X-ray absorption spectroscopy and detectors

Antonella Balerna

DAΦNE-Light Facility
INFN – Frascati National Laboratory

EDIT2015 International School
Excellence in Detectors and Instrumentation Technologies

20-29 October 2015 INFN Frascati National Laboratory (Italy)

Outline

- Light
- X-rays and Synchrotron radiation sources
  - X-rays and atoms
  - X-ray sources
- Detectors Basic Principles
  - Interactions of x-rays with matter
  - XAFS: EXAFS and XANES
- Gas Detectors
  - Ionization chambers
- Solid State Detectors
  - Silicon Drift detectors
  - Some applications of XRF to Cultural Heritage
- Conclusions

INTERNATIONAL YEAR OF LIGHT 2015

Light

Progress in science goes in parallel with the technical progress in producing and using light at different wavelengths to explore the physical world.

Light

Visible light is only a ***tiny slice of the electromagnetic spectrum***. The entire electromagnetic spectrum of light is huge, spanning from ***gamma rays on one end to radio waves***.

Visible Light is the light we can see using our eyes. This tiny human spectrum encompasses a very specific range of wavelengths from about ***380 nm to 780 nm***.

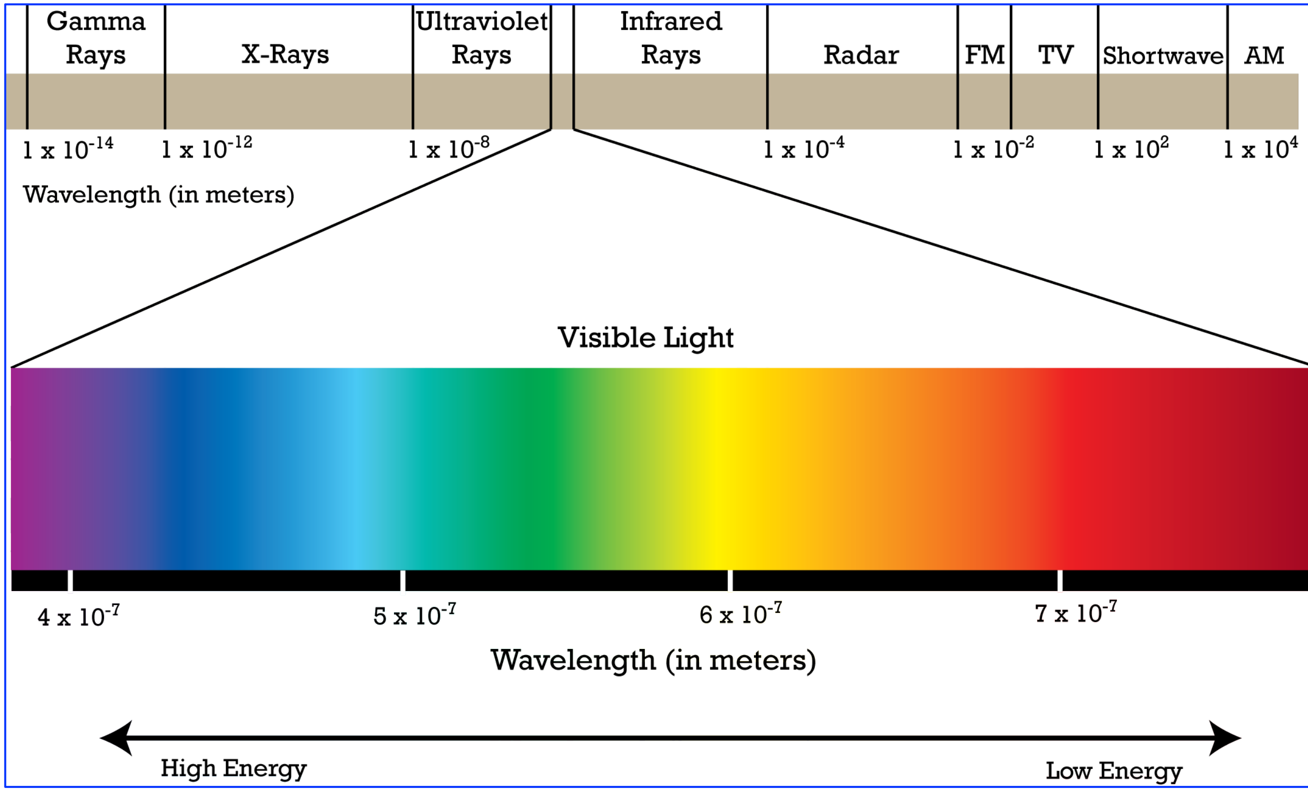

Physiologically we see these frequencies because the photoreceptors in our retinas are sensitive to them. When photons of light hit the photoreceptors this creates an electrochemical signal which is the first step in a fascinating process which ultimately results in us seeing colors.

Light and waves

Light travels as waves of energy. Waves of light have different ***wavelengths*** (the distance between the top of one wave and the top of the next). ***Different colors of visible light have different wavelengths***.

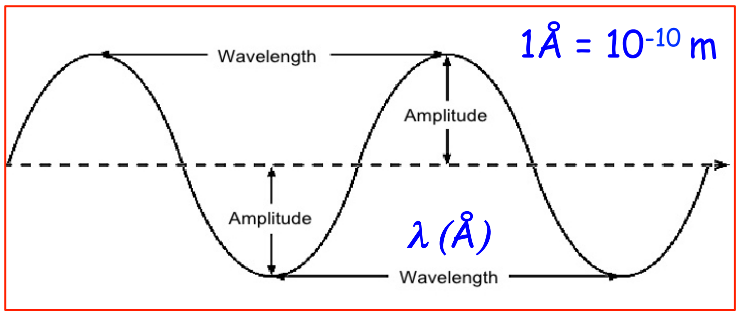

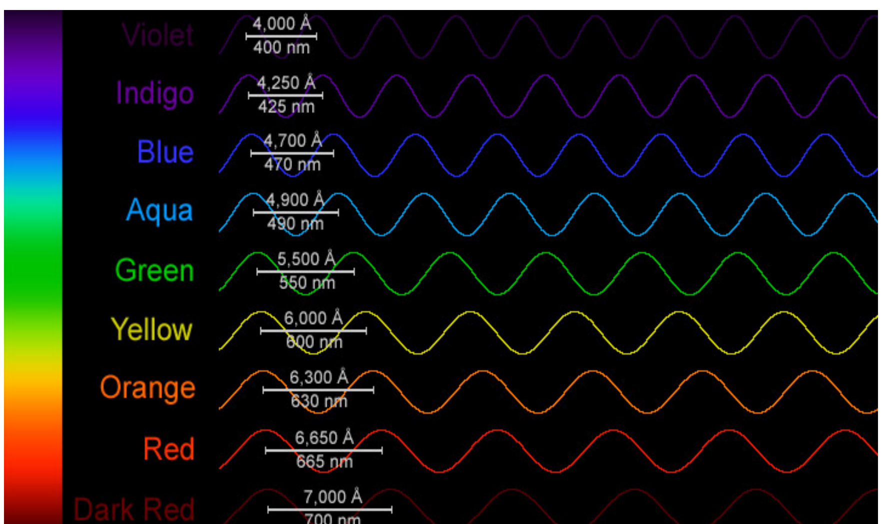

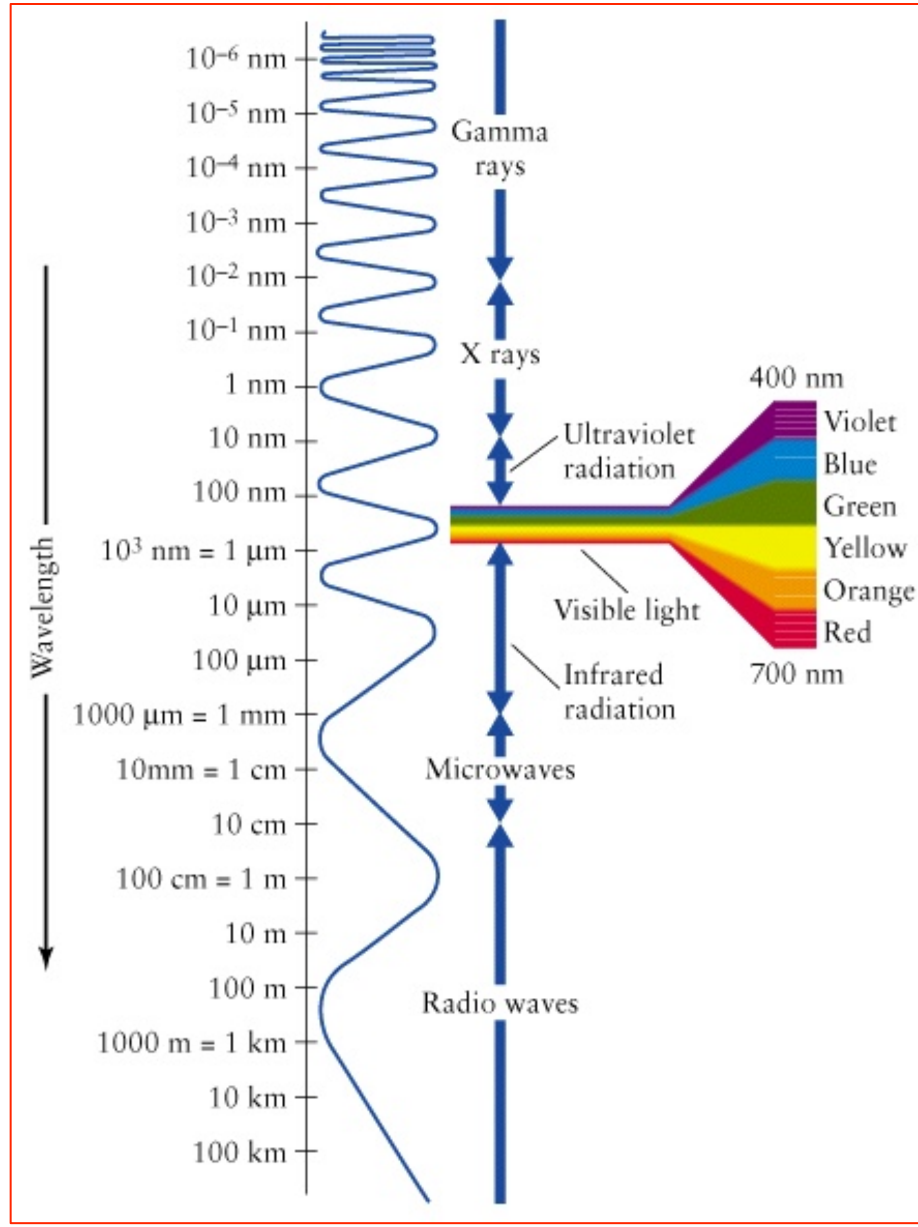

Electromagnetic Spectrum

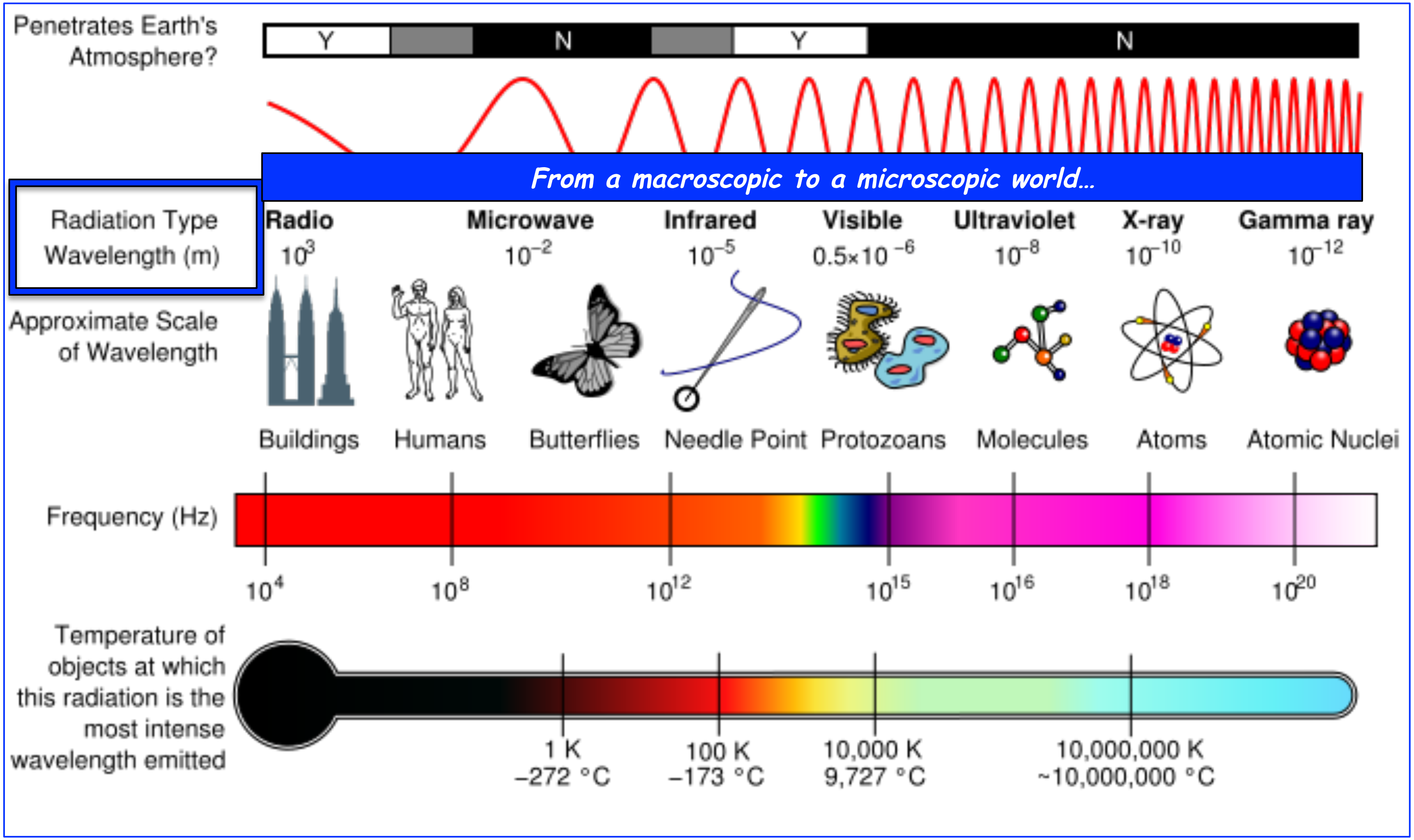

The ***wavelength*** (λ) and ***frequency*** (ν) ***of light are strictly related***: ***the higher the frequency the shorter the wavelength***! This is because ***all light waves move through vacuum at the same speed*** (*c* = speed of light) and the equation that relates wavelength and frequency for electromagnetic waves is: $\lambda\nu = c$

X-rays

Electromagnetic Spectrum and X-rays

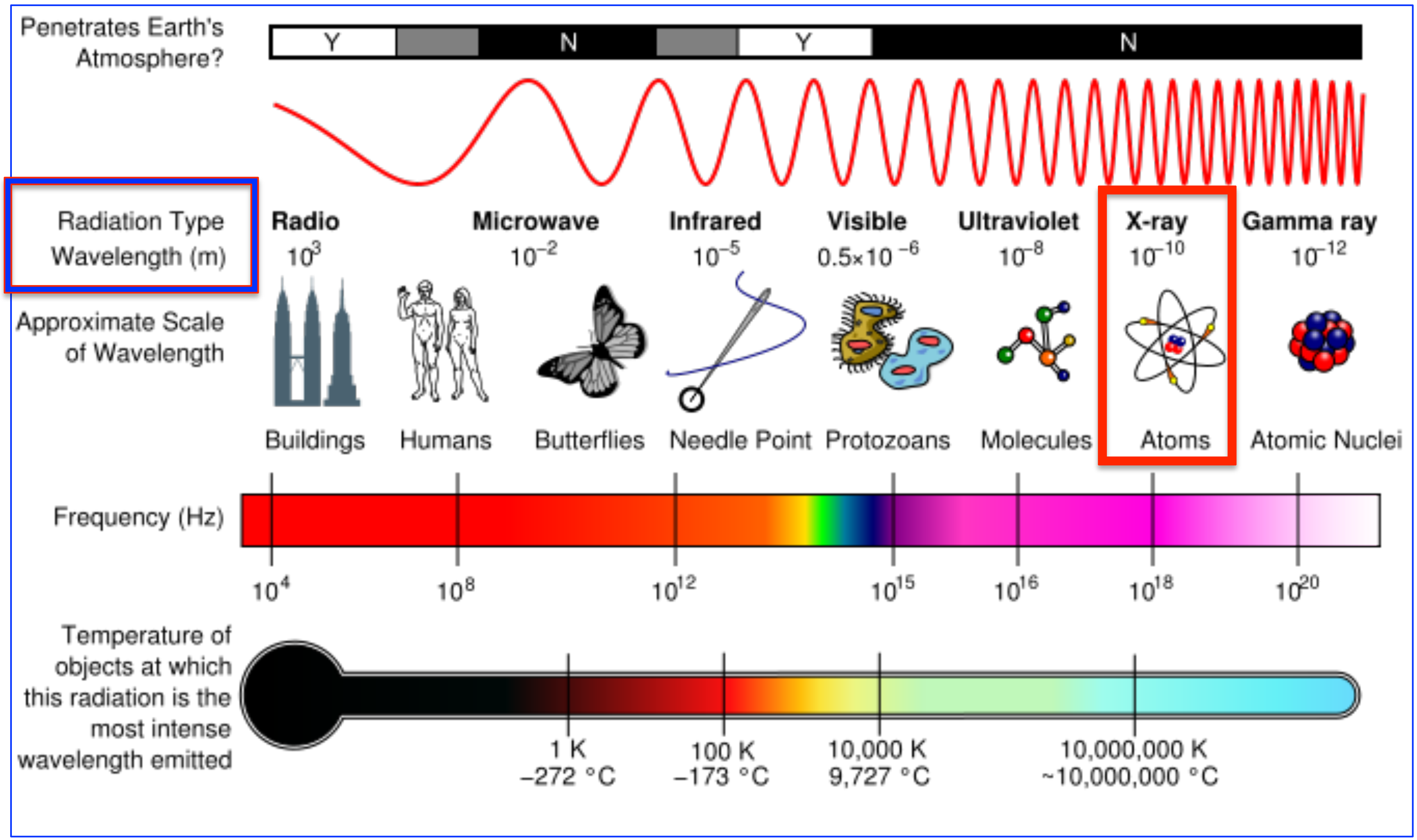

X-rays discovery


EINE NEUE ART

VON

STRAHLEN.

VON

DR. W. RÖNTGEN,

O. Ö. PROFESSOR AN DER K. UNIVERSITÄT WÜRZBURG.

WÜRZBURG.

VERLAG UND DRUCK DER STAHEL'SCHEN K. HOF- UND UNIVERSITÄTS-BUCH- UND KUNSTHANDLUNG.

Ende 1895.

60 ₰.

On a New Kind of Rays

While ***Wilhelm Roentgen*** was working on the effects of ***cathode rays*** during ***1895***, he discovered X-rays. His experiments involved the passing of electric current through gases at extremely low pressure. On **November 8, 1895** he observed that certain rays were emitted during the passing of the current through discharge tube. His experiment that involved working in a totally dark room with a well covered discharge tube resulted in the **emission of rays which illuminated a barium platinocyanide screen**. ***The screen became fluorescent even though it was placed two meters away from discharge tube***.

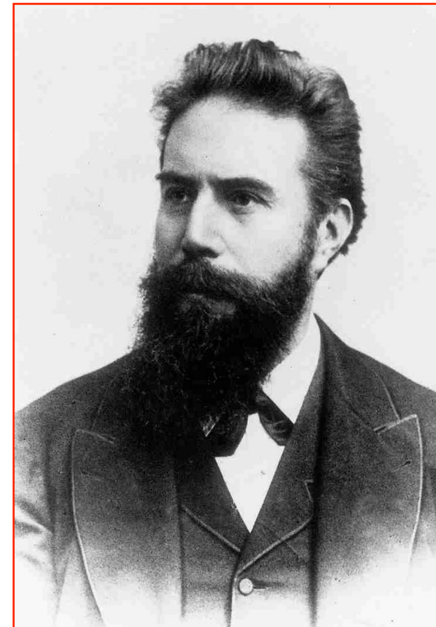

Wilhelm Conrad Roentgen

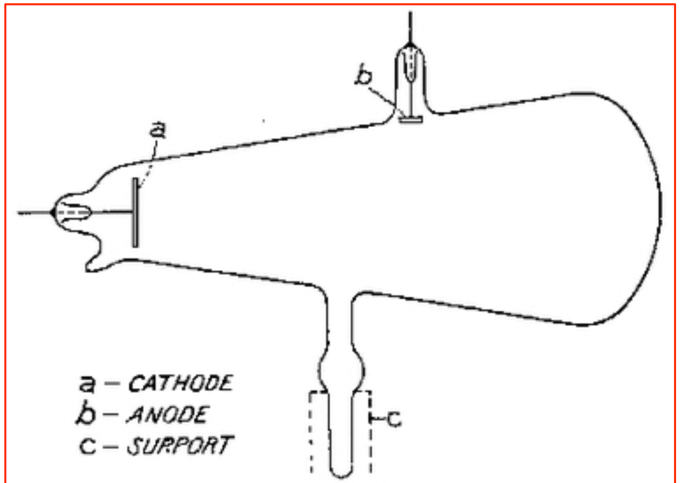

Fig. 1. Earliest type of roentgen tube.

Gas tube: electrons are freed from a **cold cathode by positive ion bombardment, thus necessitating a certain gas pressure.**

He continued his experiments using **photographic plates** and generated the very ***first "roentgenogram"*** by developing the image of ***his wife's hand*** and analyzed the variable transparency as showed by her bones, flesh and her wedding ring.

Contribution of Physics : X-ray diffraction

Max von Laue theorized and proved in 1912 that ***x-rays could be diffracted by crystalline materials.***

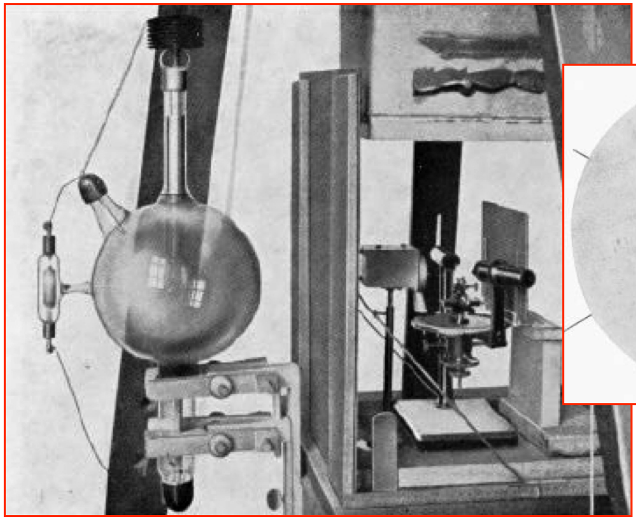

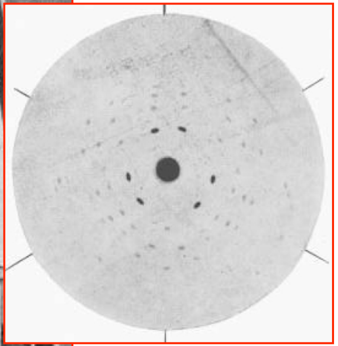

ZnS

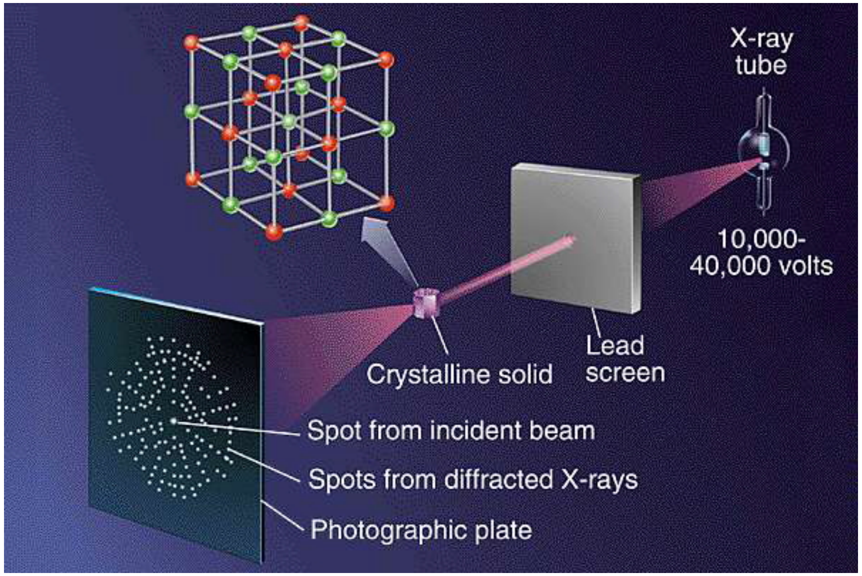

This discovery was extended by ***William Lawrence Bragg*** and his father ***William Henry Bragg*** :they showed that ***diffraction could be treated as reflection from evenly spaced planes if monochromatic x-radiation was used.***

Bragg's Law: $n\lambda = 2d \sin\theta$

λ is the ***wavelength*** of the X-radiation
d is the ***inter-planar spacing*** in the crystalline material and θ is the ***diffraction angle.***

X-rays and atoms

N. Jones, Nature 505, 602 (2014)

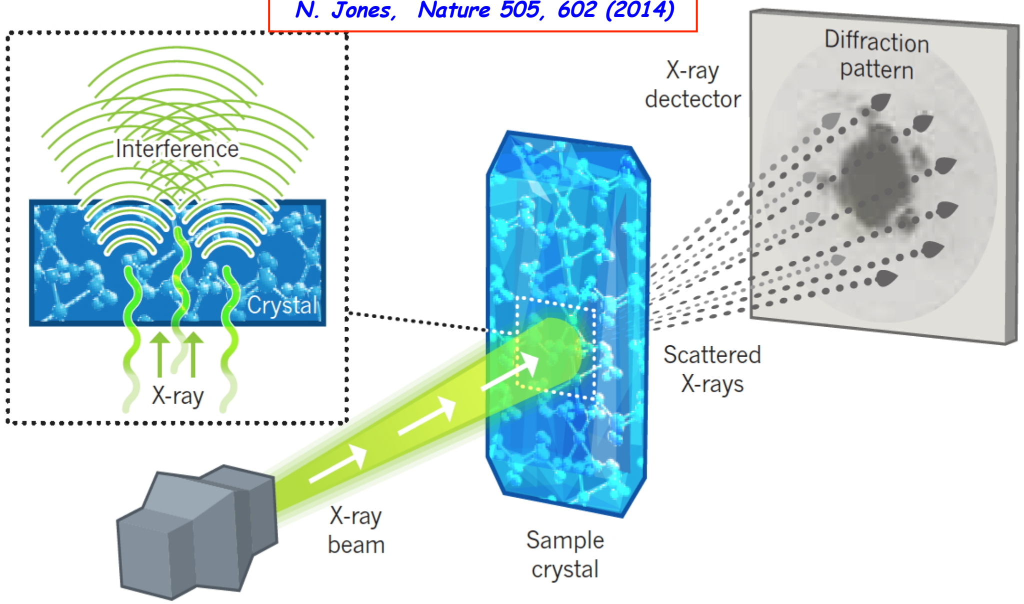

With X-rays we can study atoms because wavelengths are of the order of 10^{-10} m or 0.1 nm or 1Å

Matter is composed of atoms!

Using X-rays we can study the atomic structure of materials! The atomic structure primarily affects the chemical, physical, thermal, electrical, magnetic, and optical properties.

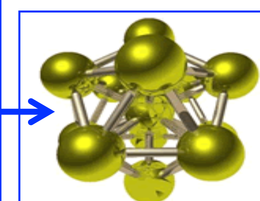

Why is this important?

X-rays and Atoms

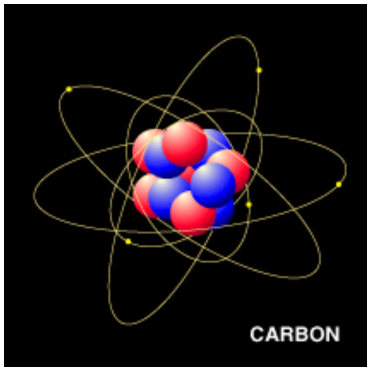

Both diamond and graphite are made entirely out of carbon!

Using x-rays to reveal the atomic structure of materials

Diamond

Graphite

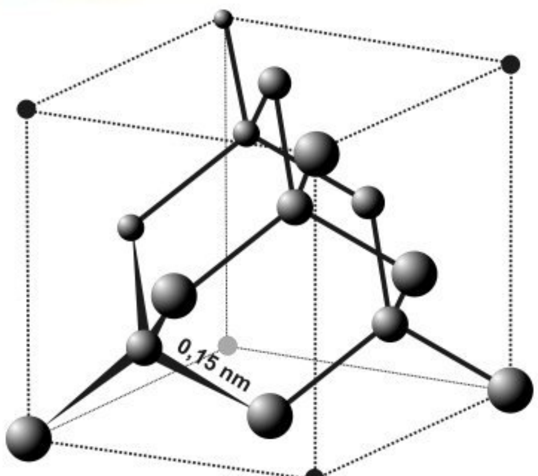

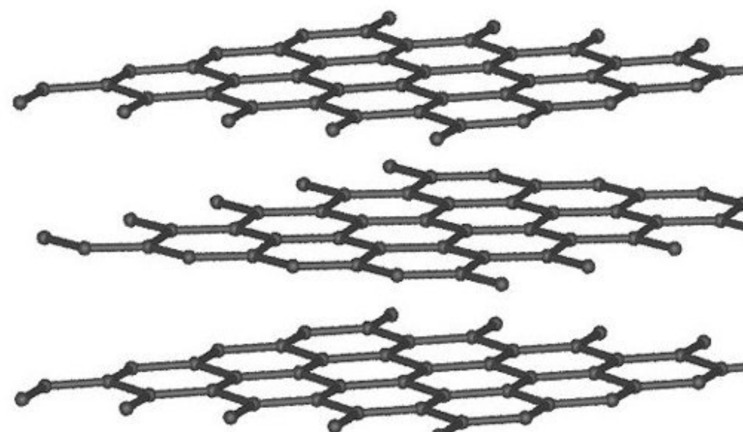

Graphite is opaque and metallic- to earthy-looking, while diamonds are transparent and brilliant.

The different properties of graphite and diamond arise from their distinct crystal structures.

X-rays application fields

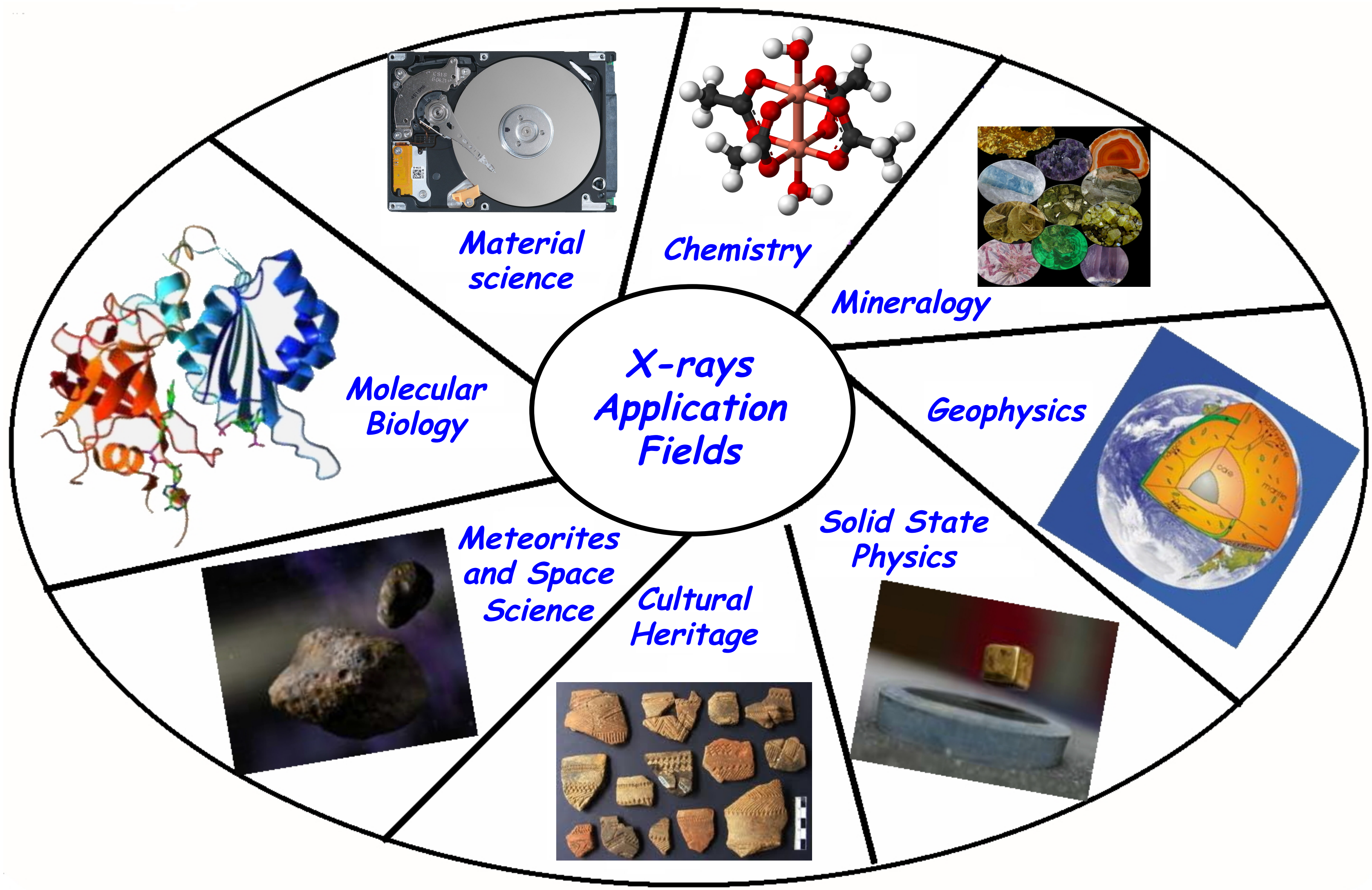

X-ray sources

X-ray conventional sources
and synchrotron radiation

X-ray conventional sources

X-rays: conventional sources

From **gas tubes** (cold cathode) to **high vacuum tubes** (hot cathode)

Crookes tube

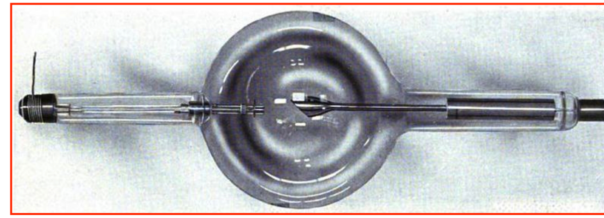

Coolidge tube

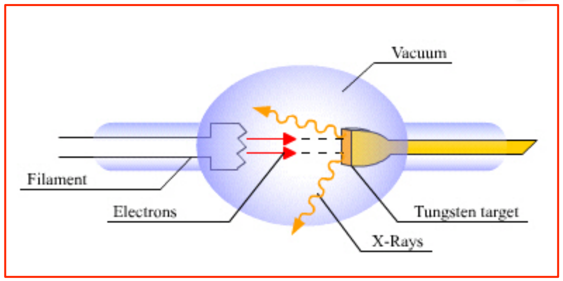

The ***Coolidge tube (1913)***, also called ***hot cathode tube***, is the most widely used. Electrons are produced by thermionic effect from a tungsten filament heated by an electric current. The filament is the cathode of the tube. The high voltage potential is between the cathode and the anode, the electrons are accelerated, and hit the anode.

The ***rotating anode tube is an improvement of the Coolidge tube*** anode surface (water cooled) is always moving, so heat is spread over a much larger surface area giving a 10-fold increase in the operating power.

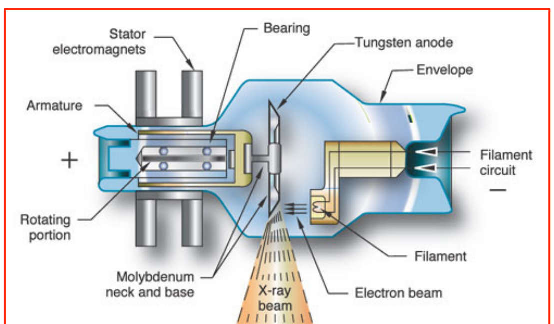

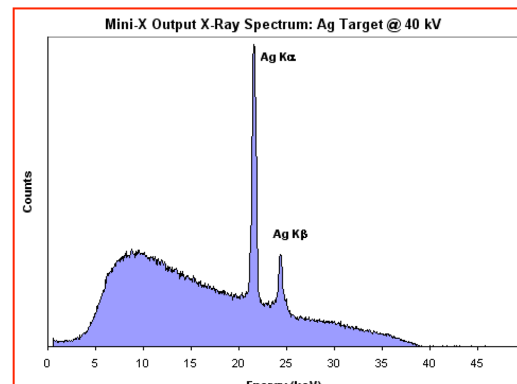

X-rays: conventional sources

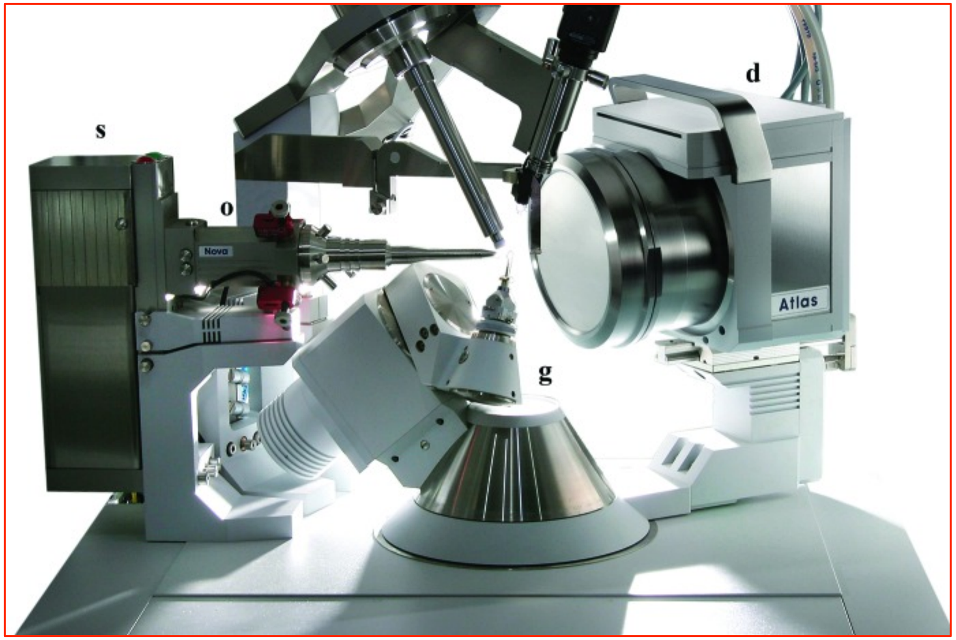

EVOLUTION

A compact X-ray in-house laboratory system consisting of ***a microfocus sealed-tube source*** (s),focusing multi-layer optics (o), a four-circle goniometer (g) and a CCD detector (d).

Pictures of ***Agilent Technologies.***

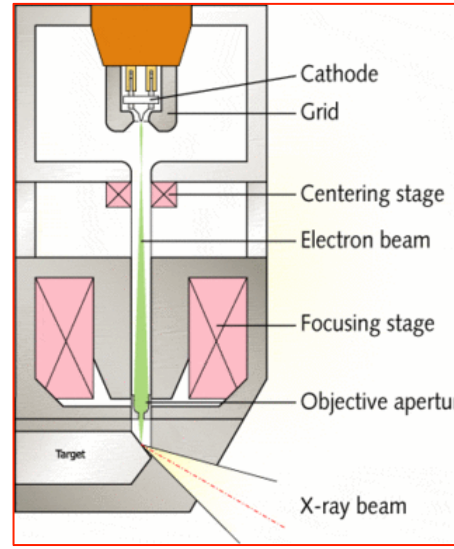

Approximate X-ray beam brilliance for the main types of in-house sources with optics

System	Power (W)	Actual spot on anode (μm)	Apparent spot on anode (μm)	Brilliance (photons s^{-1} mm^{-2} $mrad^{-1}$)
Standard sealed tube	2000	10000 × 1000	1000 × 1000	0.1×10^9
Standard rotating-anode generator	3000	3000 × 300	300 × 300	0.6×10^9
Microfocus sealed tube	50	150 × 30	30 × 30	2.0×10^9
Microfocus rotating-anode generator	1200	700 × 70	70 × 70	6.0×10^9
State-of-the-art microfocus rotating-anode generator	2500	800 × 80	80 × 80	12×10^9
Excillum JXS-D1-200	200	20 × 20	20 × 20	26×10^9

T. Skarzynski, *Collecting data in the home laboratory: evolution of X-ray sources, detectors and working practices*, ***Acta Cryst***. **D69 (2013) 1283–1288**

Synchrotron radiation sources

Light sources and brightness

When interested in nm scale details: brightness becomes fundamental.

A ***bright source*** is the one ***very effective in illuminating a specific target***. If the specific target is small a ***bright source*** is ***a small size source with emission concentrated within a narrow angular spread.***

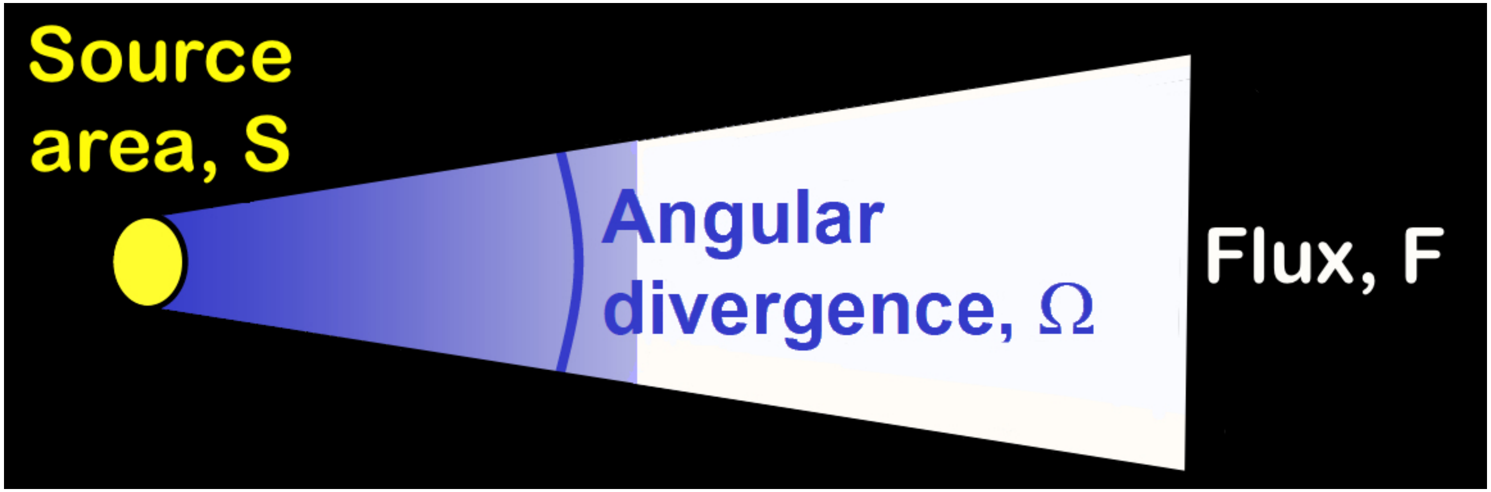

$$\textit{Brightness} = \textit{constant}\ \frac{F}{S \times \Omega}$$

Bright light sources?

HE particle accelerators

↓

Relativistic effects

↓

Synchrotron light

Synchrotron radiation and light sources

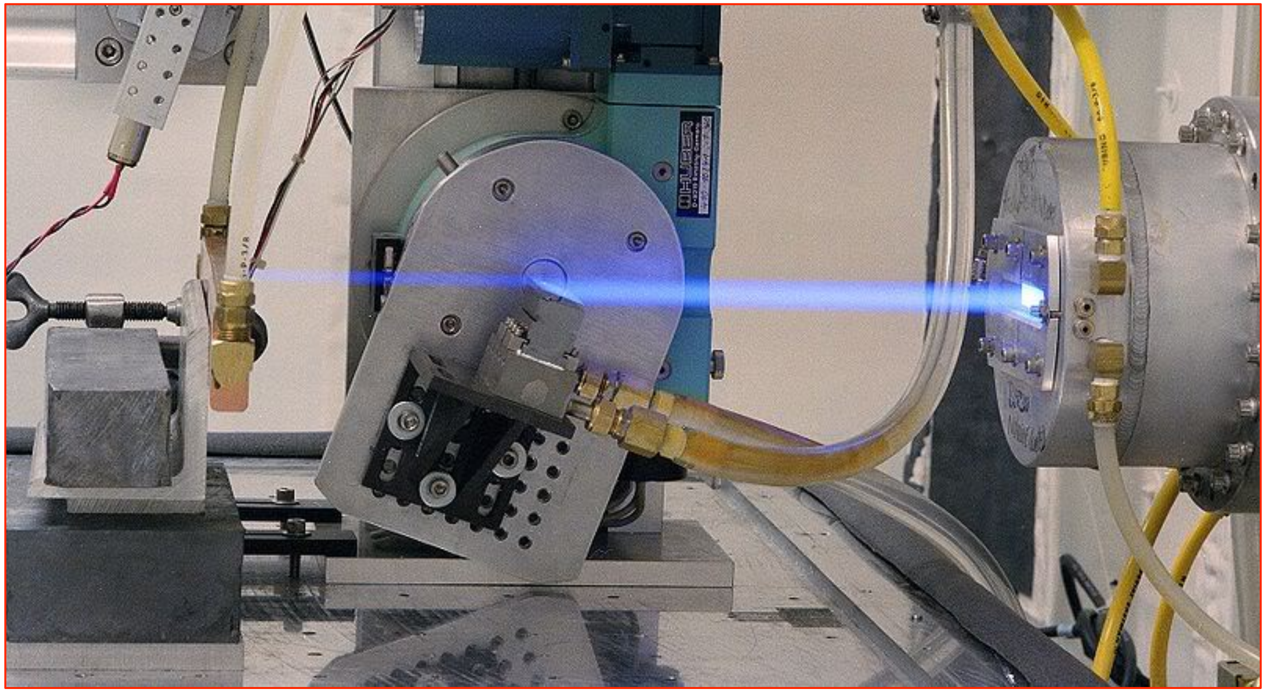

Synchrotron radiation opened a new era of accelerator-based light sources that have evolved rapidly over four generations:

- the first three-generations based on storage rings

-the forth and fifth generation light sources based on FELs.

A dramatic improvement of brightness and coherence over about 70 years.

Synchrotron light is present in nature!

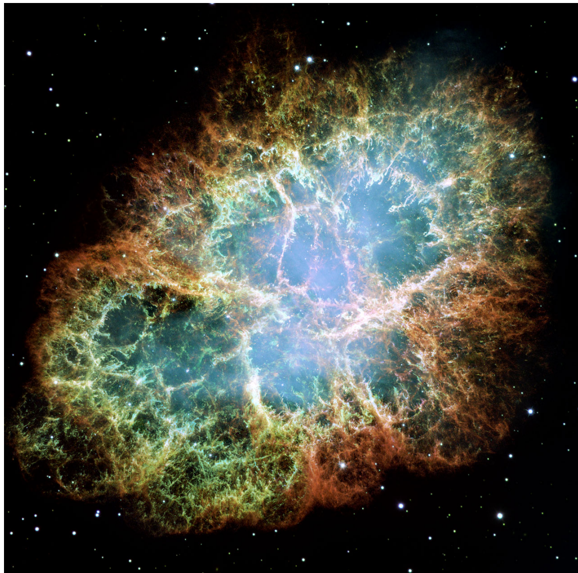

NASA Hubble Space Telescope image of the Crab Nebula (NASA, ESA and Allison Loll/Jeff Hester (Arizona State University)).

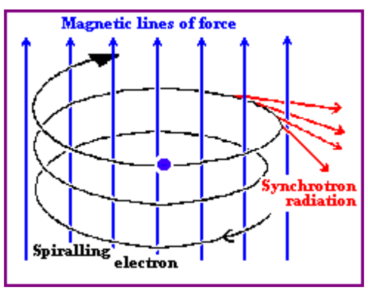

NASA's Great Observatories' View of the Crab Nebula X-Ray-blue: NASA/CXC/J.Hester (ASU); Optical-red and yellow: NASA/ESA/J.Hester & A.Loll (ASU); Infrared-purple: NASA/JPL-Caltech/R.Gehrz (Univ. Minn.)

Synchrotron radiation is a very important emission process in astrophysics!

Crab Nebula: remnant of a supernova explosion seen on earth by Chinese astronomers in 1054, at about 6500 light years from Earth in the constellation Taurus !

SR emission is produced by high energy electrons whirling around the magnetic fields lines originating from a Pulsar

The heart of the nebula is a rapidly-spinning neutron star, a pulsar, that powers the strongly polarised bluish 'synchrotron' nebula.

The ***Crab pulsar*** is ***slowing at the rate of about 10^{-8} sec per day***, and the ***corresponding energy loss agrees well with the energy needed to keep the nebula luminous***. Some of this luminosity takes the form of ***synchrotron radiation, requiring a source of energy for accelerating charged particles***.

Composite image data from ***three of NASA's Great Observatories****. The* ***Chandra X-ray Observatory image*** *is shown in blue, the* ***Hubble Space Telescope optical image*** *is in red and yellow, and the* ***Spitzer Space Telescope's infrared*** *image is in purple. The X-ray image is smaller than the others because extremely energetic electrons emitting X-rays radiate away their energy more quickly than the lower-energy electrons emitting optical and infrared light.* ***The Crab Nebula is one of the most studied objects in the sky, truly making it a cosmic icon.***

Synchrotron light is artificially produced by relativistic particles accelerated in circular orbits.

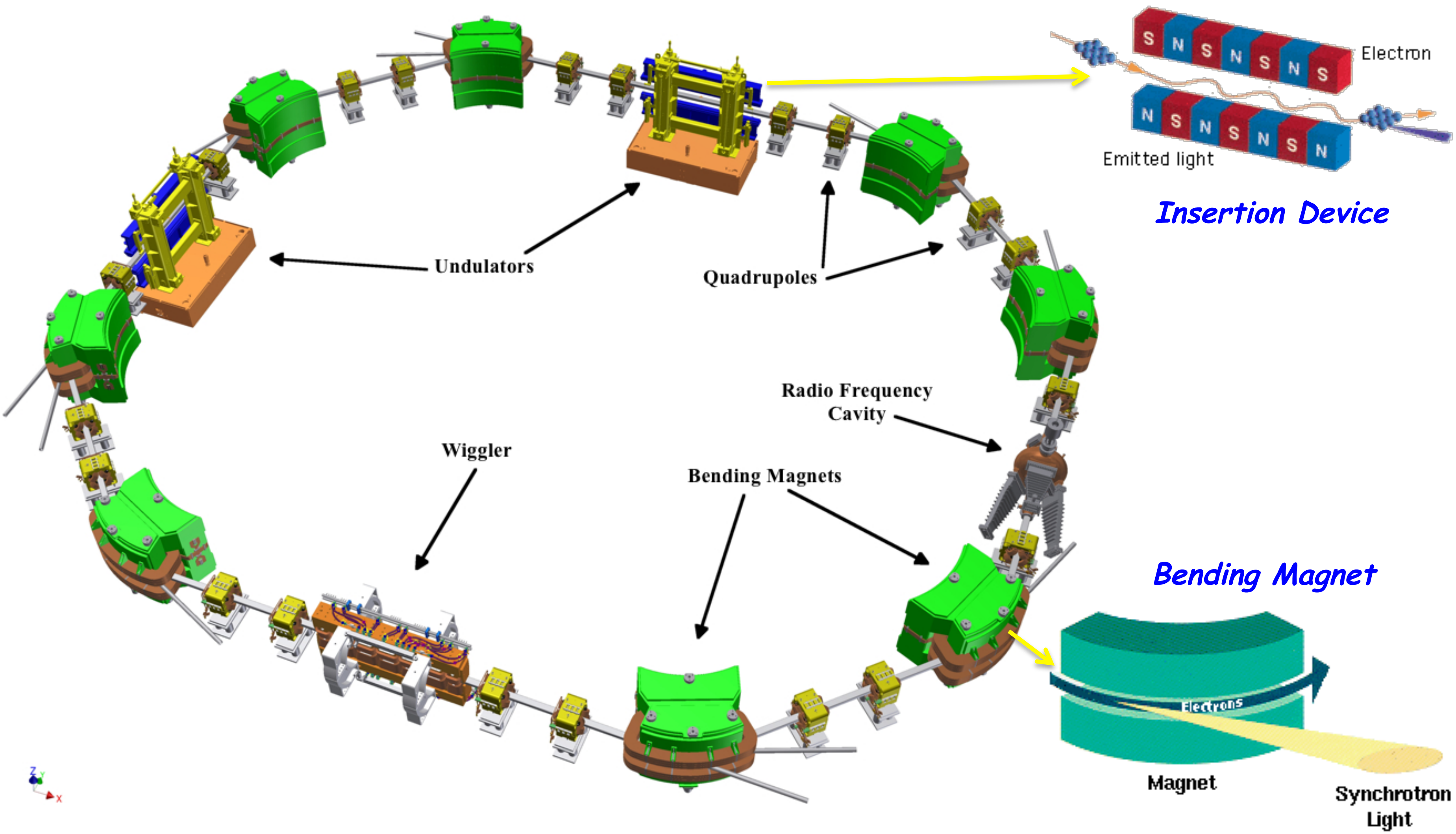

… and synchrotron radiation is also the coherent radiation emitted by the undulators of Free Electron Lasers.

Synchrotron radiation: history

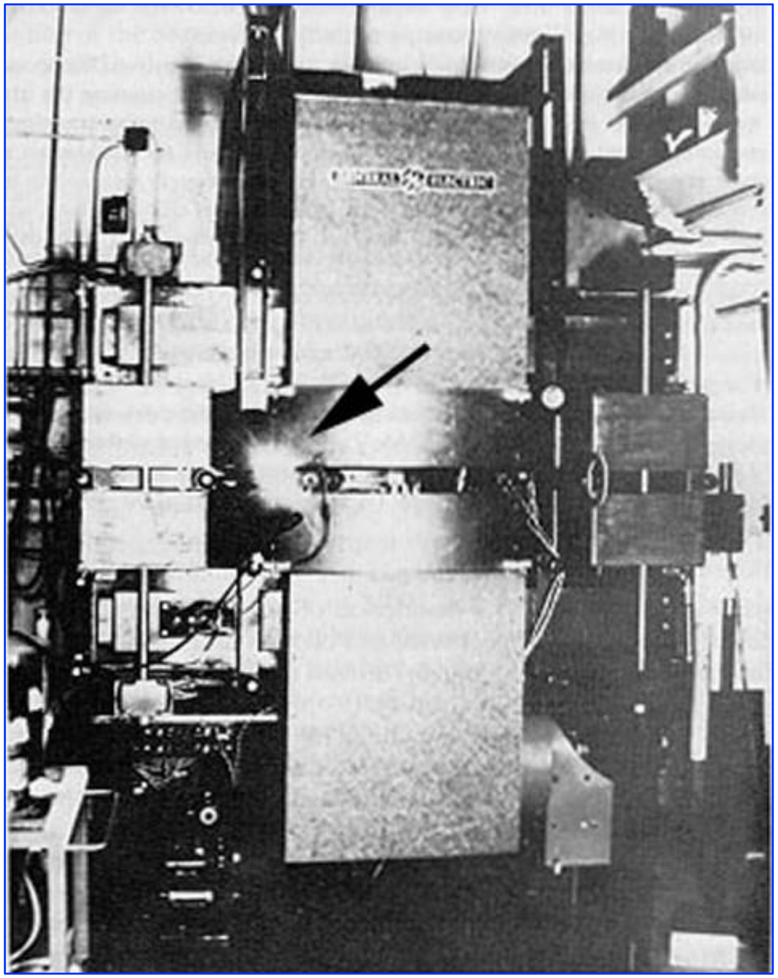

1947 *General Electric Res. Lab.* - 70 MeV Electron Synchrotron – N.Y. USA

Starting point: Proof of concepts, tests of theories!

- In the 50s and 60s machines built for High Energy Physics: synchrotrons (*1947 First 'visual observation of synchrotron radiation*).
- Synchrotron radiation was considered a ***nuisance by particle physicists***: ***unwanted but unavoidable loss of energy***!
- 1961 US National Bureau of Standards (now NIST) modified their electron synchrotron : ***access to the synchrotron radiation users***.
- Synchrotron radiation scientists became ***parasites*** of nuclear physics experiments. (*1961 Frascati – CNEN Electrosynchrotron – (0.4-1.1) GeV*)
- 1968 *First storage ring dedicated* to synchrotron radiation research: *Tantalus* (University of Wisconsin) only ***bending magnets.***

F.R. Elder, A.M. Gurewitsch, R.V. Langmuir, and H.C. Pollock, *Radiation from Electrons in a Synchrotron*, *Phys. Rev.* *71*, *829* (*1947*)
G. C. Baldwin and D.W. Kerst, *Origin of Synchrotron Radiation*, Physics Today, **28**, 9 (*1975*)

Synchrotrons and Storage Rings

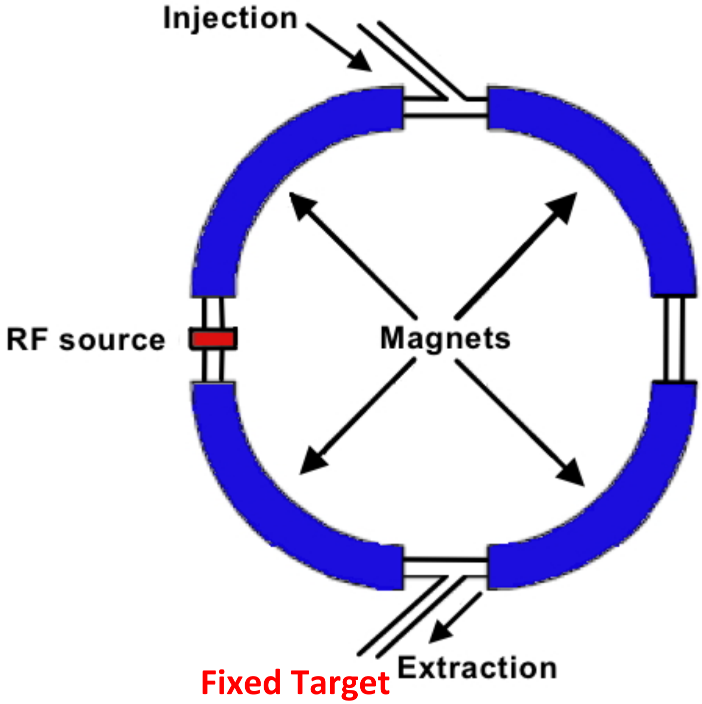

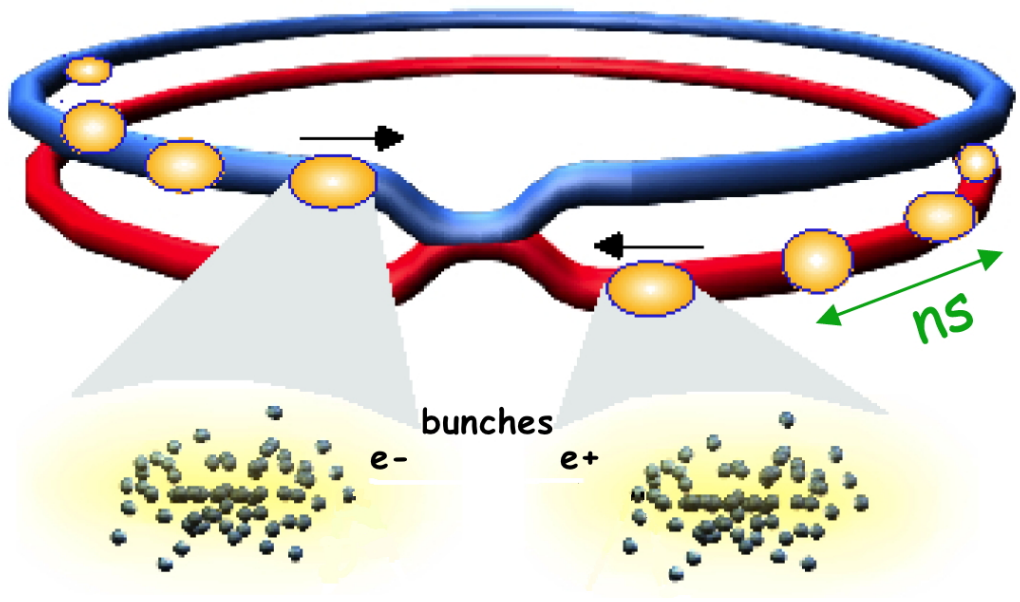

Synchrotron

Particle beam on fixed target

$E_{CM} = (mE)^{1/2}$

Storage rings

Colliding particle beams

$E_{CM} = 2E$

Colliding beams more efficient

E= particle energy >> m_0c^2 $\quad$ E_{CM}= center-of-mass energy

Comparing synchrotrons and storage rings

Synchrotrons

- *Cyclic* - the guiding magnetic field used to bend the particles into a closed path, is time-dependent, being *synchronized* to a particle beam of increasing kinetic energy.
- ***Emitted photon spectrum varies*** as e^- energy changes during each cycle.
- ***Photon intensity varies*** as e^- energy changes during each cycle (also cycle to cycle variations).
- ***Source position varies*** during the acceleration cycle.
- ***High Energy Radiation Background*** (Bremsstrahlung + e^-): ***high***, due to loss of all particles on each cycle.

Storage rings

- ***Constant***: as special type of synchrotron in which the kinetic energy of the particles is kept constant.
- ***Emitted photon spectrum constant.***
- ***Photon intensity decays slowly*** over many hours.
- ***Source position constant***- submicron source stability.
- ***High Energy Radiation Background: low*** because same particles are stored for many hours.

H. Winick, ***From Röntgen to X-ray Free-electron Lasers***, http://indico.cern.ch/event/145296/contribution/47/material/slides/1.pdf, *2012*

Synchrotron radiation: in the early history

Frascati: ElettroSynchrotron, ADA and ADONE

Frascati - CNEN (Comitato Nazionale Energia Nucleare)
Laboratory ElettroSincrotrone – (0.4-1.1) GeV, C= 28 m
(1959-1975)

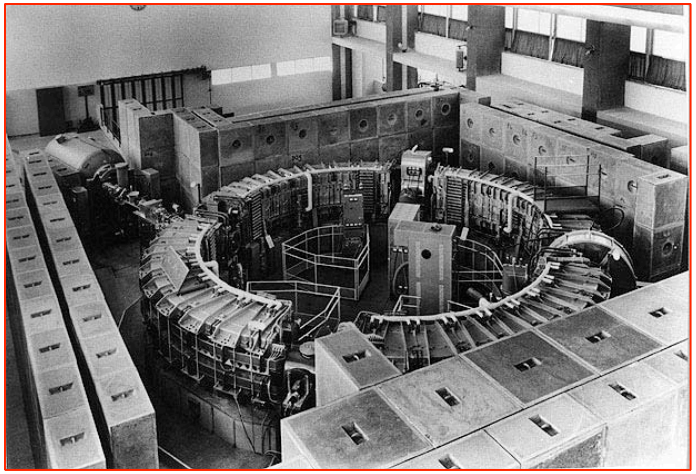

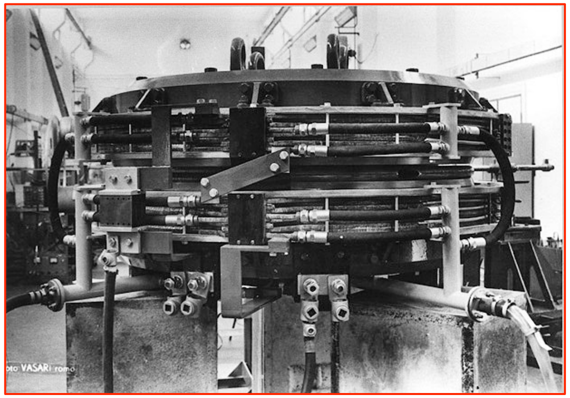

LNF ADA (Anello Di Accumulazione) – first electron-positron storage ring (proposed by B. Touschek) 0.25 GeV, C= 5 m
(1961-1964)

LNF ADONE (big ADA) electron-positron storage ring 1.5 GeV per beam, C = 105 m
(1969-1993)

1976-1993 LNF ADONE 1.5 GeV parasitic/dedicated use for SR experiments after its use for HE experiments.

Increasing brightness

Brightness is the main figure of merit of synchrotron radiation sources and its huge increase, was obtained designing low emittance machines, minimizing the source size and the beam divergence.

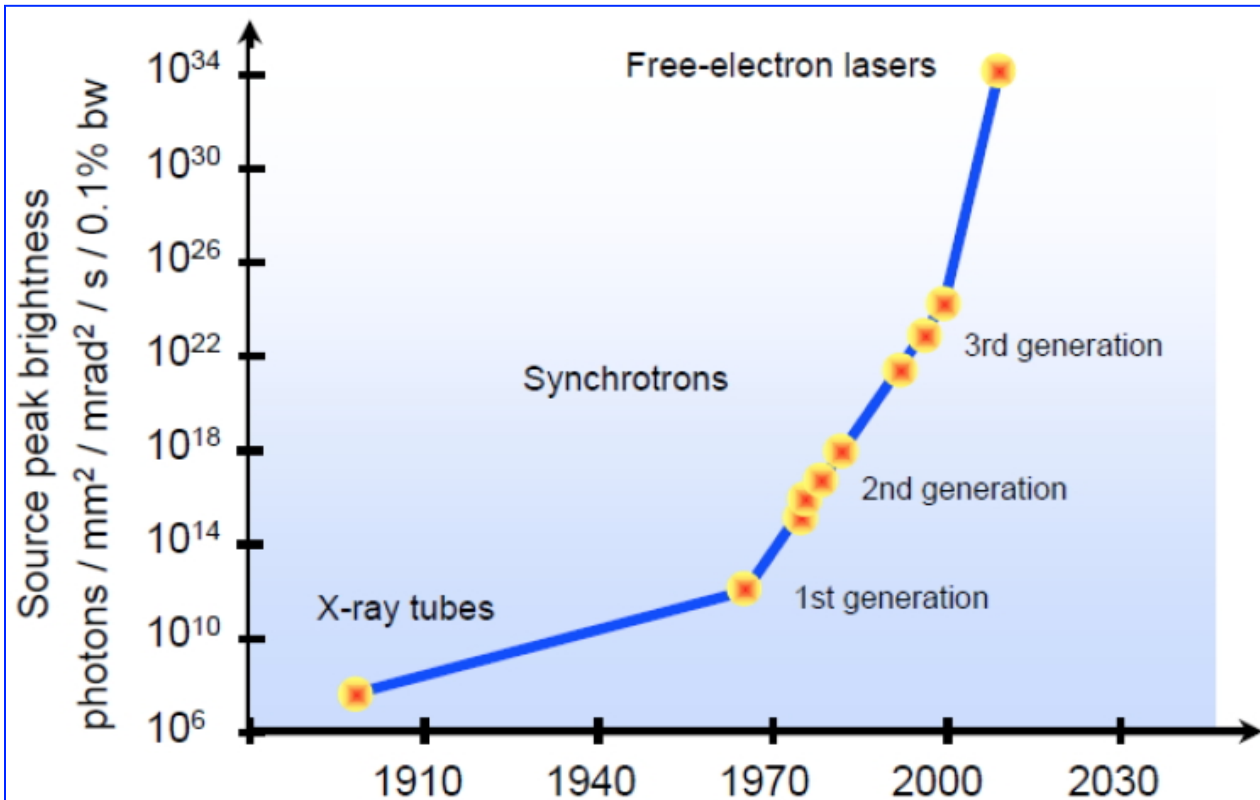

Increase of a factor 1000 every 10 years!!!

Synchrotron radiation: optimized sources

Third generation sources

Synchrotron light is now a unique tool for science!

ESRF, Grenoble - France 6 GeV, C = 844 m
opened to users in 1994

- Sources designed specifically for high brightness or low emittance.
- Emphasis on research with insertion devices like undulators!
- High-energy machines able to generate hard x-rays
- Larger facilities to support rapidly growing user community, many beamlines high number of users.

Synchrotron radiation facilities

18 in America
25 in Asia
25 in Europe
1 in Oceania
including facilities under design and FELS

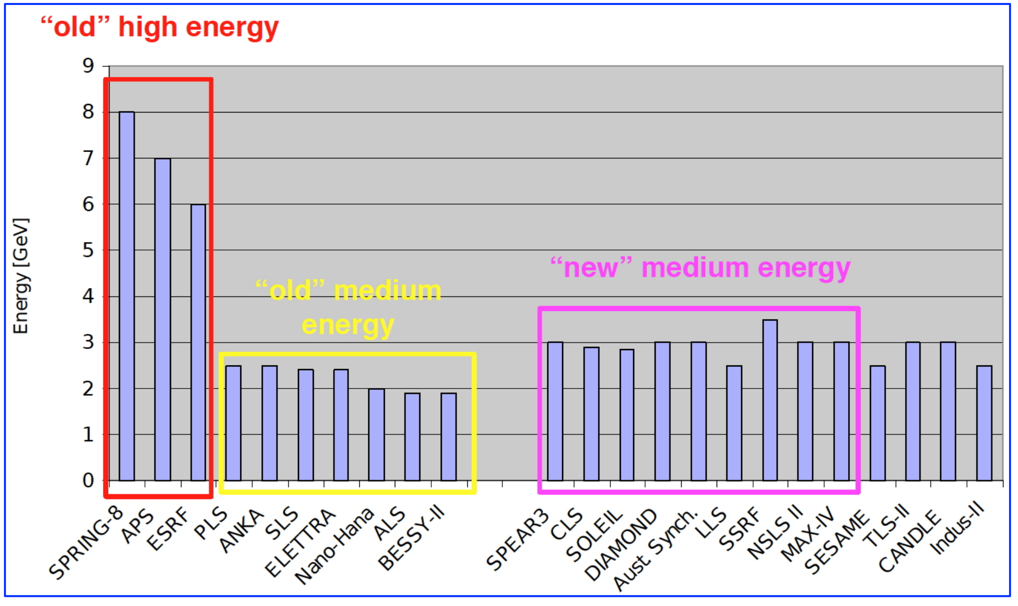

wayforlight
the european lightsources single entry point

Info on European Synchrotron Radiation Facilities: www.wayforlight.eu
About 67 operational Synchrotron Radiation Facilities Around the World information on: www.lightsources.org

Schematic view of a Synchrotron Radiation facility

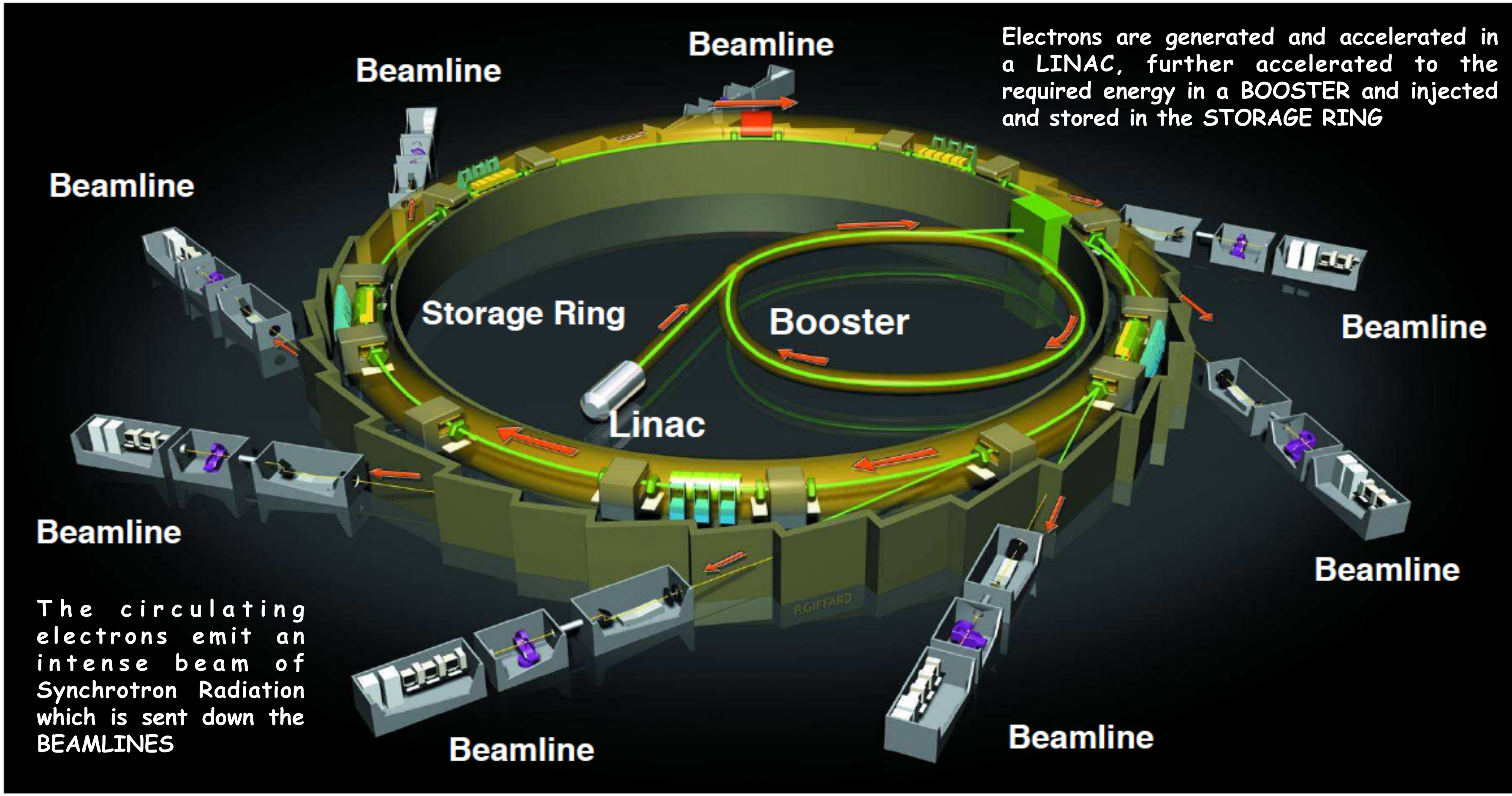

As a function of the energy range to be used each beamline must be optimized for a particular field of research.

Beamline schematic composition:

- *Front end*
- *Optical hutch*
- *Experimental hutch*
- *Control and computing*

The ***front end*** isolates the beamline vacuum from the storage ring vacuum; **defines the angular acceptance of the synchrotron radiation** via an aperture; blocks(beam shutter) when required, the x-ray and Bremsstrahlung radiation during access to the other hutches.

Synchrotron radiation @ INFN-Frascati National Laboratory

DAΦNE-Light

INFN-LNF Synchrotron Radiation Facility

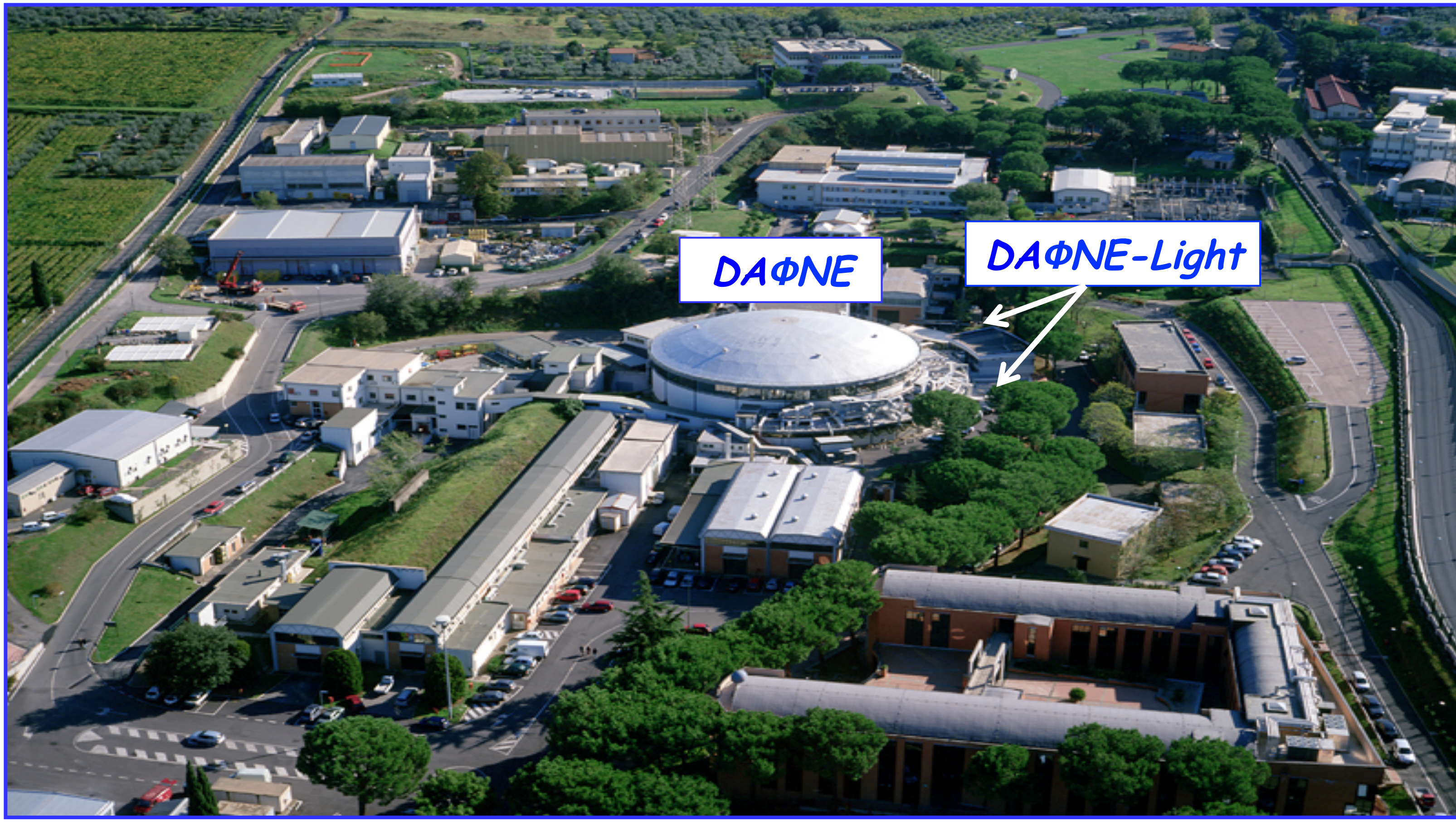

Beamlines @ DAΦNE

1) SINBAD - IR beamline (1.24 meV - 1.24 eV)

2) DXR1- Soft x-ray beamline (900-3000 eV)

Open to Italian and EU users

3) DXR2 – UV-VIS beamline (2-10eV) new setup.

XUV beamlines

4) Low Energy Beamline (35-200 eV) ready for commissioning;

5) High Energy Beamline (60-1000eV) ready for commissioning.

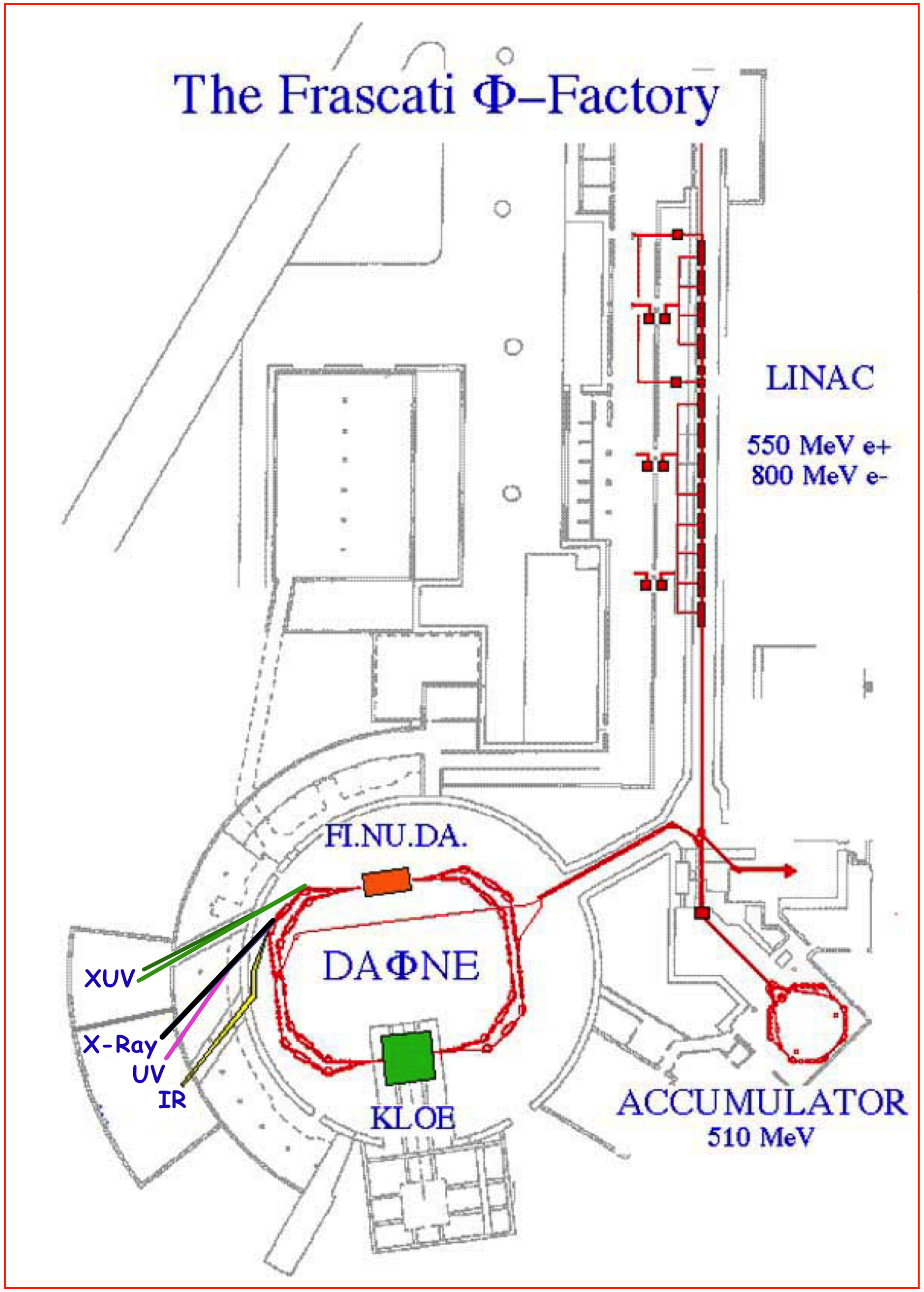

Available techniques

- FTIR spectroscopy, IR microscopy and IR imaging
- UV-Vis absorption spectroscopy
- Photochemistry: UV irradiation and FTIR micro-spectroscopy and imaging.
- Soft x-ray spectroscopy: XANES (X-ray Absorption Near Edge Structure) light elements from Na to S
- SEY (secondary electron yield) and XPS (X-ray photoelectron spectroscopy) – by electron and photon bombardment

From accelerators to applications

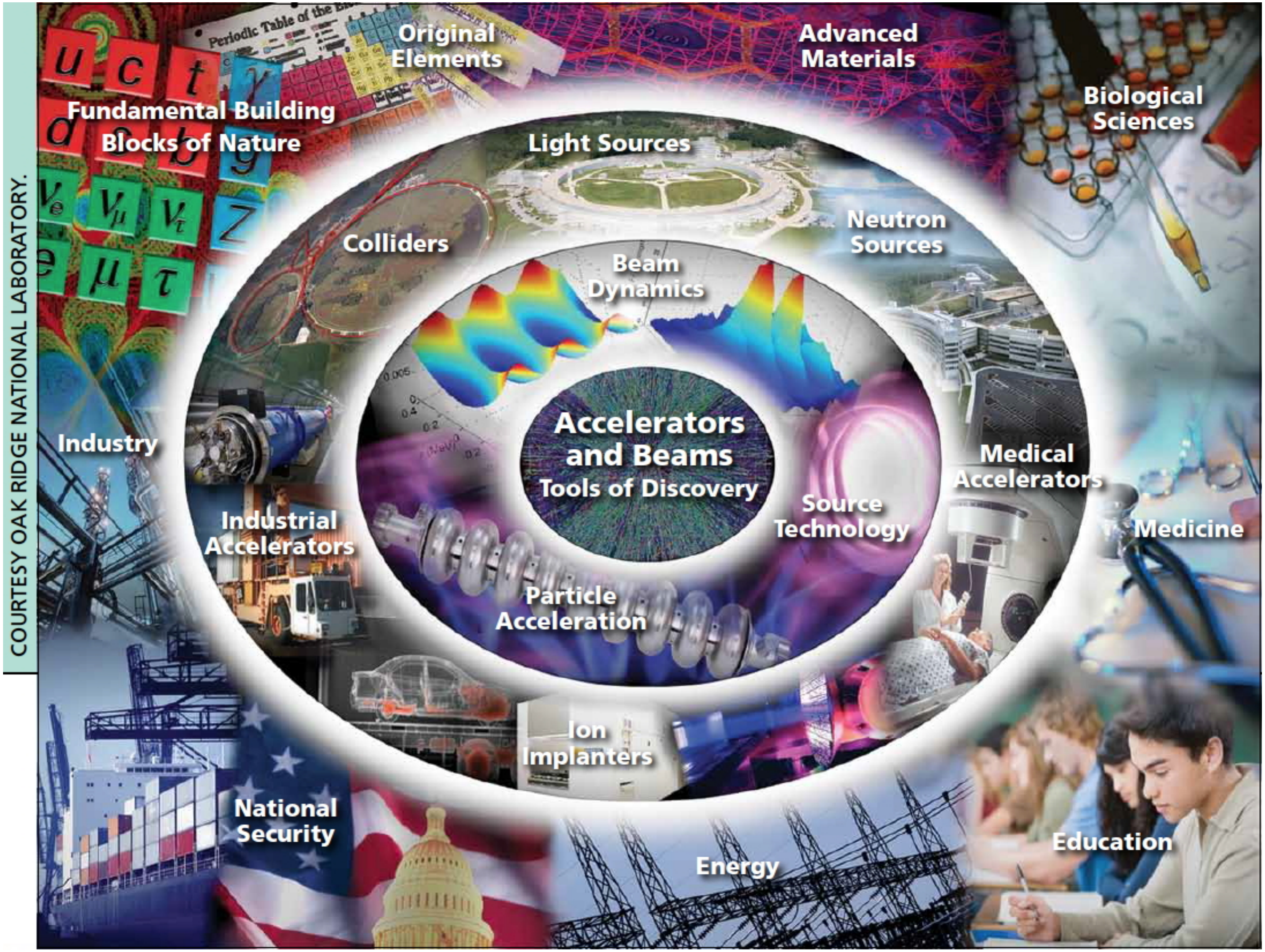

E. Malamud *Ed.*, ***Accelerators and Beams tools of discovery and innovation*** (http://www.aps.org/units/dpb/news/edition4th.cfm) ***2013***

Interactions of x-rays with matter

Interaction of X-rays with matter

Attenuation mechanisms for X-rays

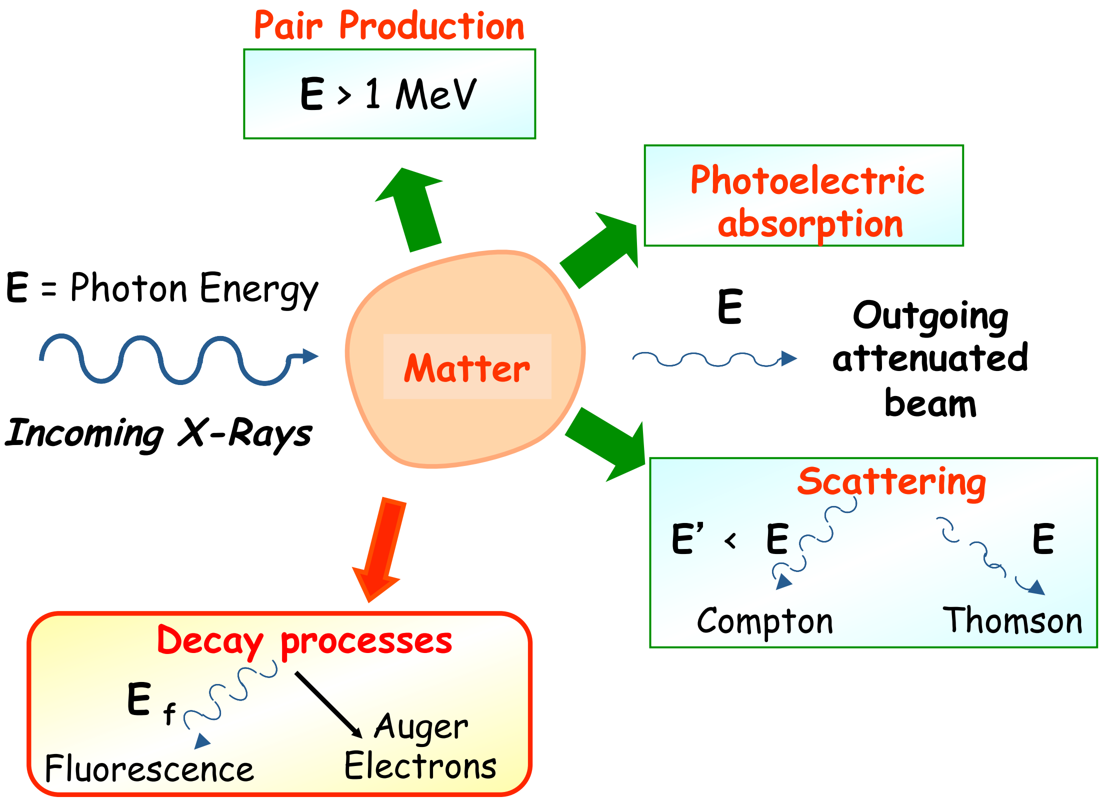

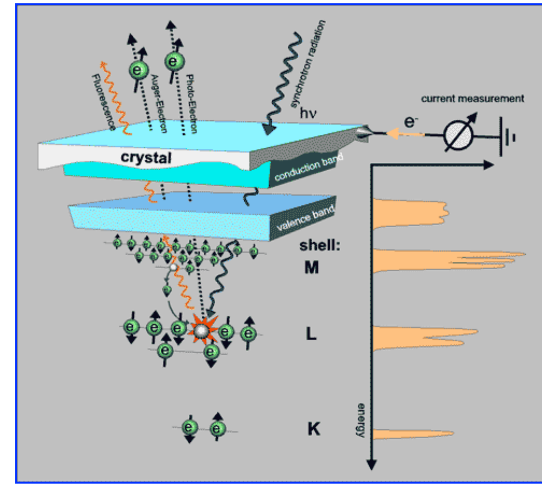

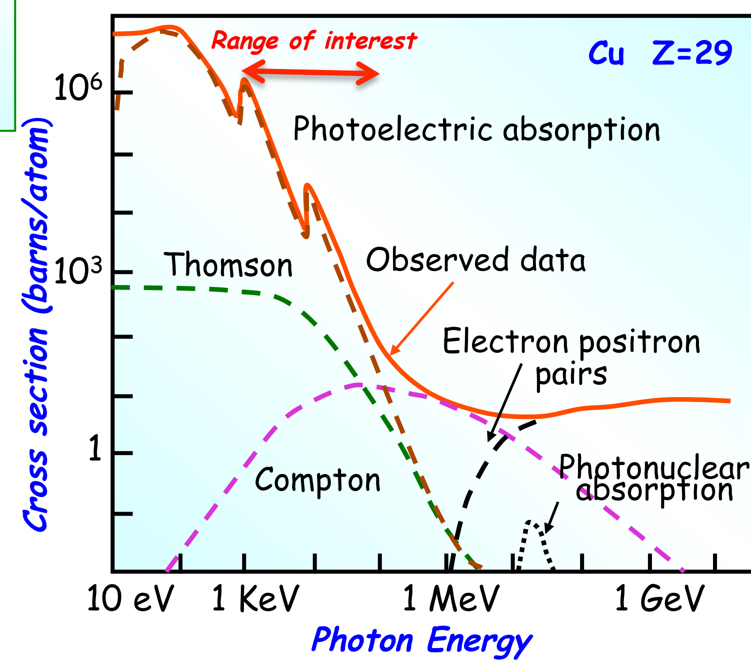

There are different types of interaction of X-rays with matter but taking into account the energy range of interest the ones that will be taken into account are ***absorption*** and ***elastic*** or ***Thomson scattering***.

X-rays interactions with matter and experimental techniques

X-rays, interactions and experimental techniques

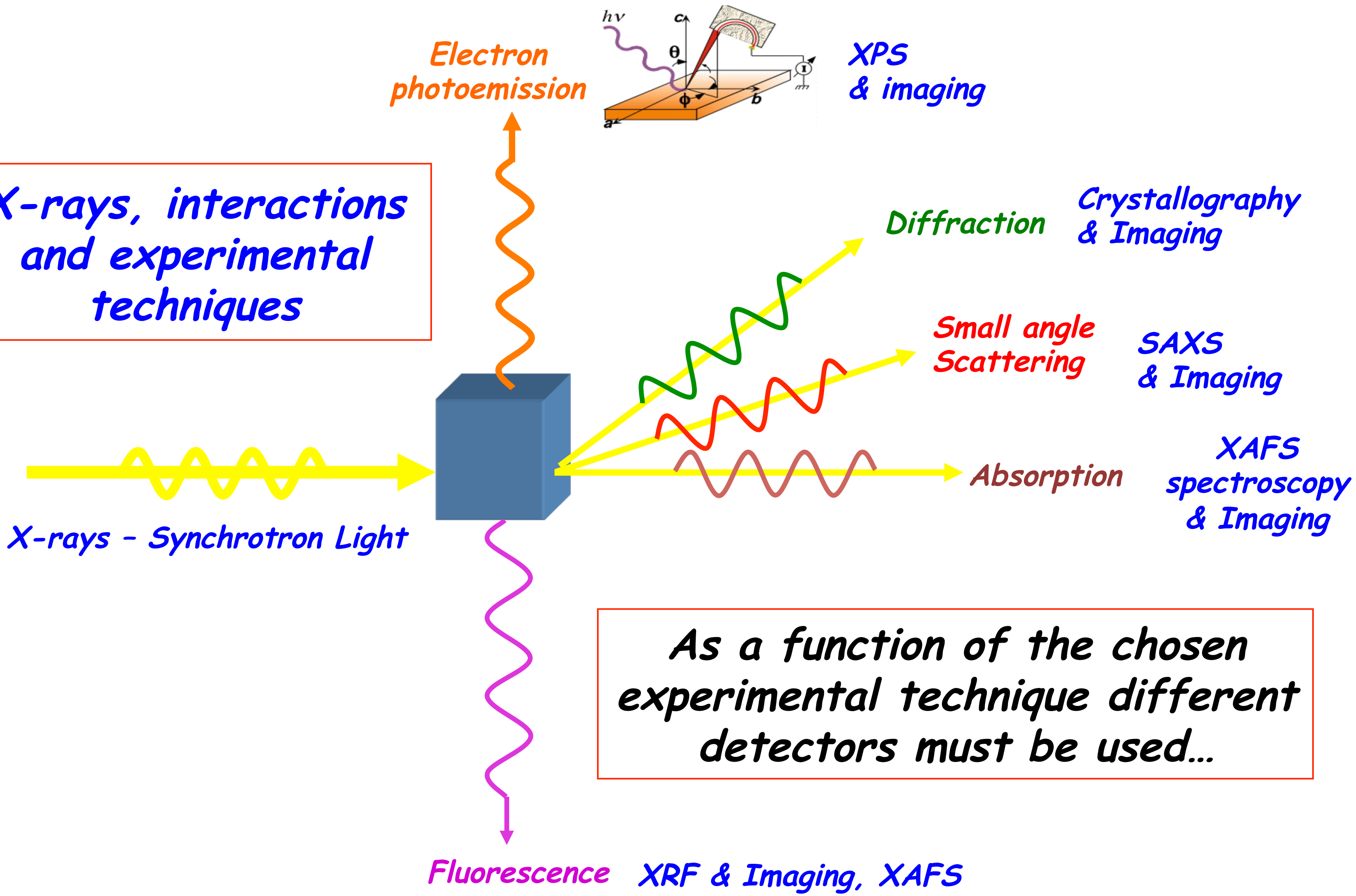

As a function of the chosen experimental technique different detectors must be used…

Some X-ray techniques

Imaging

Conventional radiology relies on X ray absorption

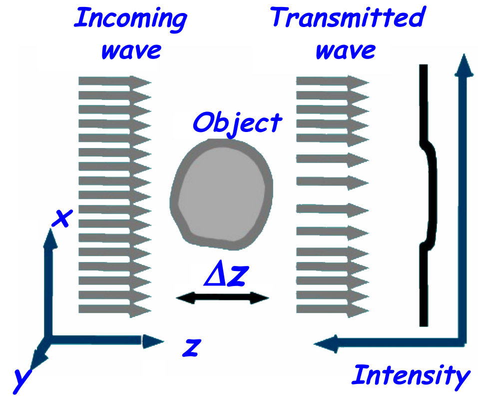

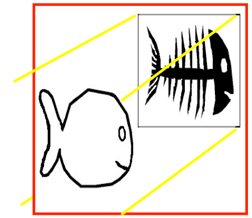

Scattering

Elastic scattering :
Thomson (elastic) if $E<E_{binding}$

$$n\lambda=2d\sin\theta \quad \text{Bragg's Law}$$

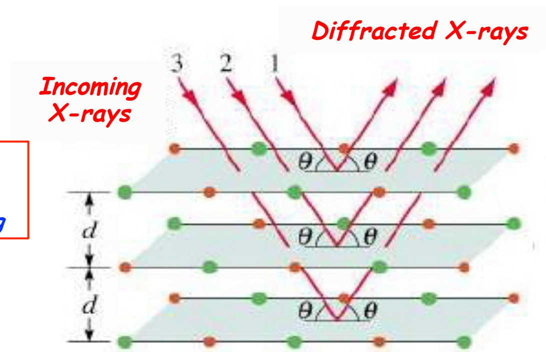

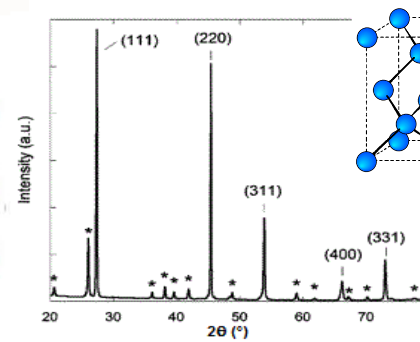

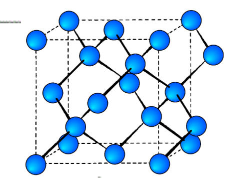

Ge crystal structure

Spectroscopy

X ray Absorption Fine Structure (XAFS)

Transmission and fluorescence mode

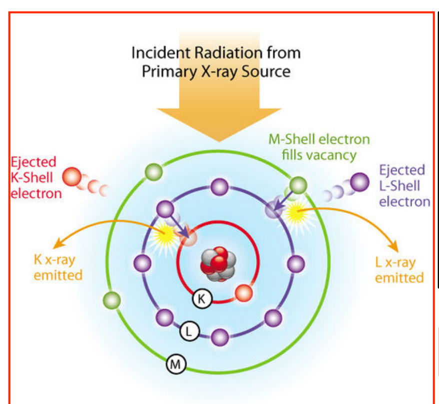

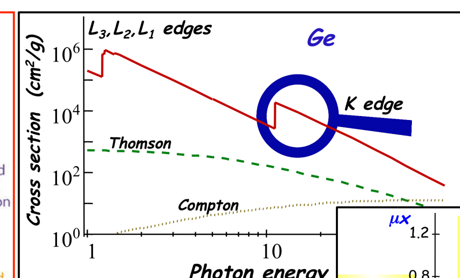

XAFS=XANES+EXAFS

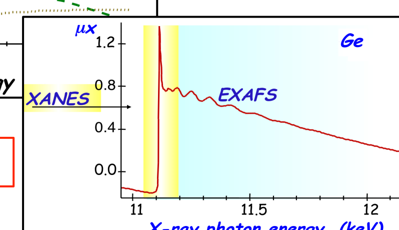

X-ray Absorption Spectroscopy

XAS local sensitive and chemical selective probe
that can provide structural, electronic and magnetic information.

DAFNE-L DXR1 beam line absorption spectroscopy

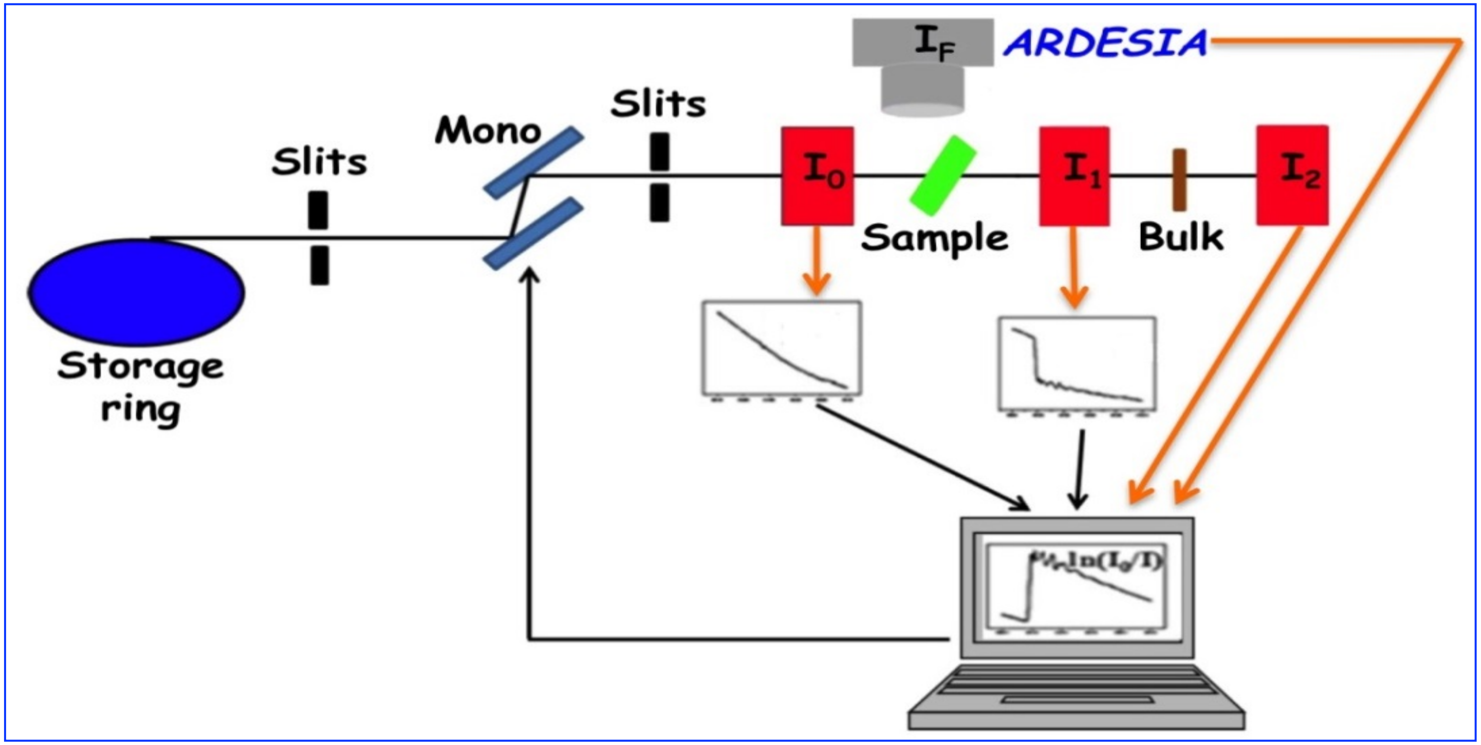

I_0, I_1, I_2 Gas ionization chambers - I_F SDD solid state detector

Photons as Ionizing Radiation

- ***Photoelectric effect***
  - Causes ejection of an inner orbital electron and thus also characteristic radiation (energy of fluorescence lines $E_F \approx Z^2$) as orbital hole is filled
  - Energy of ejected photoelectron: $E_e = h\nu - E_B$

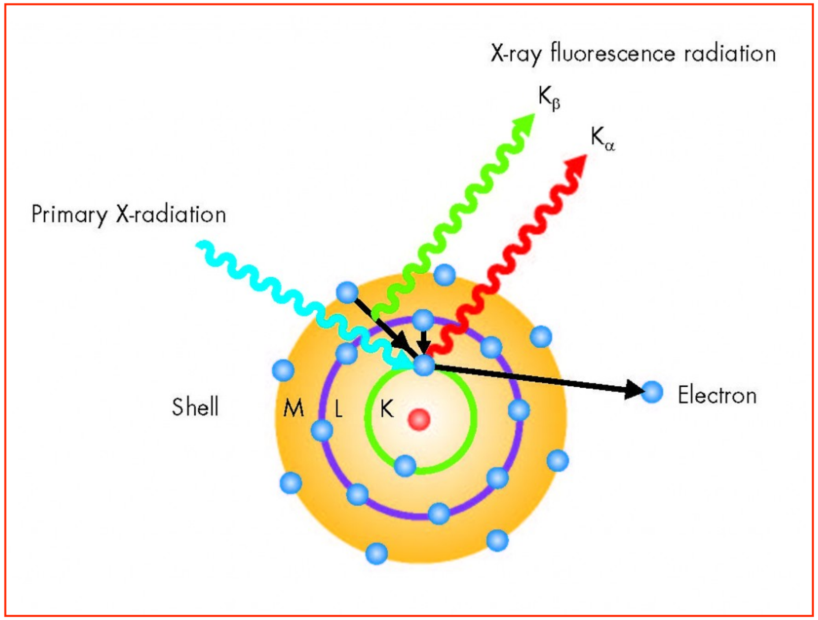

Photoelectric absorption

The probability of a photoelectric interaction is a function of the photon energy and the atomic number of the target atom.
A photoelectric interaction cannot occur unless the incident x-ray has energy equal to or greater than the electron binding energy.

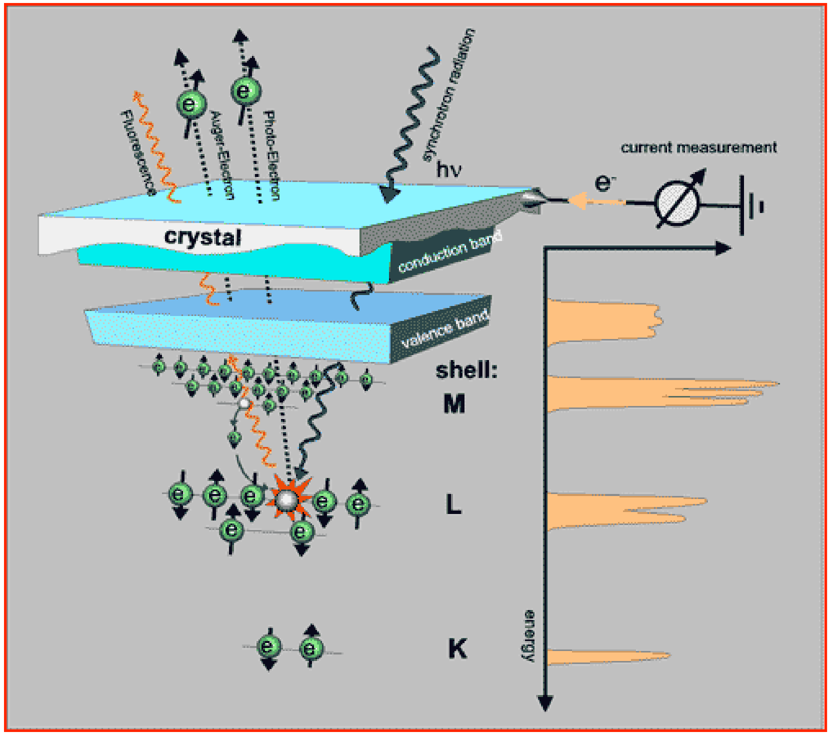

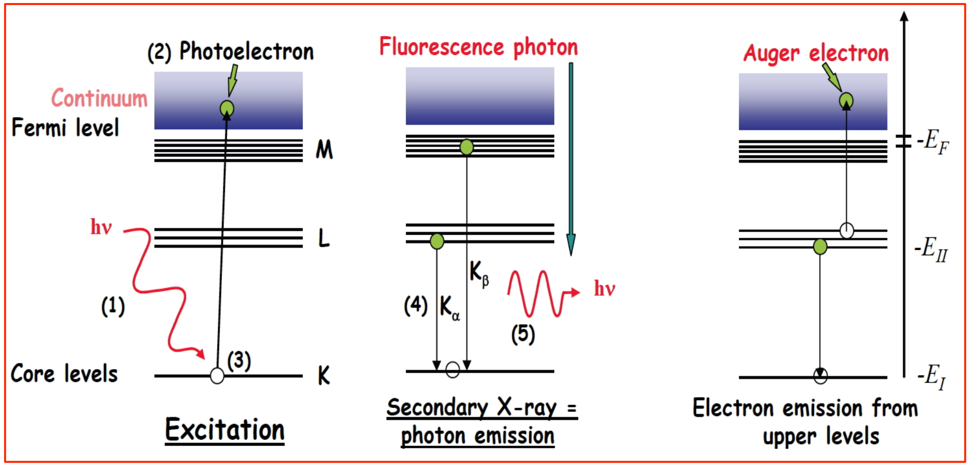

Absorption and decay effects XRF (X Ray Fluorescence) and AES (Auger Electron).

XRF - X Ray Fluorescence Spectroscopy

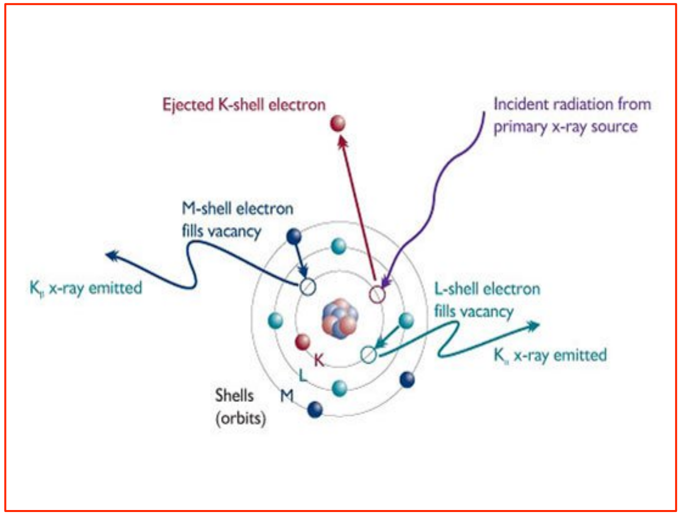

X-ray absorption

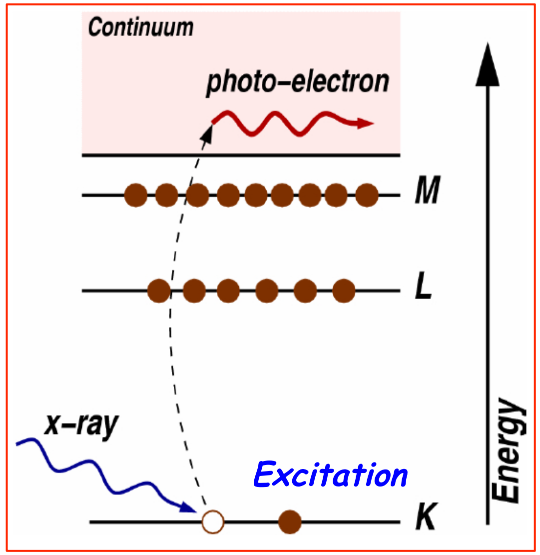

X-ray fluorescence

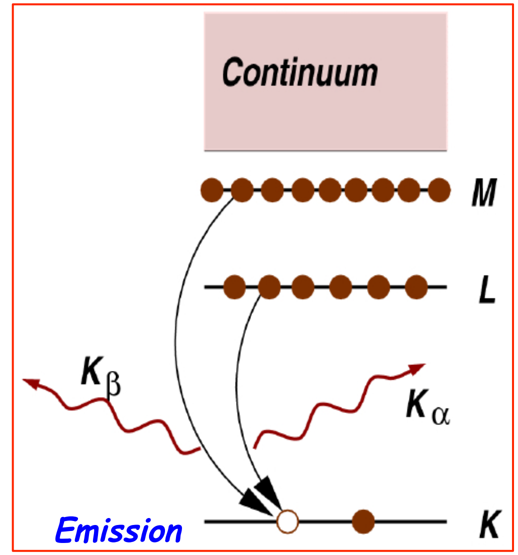

Principle X-ray Fluorescence Emission Lines

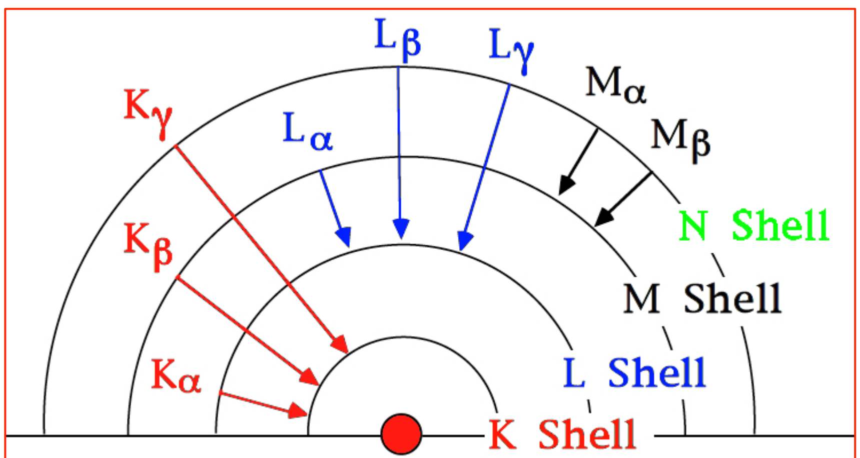

For each atom every shell has a unique energy level determined by the atomic configuration for that element -
Moseley's Law $E \approx Z^2$

X-ray absorption fine structure spectroscopy - XAFS

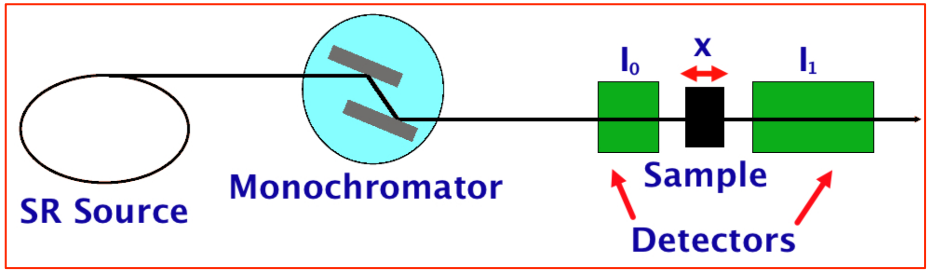

$$I_1 = I_o \exp[-\mu(E)\, x]$$

Exponential attenuation or equation of Beer-Lambert

Attenuation coefficient

$$\mu(E) = \frac{1}{x} \ln\left(\frac{I_0}{I_1}\right)$$

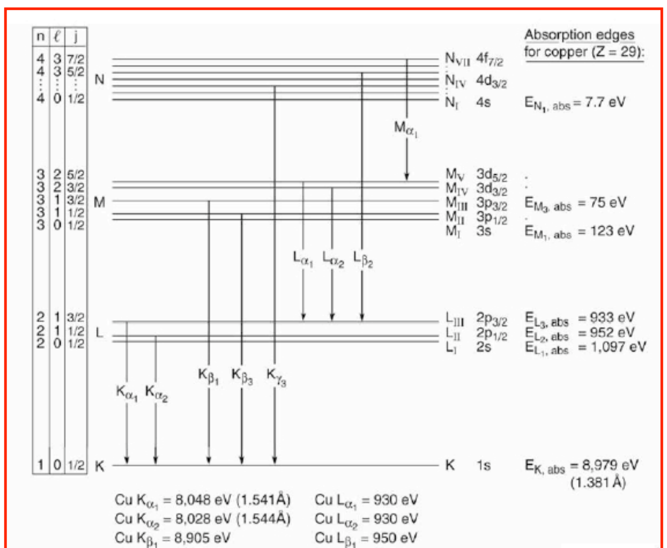

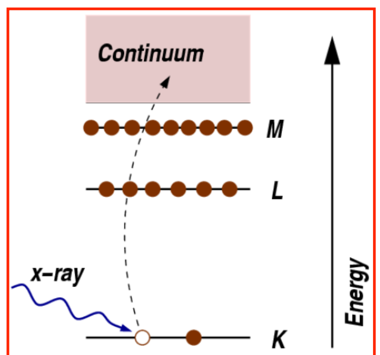

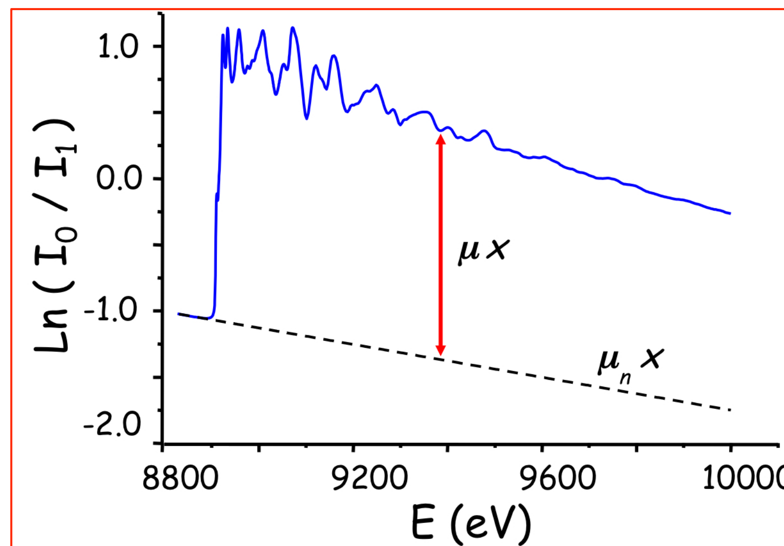

XAFS in transmission or fluorescence geometries

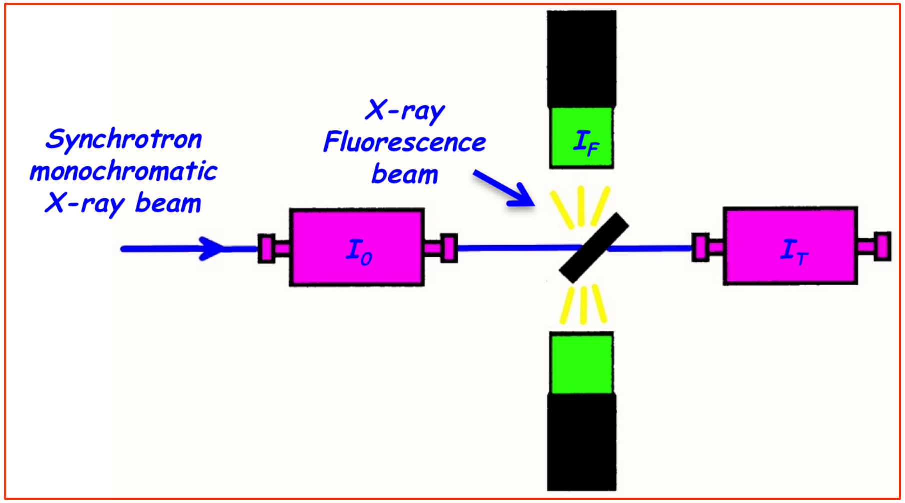

XAFS can be measured either in transmission or fluorescence geometries.
The energy dependence of the absorption coefficient μ(E):

$$\mu(E)x = \ln\left(\frac{I_0}{I_1}\right)$$

Transmission geometry

$$\mu(E)x = \left(\frac{I_F}{I_0}\right)$$

Fluorescence geometry

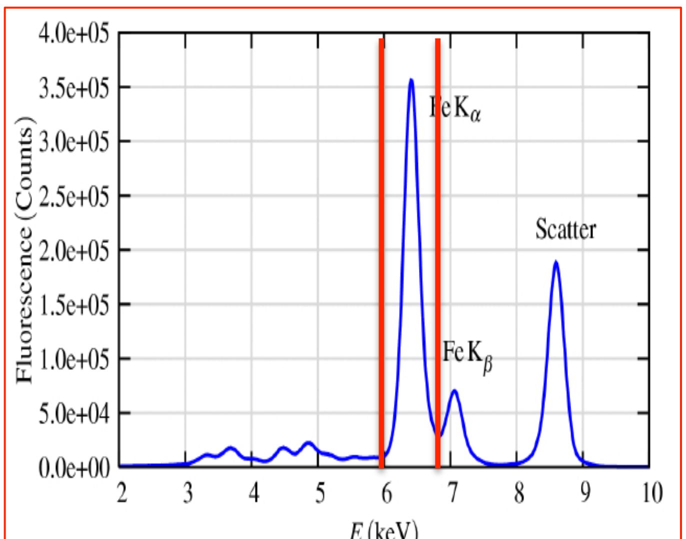

The probability of fluorescence emission is directly proportional to the absorption probability. So in fluorescence mode the variation of the intensity of the fluorescence line as a function of energy gives the XAFS spectra.

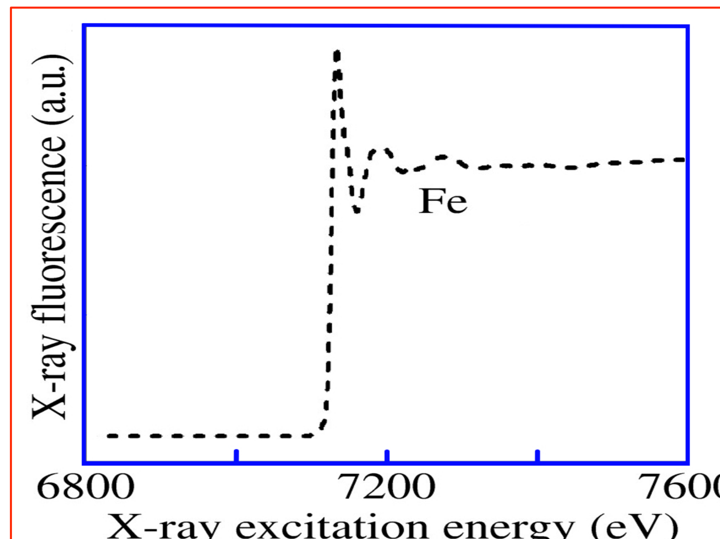

Fermi's golden rule

$$\mu(\omega) = \frac{4\pi n\alpha}{\omega} \sum_f \left| \langle i | d | f \rangle \right|^2 \delta(\hbar\omega + E_i - E_f)$$

α = 1/137 fine structure constant

$E = \hbar\omega + E_i$

Transition probability

INITIAL STATE

$|i\rangle$

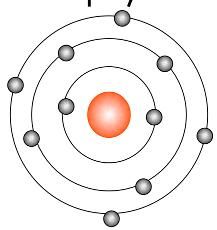

Ground state

INTERACTION

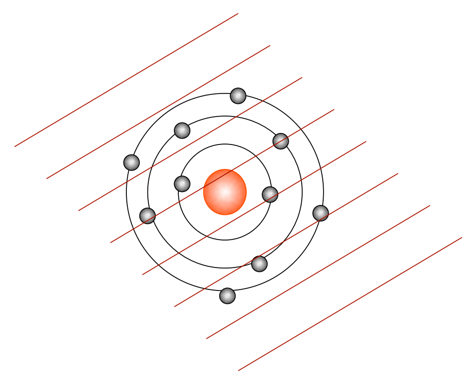

FINAL STATE

$|f\rangle$

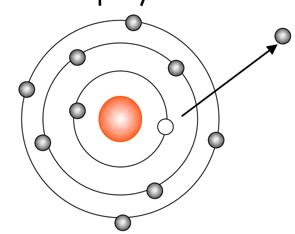

Core hole + excitation or ionization

$$d = \hat{\epsilon} \cdot \vec{r}\, e^{i\vec{k}\cdot\vec{r}} = (\hat{\epsilon} \cdot \vec{r}) + i(\hat{\epsilon} \cdot \vec{r})(\vec{k} \cdot \vec{r}) + \ldots$$

Photon polarisation vector

Wavevector of the Incident plane wave

Electric Dipole Term

Electric Quadrupole Term

d = Interaction Hamiltonian describing the coupling to the X-ray field.

XAFS spectroscopy

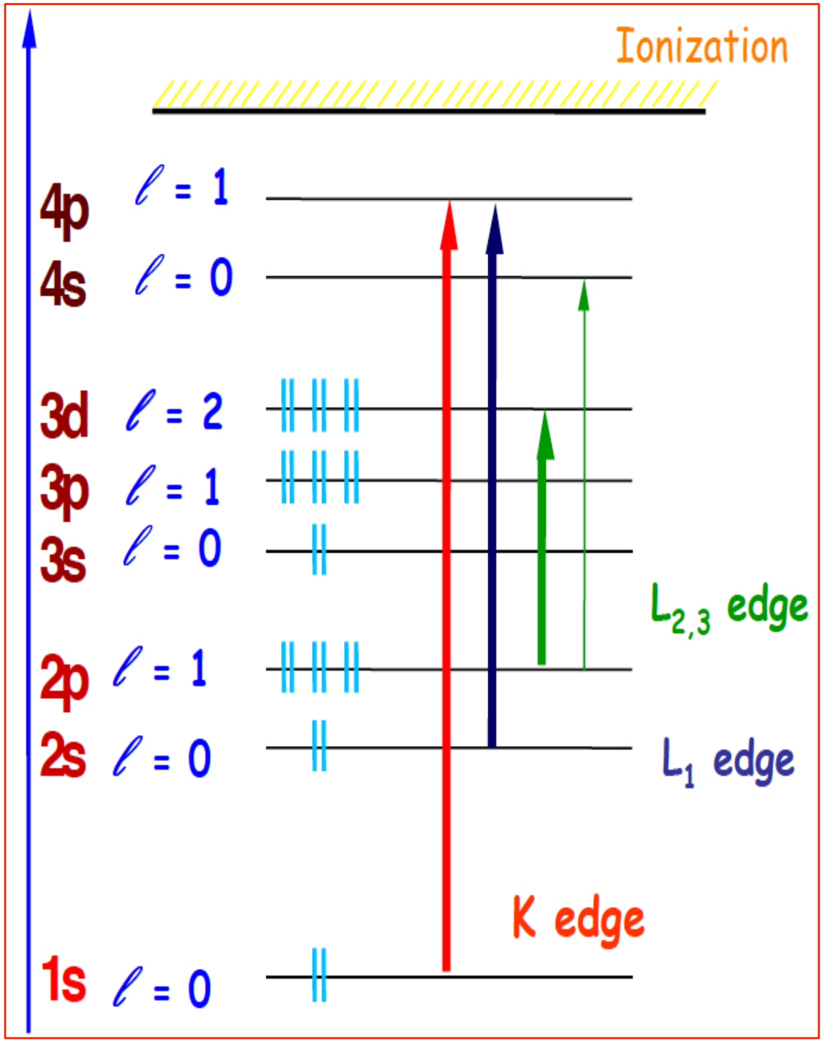

Element specific, angular momentum selective which probes density of unoccupied states.

Selection rules:

Dipole transition $\Delta l = \pm 1$

K edge: 1s → p
L edge: 2s → p, 2p → s,d

Quadrupole transition *(Much weaker)* $\Delta l = \pm 2$

K edge: s → d, p → f

Absorption edges:

1s – **K edge**
2s, 2p – **L edges**
3s, 3p, 3d – **M edges**
4s, 4p, 4d, 4f – **N edges**

XAFS = XANES + EXAFS

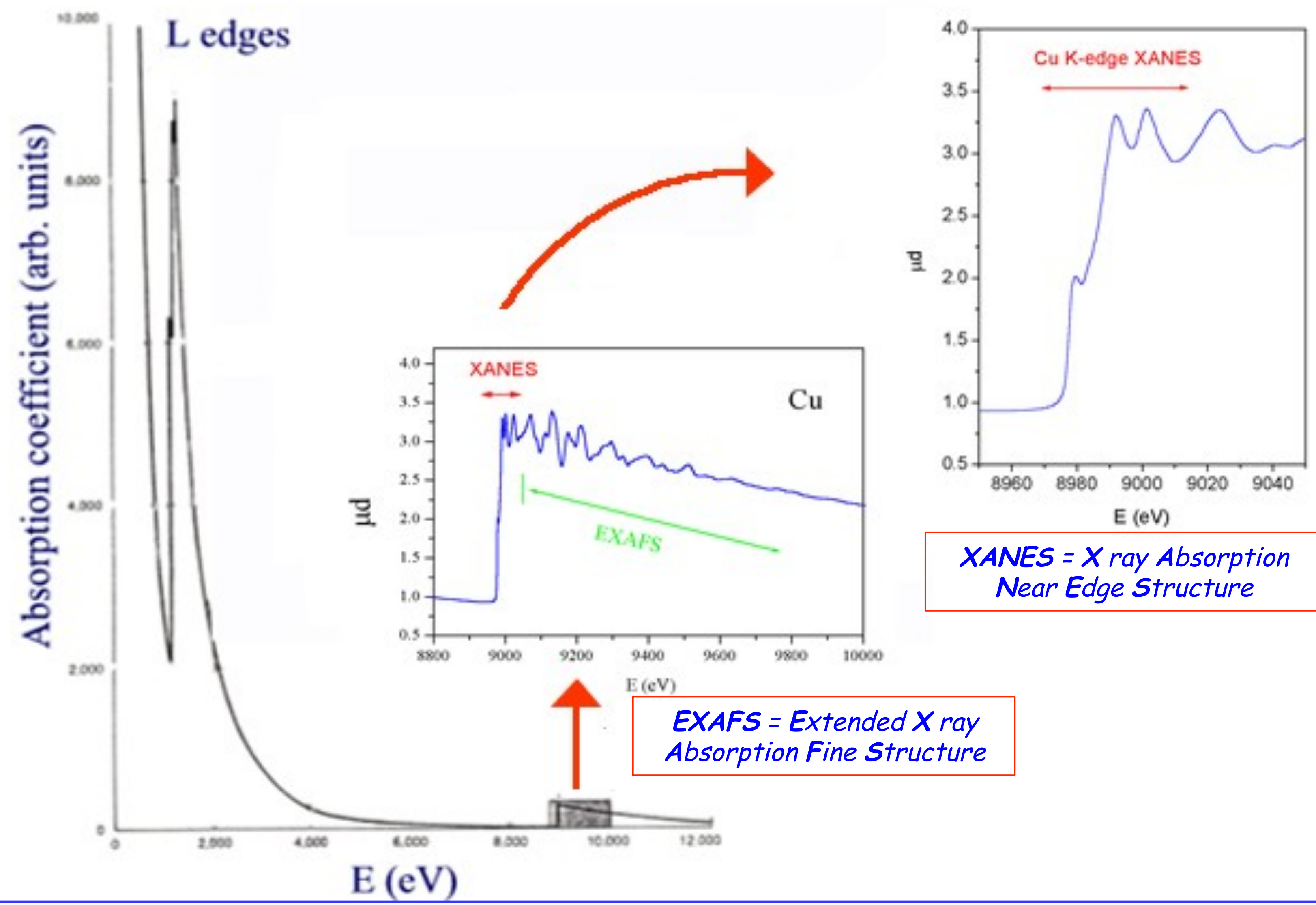

XANES = X ray Absorption Near Edge Structure

EXAFS = Extended X ray Absorption Fine Structure

XAFS and Carbon K edge

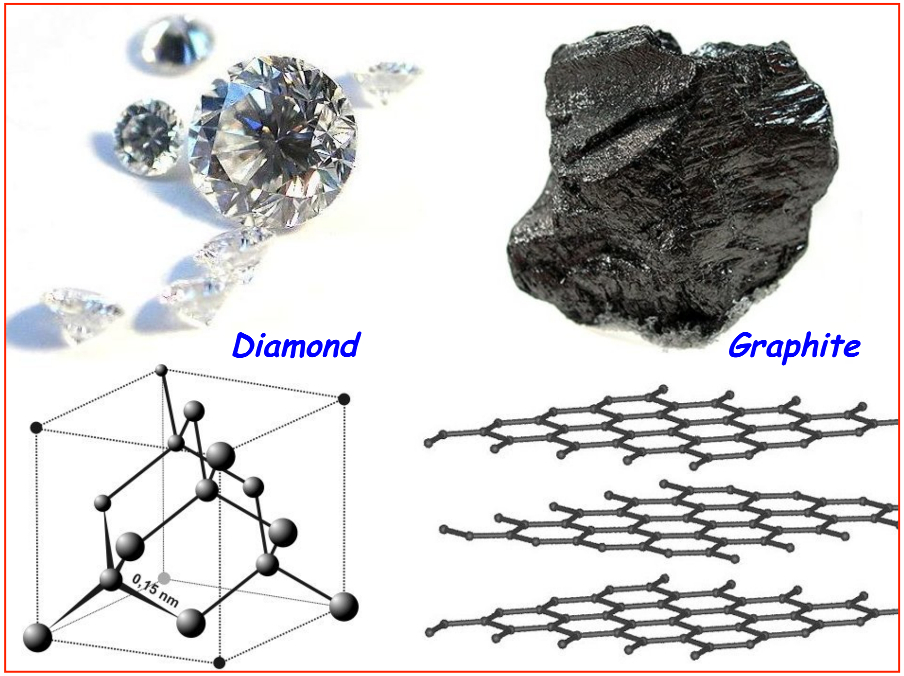

The quite different XAFS spectra of graphite and diamond.

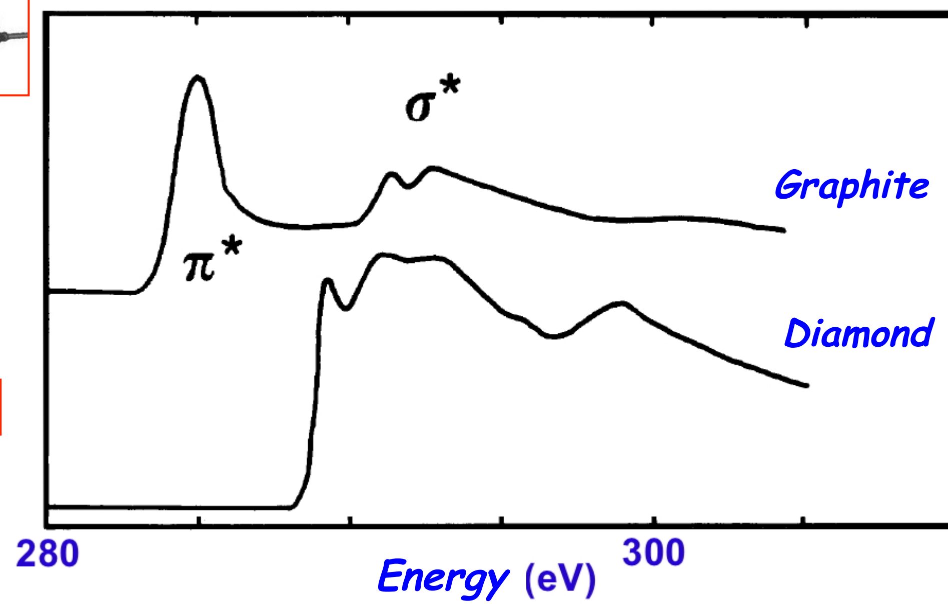

J. Robertson, Prog Solid St. Chem 21, 199 (1991)

EXAFS

Extended X ray Absorption Fine Structure

EXAFS phenomenological interpretation

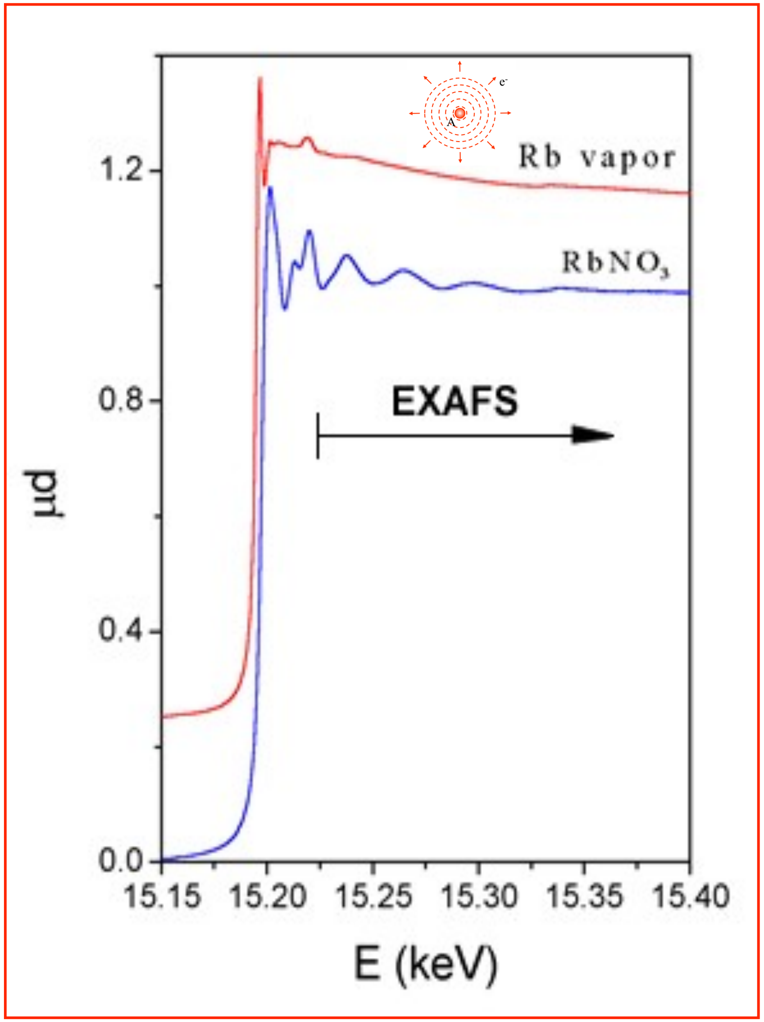

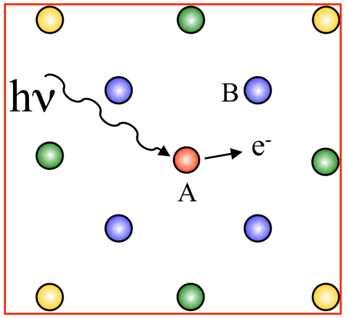

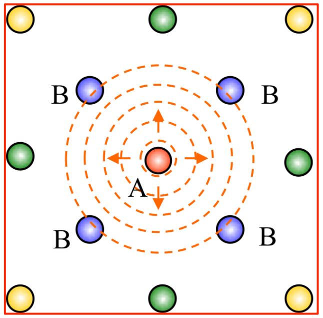

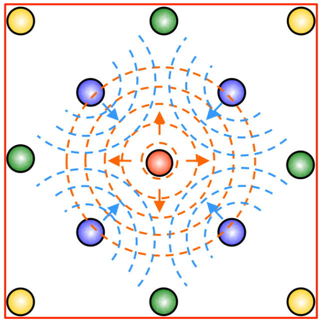

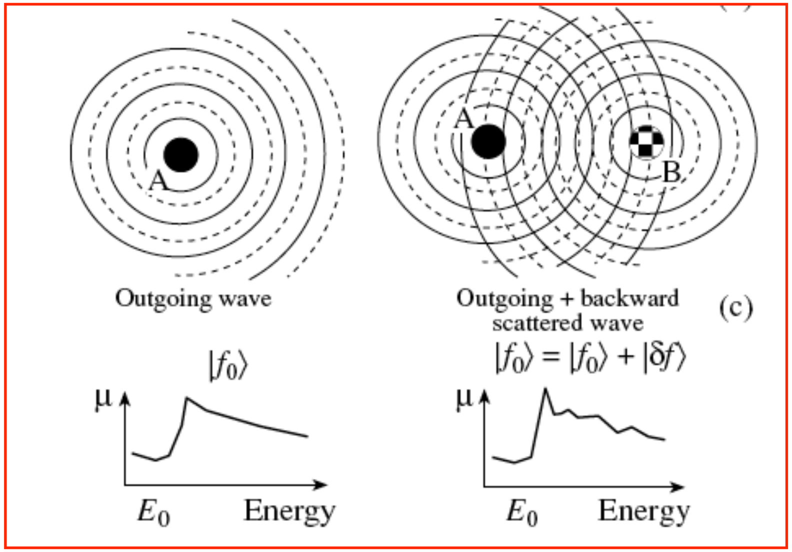

Auto -interference phenomenon of the outgoing photoelectron with its parts that are backscattered by the neighbouring atoms

EXAFS phenomenological interpretation

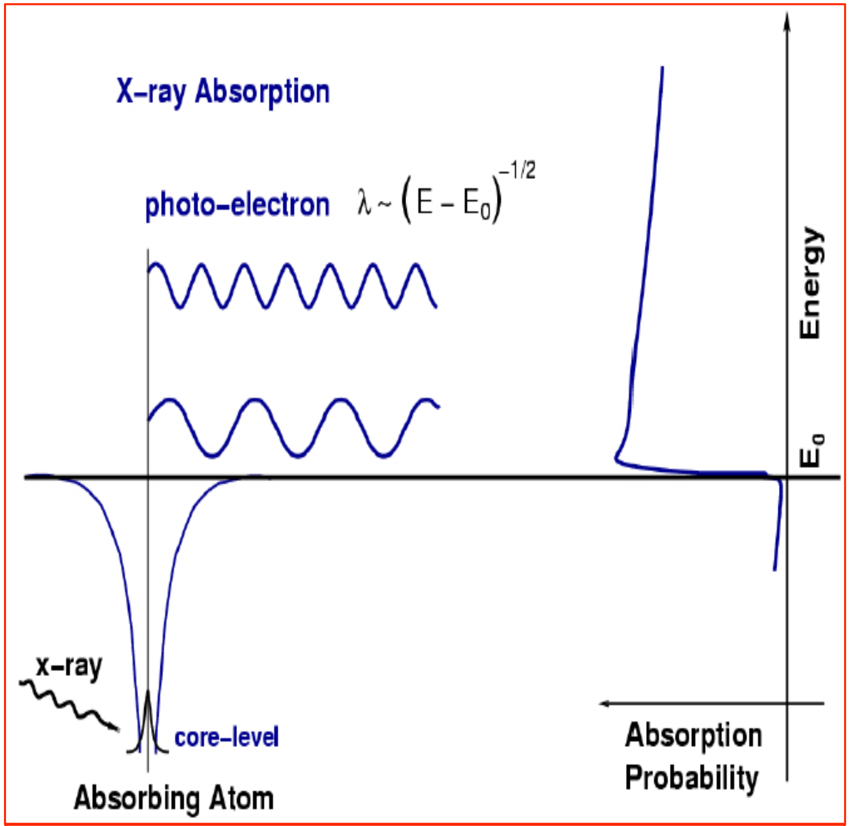

Photoelectric effects in the presence of no scattering atom = a photo-electron is created that travels as a wave with wave number proportional $(E-E_0)^{-1/2}$

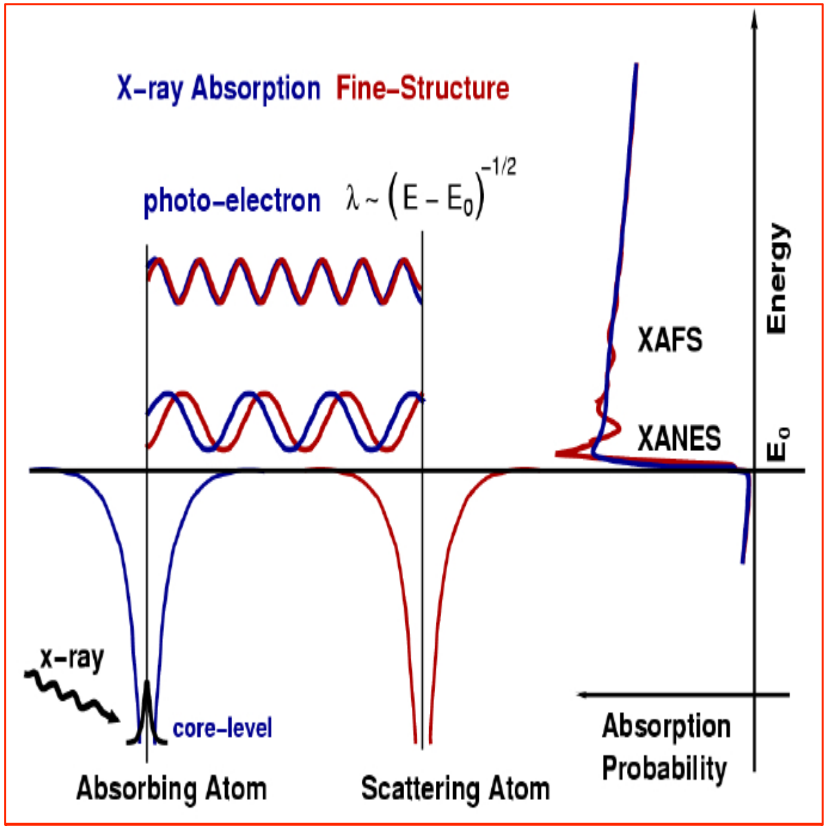

The photo-electron scattered by a neighboring atom can return to the absorbing atom, modulating the amplitude of the photo-electron wave-function at the absorbing atom. This in turn modulates the absorption coefficient μ(E), causing EXAFS.

M. Newville - Fundamentals of XAFS -2004

EXAFS formula

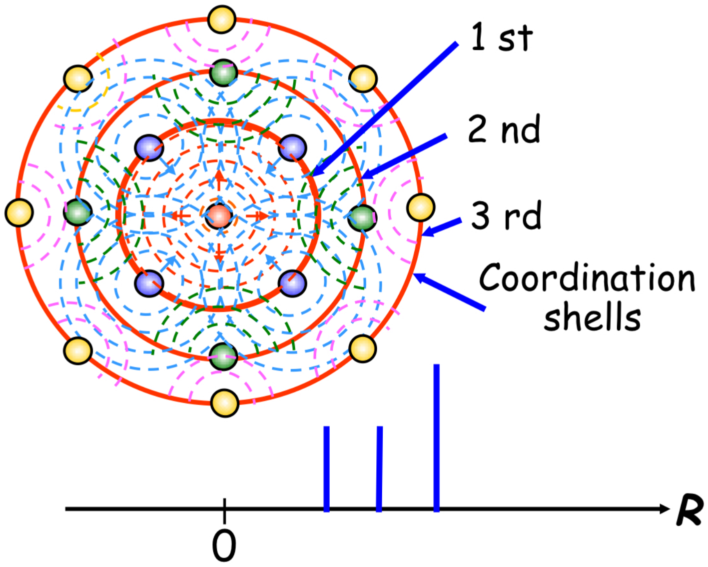

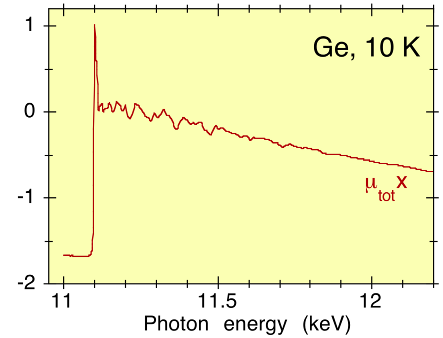

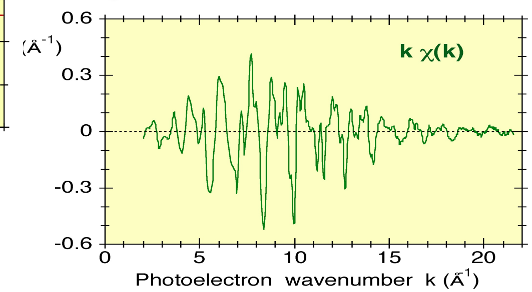

$$\chi(k) = -\frac{S_0^2}{k}\sum_s N_s \frac{\left|f_s(\pi,k)\right|}{R_s^2}\, e^{-k^2/\sigma_s^2}\, e^{-2R_s/\lambda_s}\, \sin\left(2kR_s + \phi_s(k)\right)$$

Coordination number

Debye Waller factor

Interatomic distance

$$k = \sqrt{\frac{2m}{\hbar^2}\left(E - E_0\right)}$$

k = wavenumber

Thermal disorder: e^{-k^2/σ^2}

Electron mean free path: λ

Inelastic scattering effect: S_0^2

EXAFS

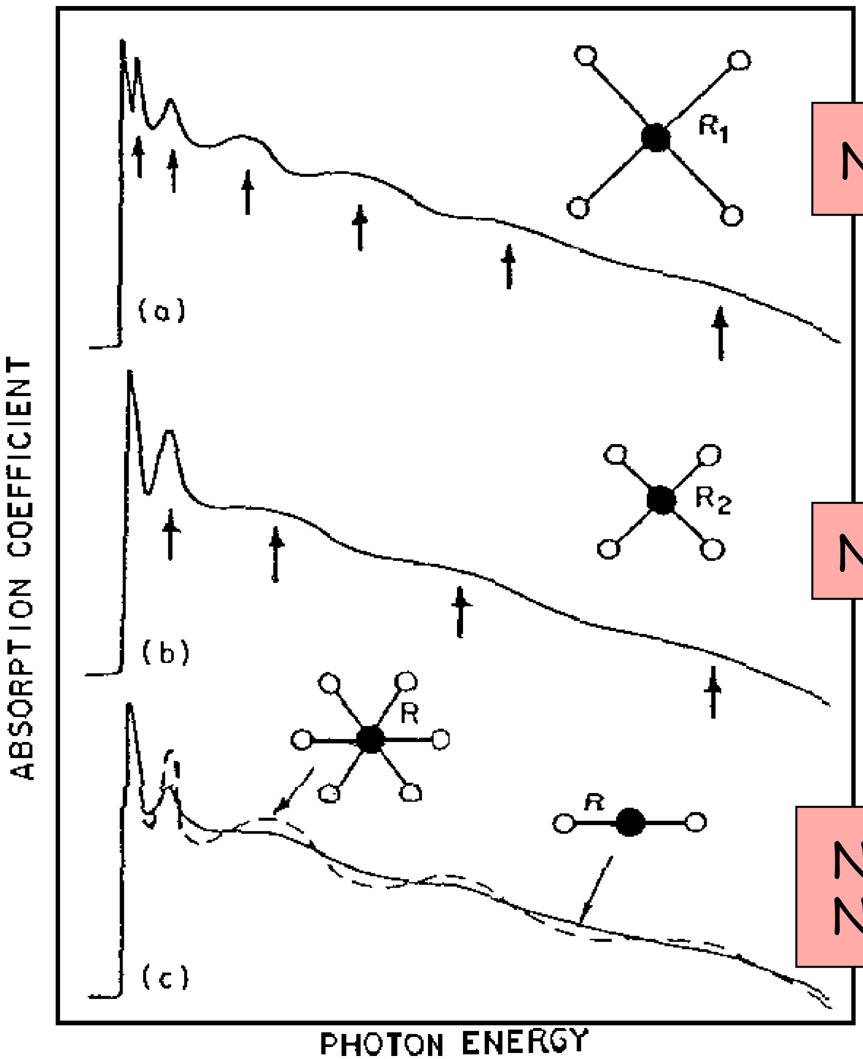

N=4 R=R_1

N=4 R=R_2

N=6 R=R
N=2 R=R

EXAFS and structural information

$$\chi(k) = -\frac{S_0^2}{k}\sum_s N_s \frac{|f_s(\pi,k)|}{R_s^2} e^{-k^2/\sigma_s^2} e^{-2R_s/\lambda_s} \sin\left(2kR_s + \phi_s(k)\right)$$

Coordination number

Debye Waller factor

Interatomic distance

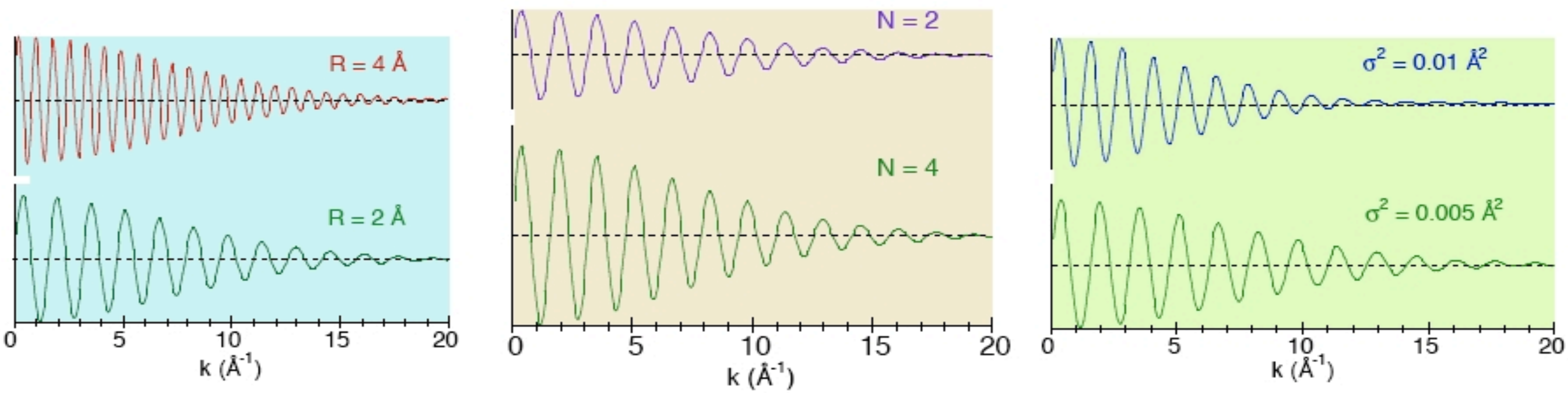

Frequency → Inter-atomic distance — R

Amplitude → Coordination number — N

Damping → Disorder — σ^2

EXAFS data analysis

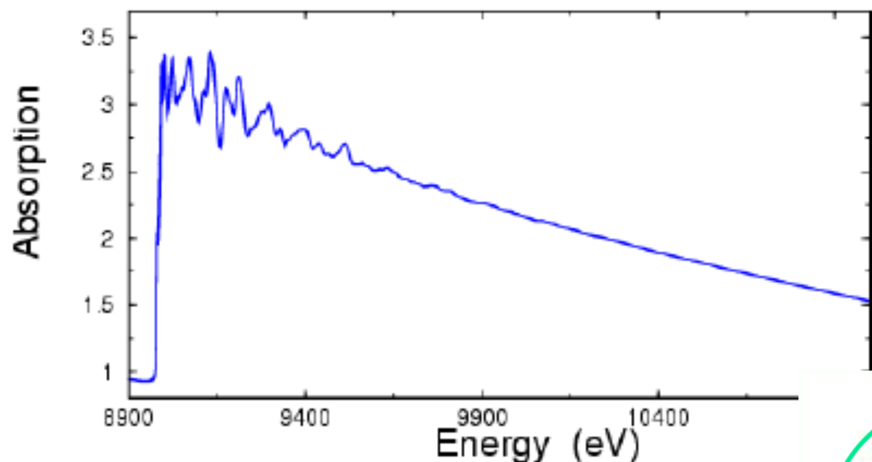

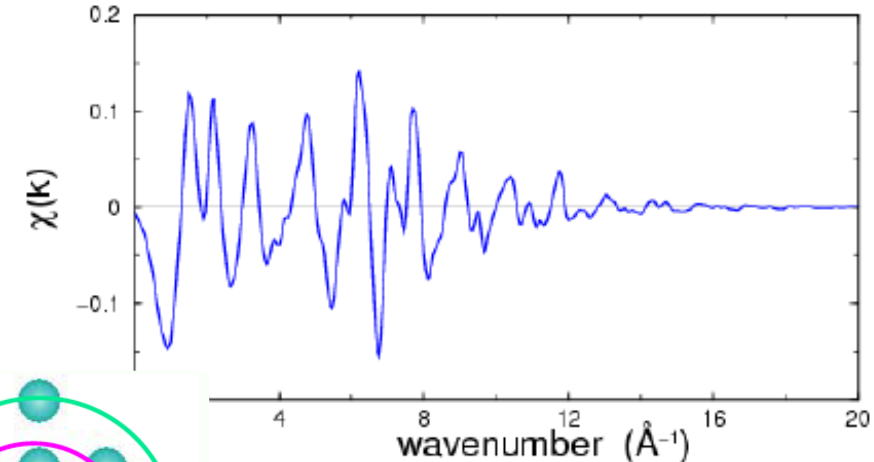

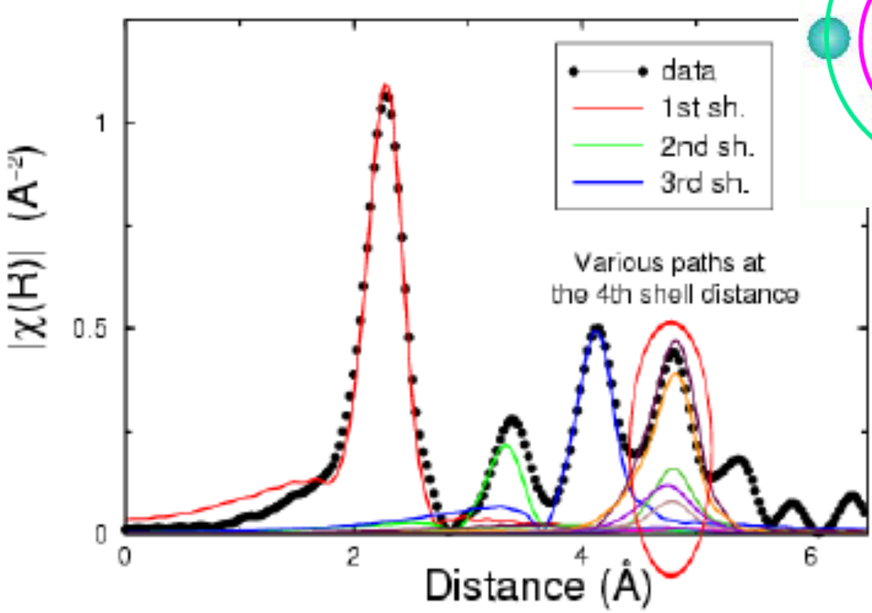

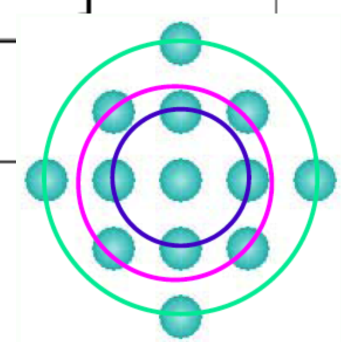

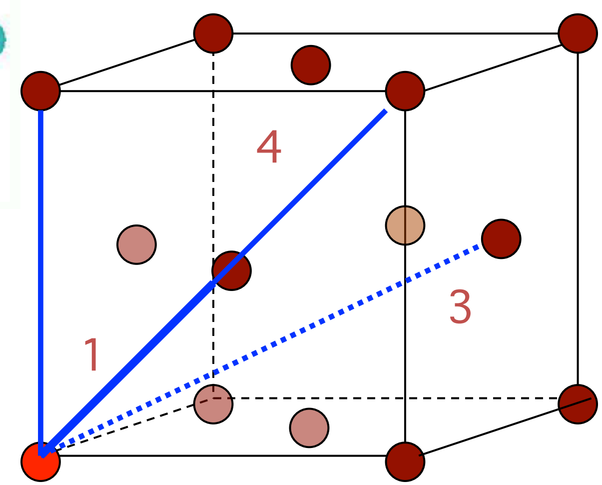

Metallic Copper – FCC or Face Centered Cubic structure.

Cu foil and temperature effects

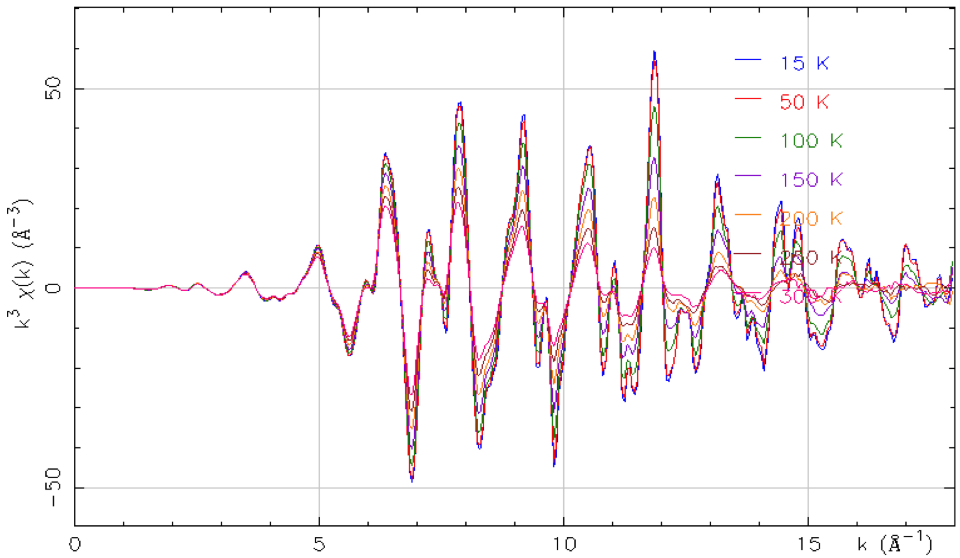

EXAFS spectra as a function of temperature.

Thermal disorder: e^{-k^2/σ^2}

Fourier transforms of the EXAFS spectra.

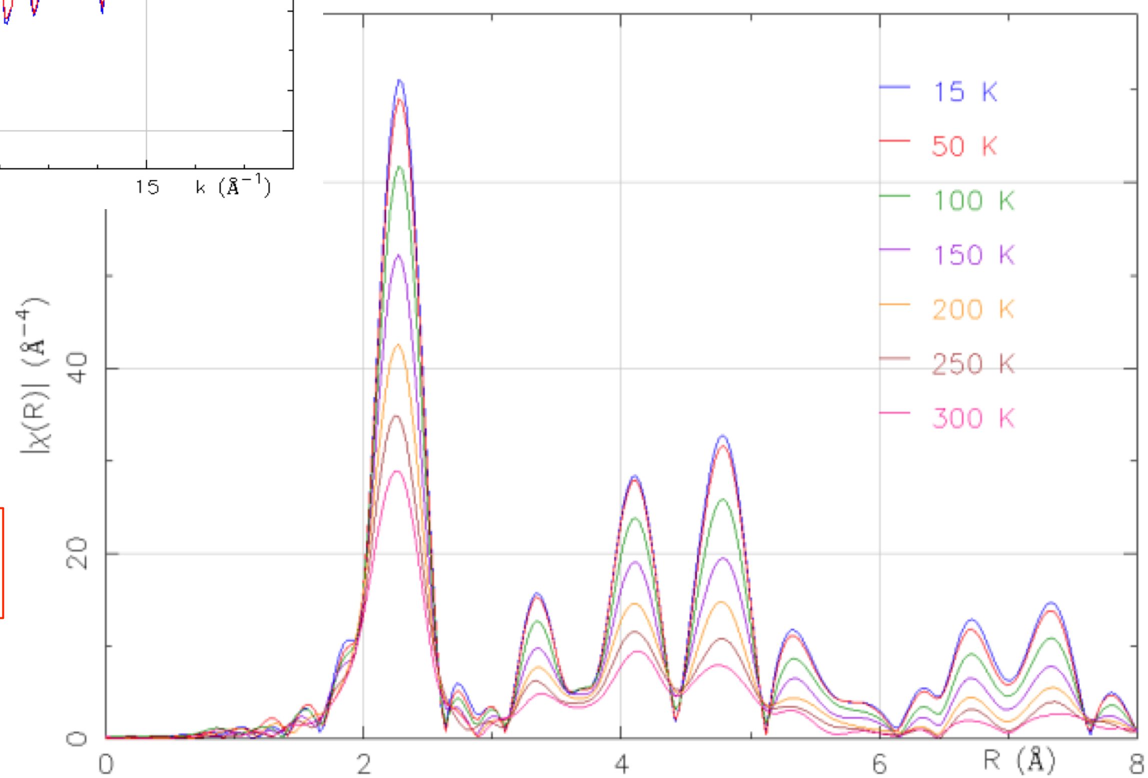

EXAFS data analysis

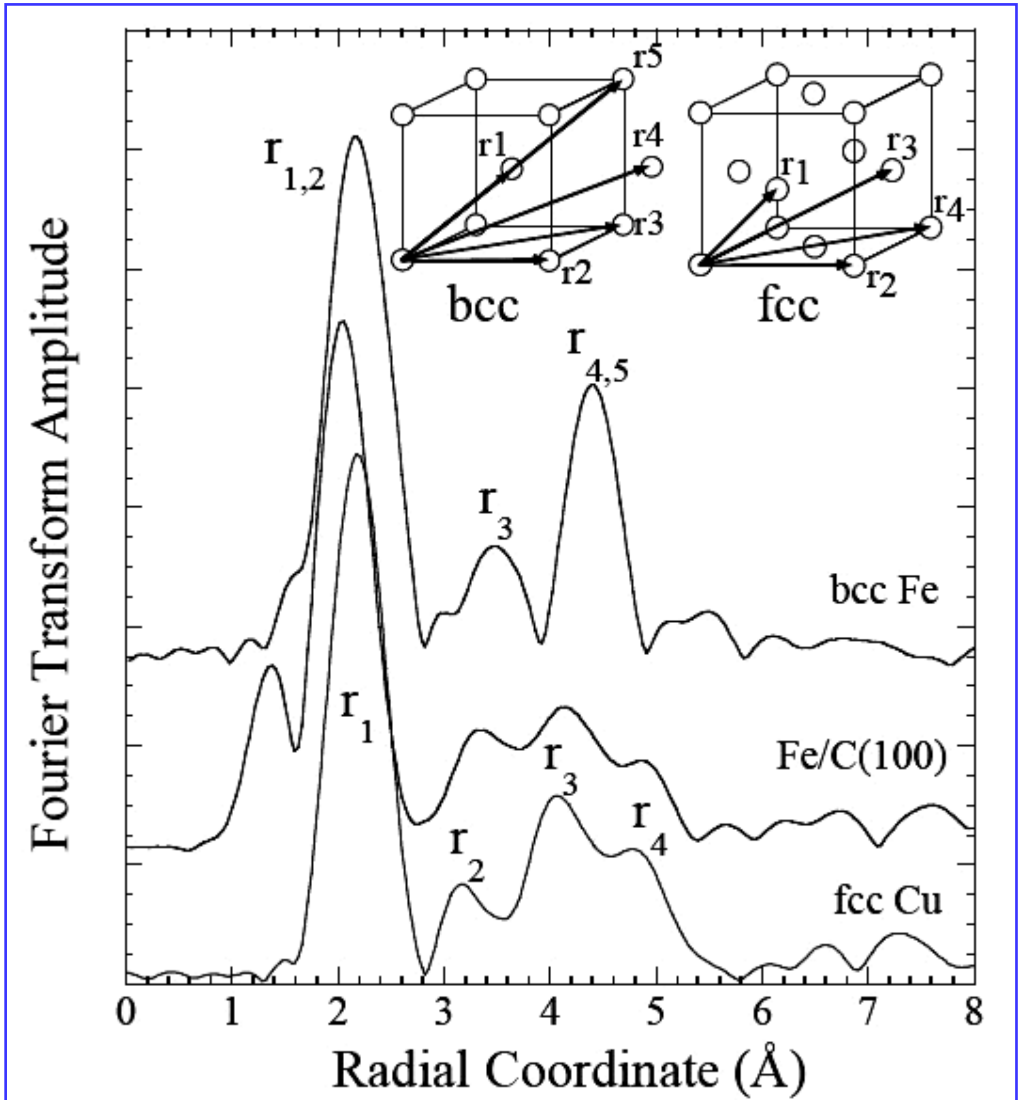

EXAFS data analysis

EXAFS signals

Fourier transforms

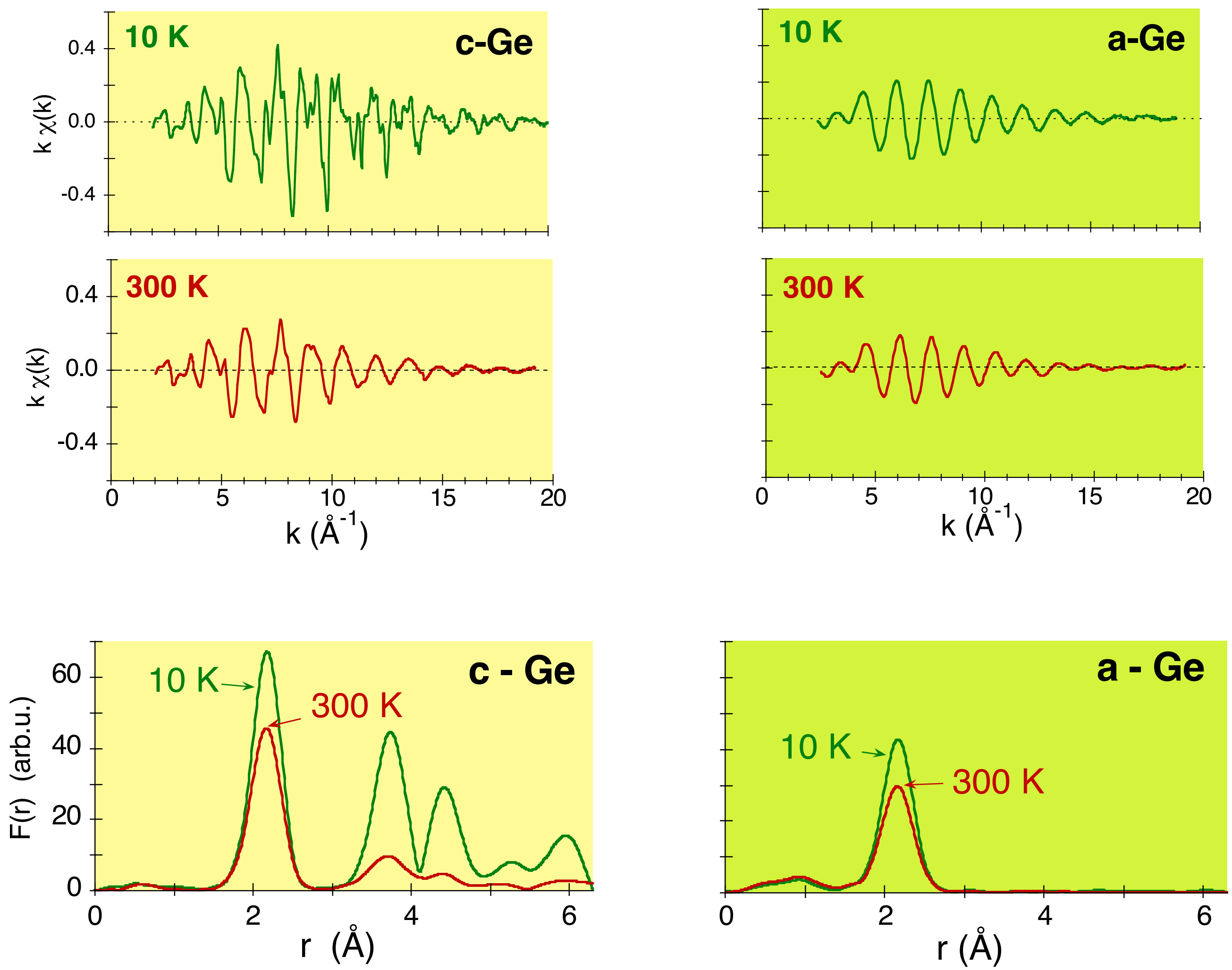

Cu Cu_2O CuO

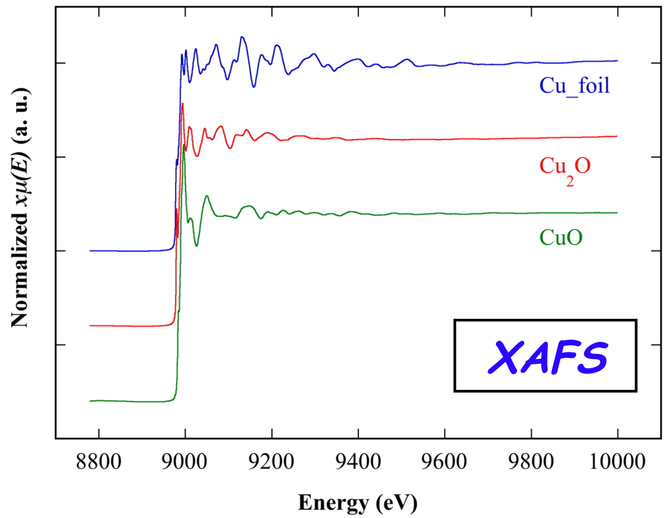

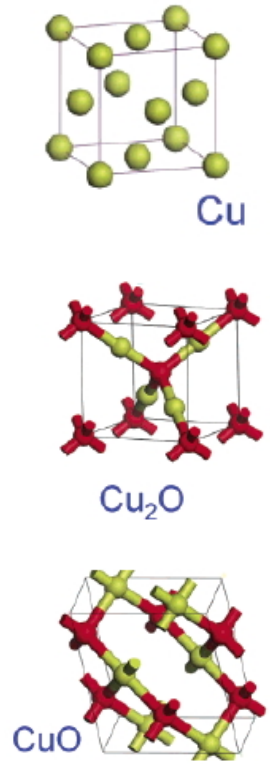

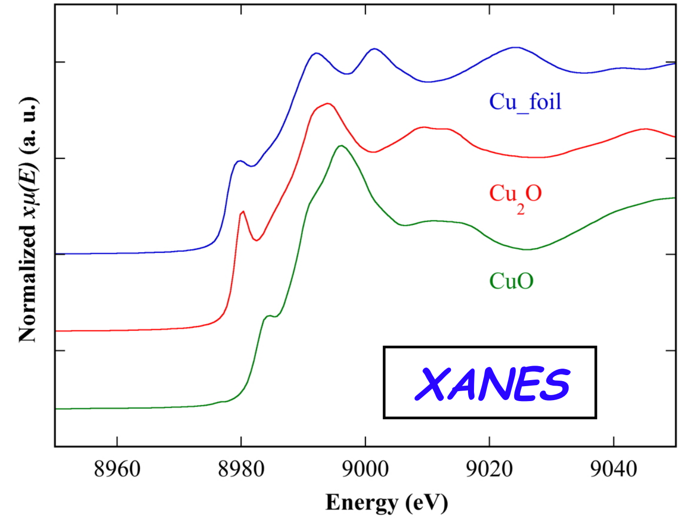

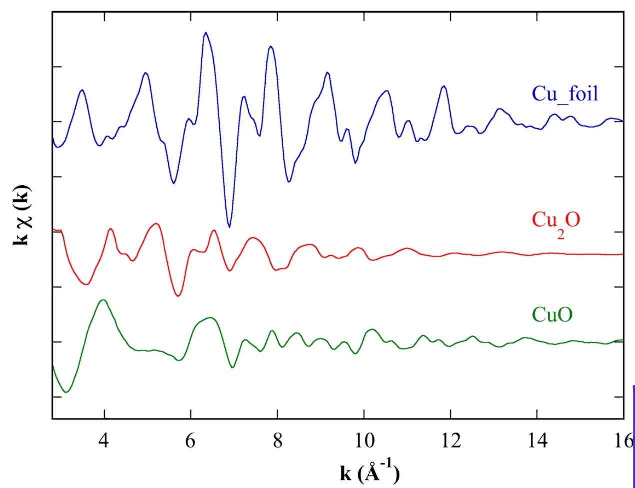

EXAFS

	Cu_2O	CuO
Lattice parameter	Cubic $a = 4.27$ Å	Monoclinic $a = 4.6837$ Å $b = 3.4226$ Å $c = 5.1288$ Å $\beta = 99.54°$
Shortest distances		
$d_{Cu\text{-}O}$	1.84 Å	1.95 Å
$d_{O\text{-}O}$	3.68 Å	2.62 Å
$d_{Cu\text{-}Cu}$	3.02 Å	2.90 Å

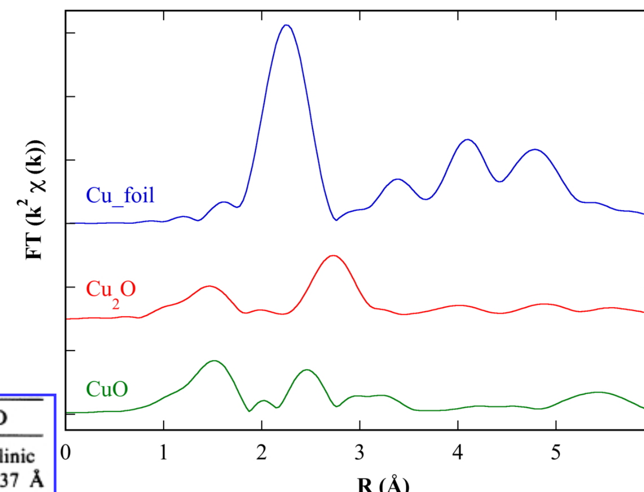

Fourier Transform

Cu metal FCC a= 3.61Å

DXR1 XAFS beamline

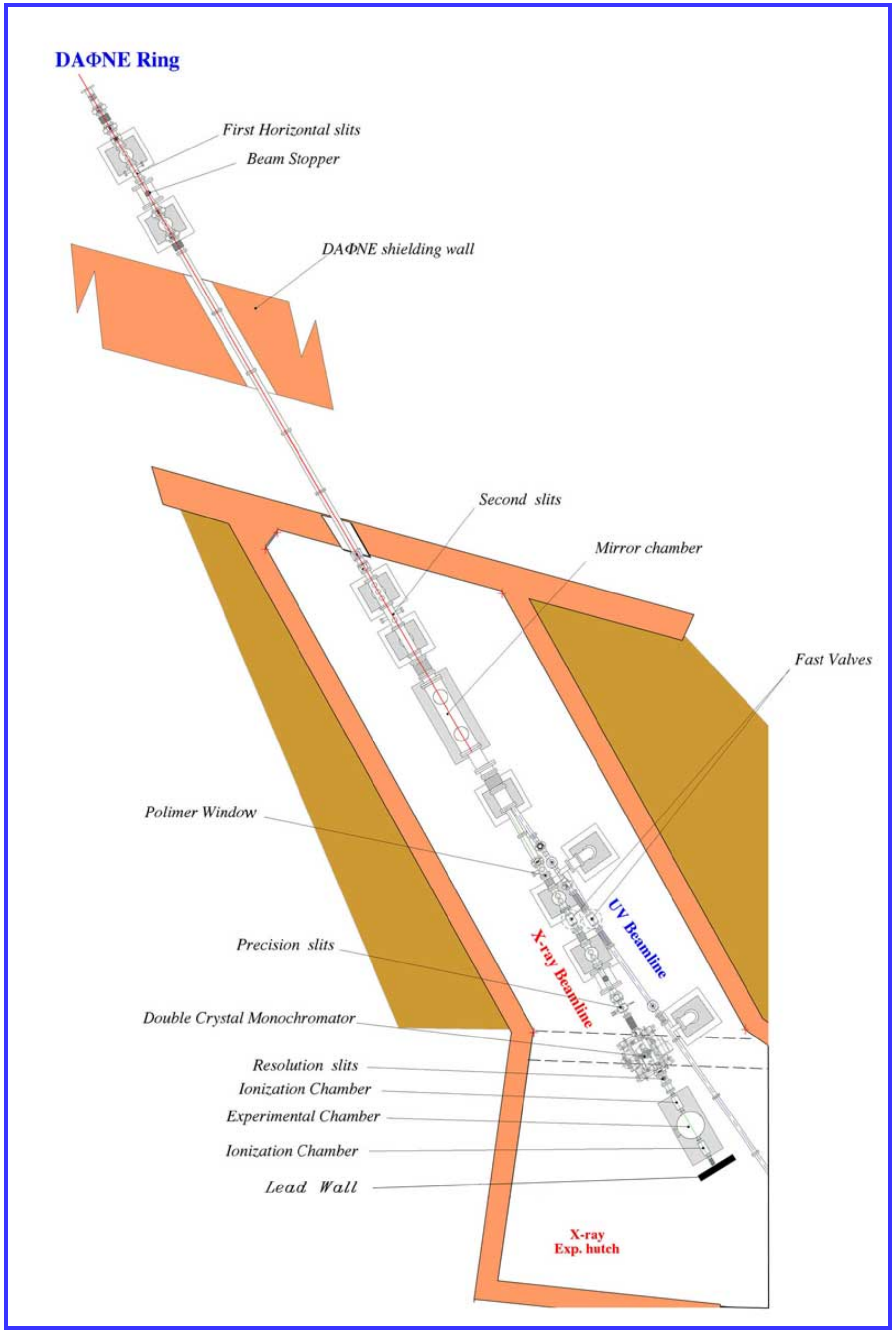

DAΦNE Soft X-ray DXR1 Beamline

- Wiggler soft x-ray beam line
- Critical energy E_c = 284 eV
- Working range 0.9 - 3.0 keV
- TOYAMA double crystal monochromator with KTP (011), Ge (111), Si (111), InSb (111) and Beryl (10-10) crystals
- Soft X-ray absorption spectroscopy and tests of Soft x-ray optics and detectors.

DXR1 Beamline

As a function of the energy range to be used each beamline must be optimized for a particular field of research.
The front end isolates the beamline vacuum from the storage ring vacuum; defines the angular acceptance of the synchrotron radiation via an aperture; blocks (beam shutter) when required, the x-ray and Bremsstrahlung radiation during access to the other hutches.

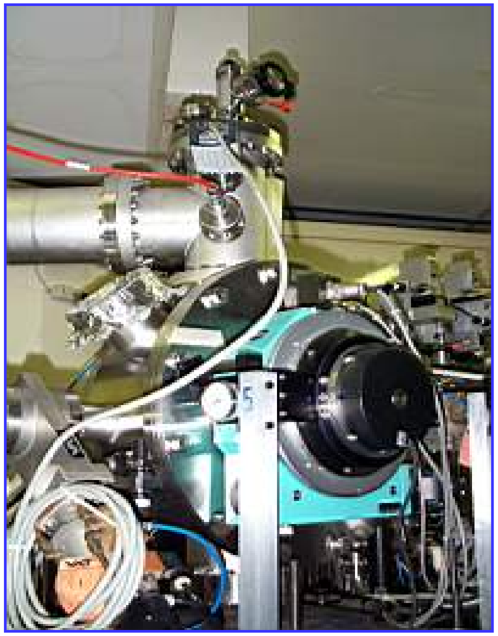

Monochromator

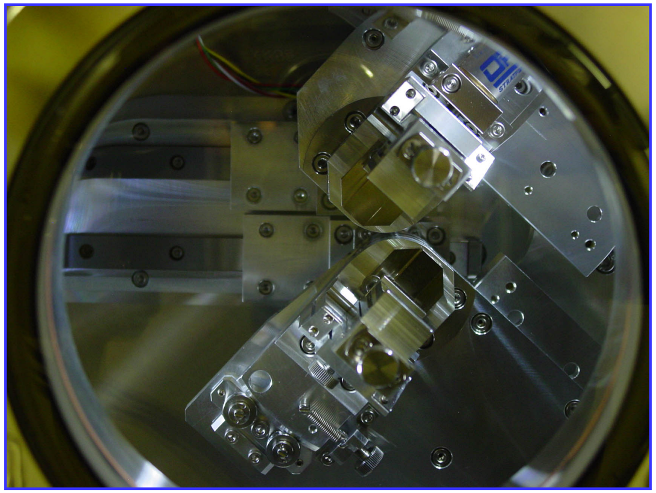

Monochromator

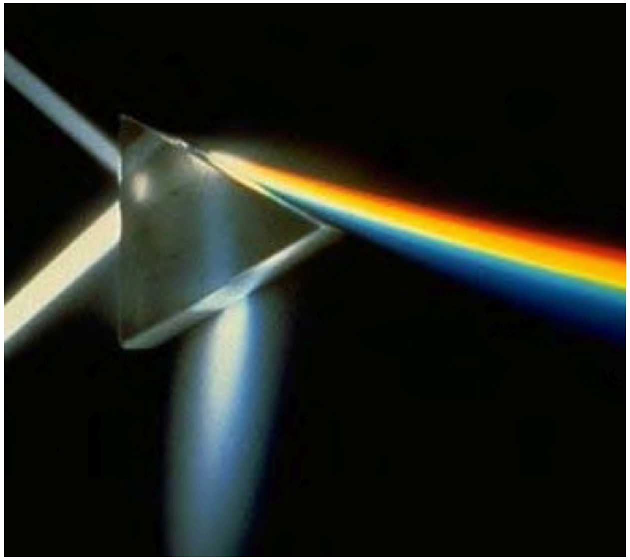

Prism and visible light

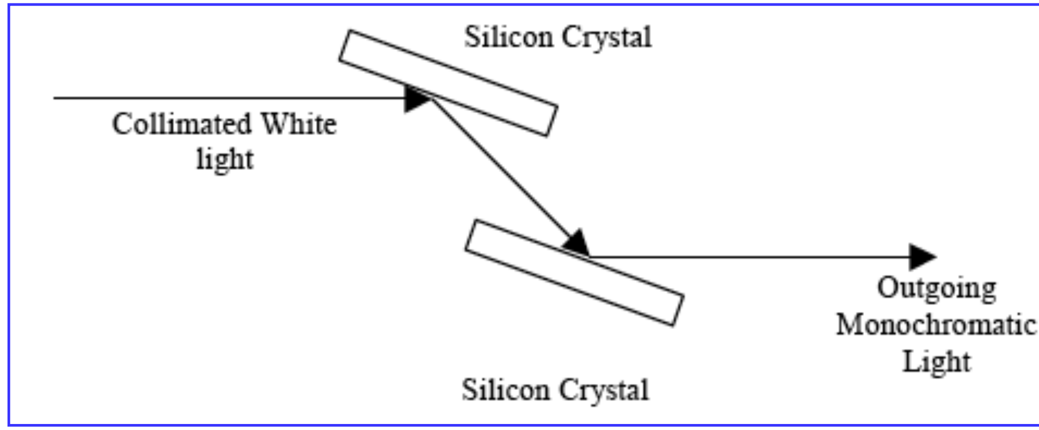

X-rays and crystals

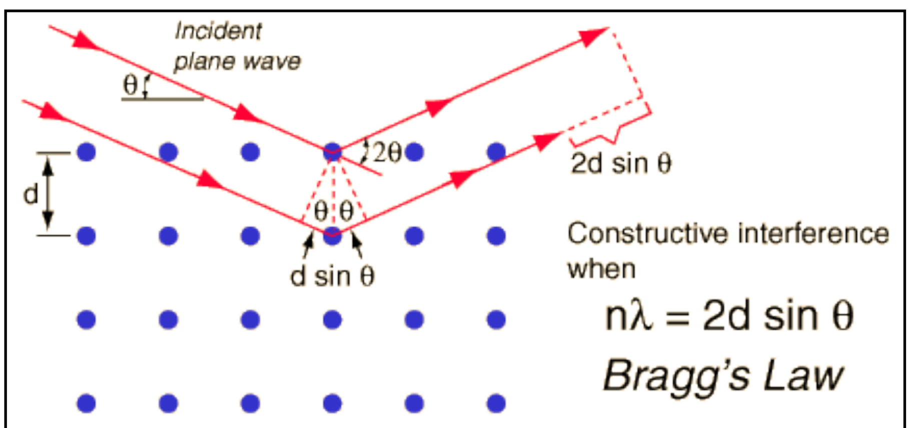

Crystal type	2d spacing (Å)	Energy range (eV)	Absorption edges
Beryl (10-10)	15.954	1000 - 1560	Na K, Mg K, Cu L
KTP (011)	10.950	1200 - 2200	Mg K, Al K
InSb (111)	7.481	1800 - 3100	Si K, P K, S K, Cl K
Ge (111)	6.532	2100 - 3100	P K, S K, Cl K

$$n\lambda = 2d\sin\theta$$

Bragg's Law

Elements that can be investigated

K- edges

L - edges

M - edges

1 H 1.00794																1 H 1.00794	2 He 4.002602
3 Li 6.941	4 Be 9.012182											5 B 10.811	6 C 12.0107	7 N 14.00674	8 O 15.9994	9 F 18.9984032	10 Ne 20.1797
11 Na 22.989770	12 Mg 24.3050											13 Al 26.981538	14 Si 28.0855	15 P 30.973761	16 S 32.066	17 Cl 35.4527	18 Ar 39.948
19 K 39.0983	20 Ca 40.078	21 Sc 44.955910	22 Ti 47.867	23 V 50.9415	24 Cr 51.9961	25 Mn 54.938049	26 Fe 55.845	27 Co 58.933200	28 Ni 58.6934	29 Cu 63.546	30 Zn 65.39	31 Ga 69.723	32 Ge 72.61	33 As 74.92160	34 Se 78.96	35 Br 79.904	36 Kr 83.80
37 Rb 85.4678	38 Sr 87.62	39 Y 88.90585	40 Zr 91.224	41 Nb 92.90638	42 Mo 95.94	43 Tc (98)	44 Ru 101.07	45 Rh 102.90550	46 Pd 106.42	47 Ag 107.8682	48 Cd 112.411	49 In 114.818	50 Sn 118.710	51 Sb 121.760	52 Te 127.60	53 I 126.90447	54 Xe 131.29
55 Cs 132.90545	56 Ba 137.327	57 La 138.9055	72 Hf 178.49	73 Ta 180.9479	74 W 183.84	75 Re 186.207	76 Os 190.23	77 Ir 192.217	78 Pt 195.078	79 Au 196.96655	80 Hg 200.59	81 Tl 204.3833	82 Pb 207.2	83 Bi 208.98038	84 Po (209)	85 At (210)	86 Rn (222)
87 Fr (223)	88 Ra (226)	89 Ac (227)	104 Rf (261)	105 Db (262)	106 Sg (263)	107 Bh (262)	108 Hs (265)	109 Mt (266)	110 (269)	111 (272)	112 (277)		114 (289) (287)		116 (289)		118 (293)

58 Ce 140.116	59 Pr 140.90765	60 Nd 144.24	61 Pm (145)	62 Sm 150.36	63 Eu 151.964	64 Gd 157.25	65 Tb 158.92534	66 Dy 162.50	67 Ho 164.93032	68 Er 167.26	69 Tm 168.93421	70 Yb 173.04	71 Lu 174.967
90 Th 232.0381	91 Pa 231.03588	92 U 238.0289	93 Np (237)	94 Pu (244)	95 Am (243)	96 Cm (247)	97 Bk (247)	98 Cf (251)	99 Es (252)	100 Fm (257)	101 Md (258)	102 No (259)	103 Lr (262)

DXR1 EXAFS examples

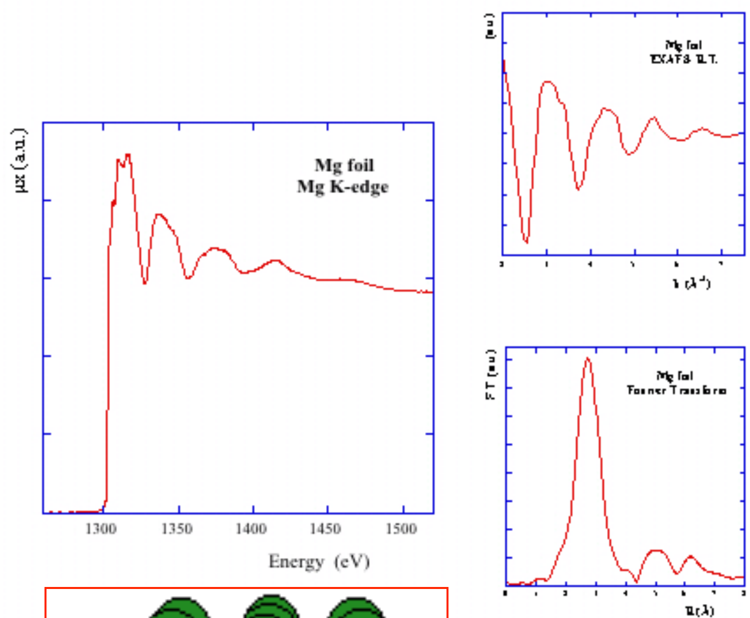

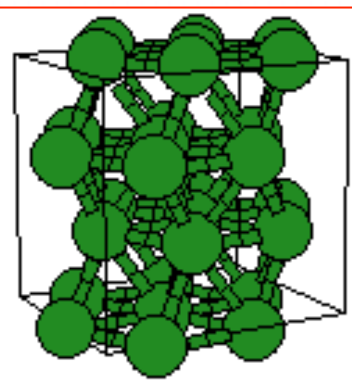

Mg hcp crystal structure

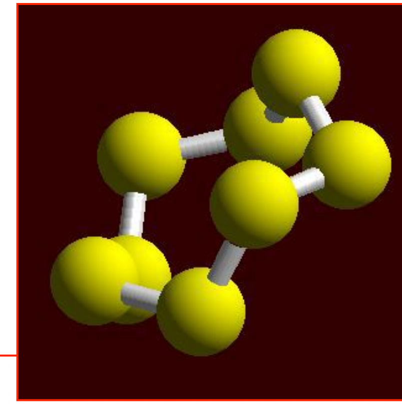

S_8

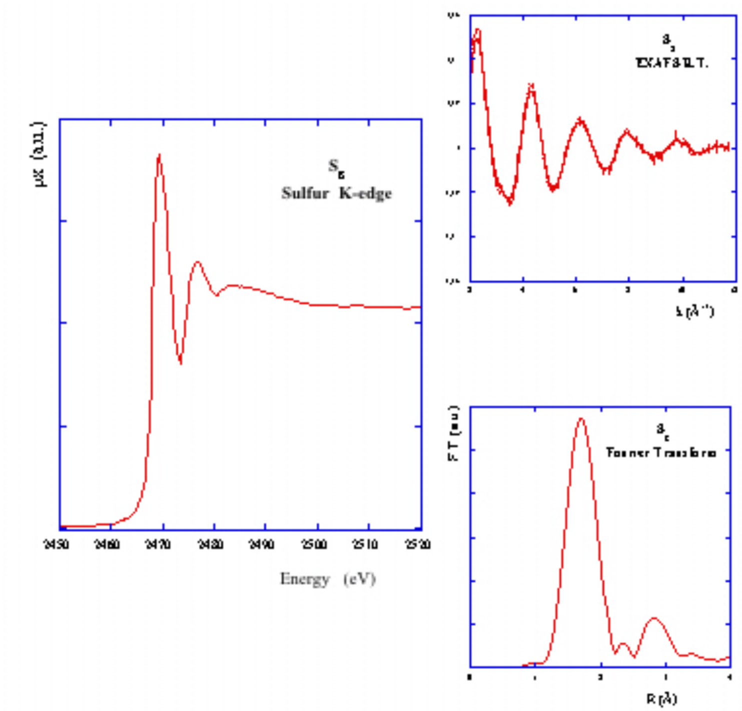

X-ray absorption studies of adducts of gold and ruthenium anticancer metallo-drugs with a serum protein

Due to the ***clinical success of platinum-based anticancer drugs***, much attention has been focused on similar metal complexes of potential use in cancer treatment.

Specifically, a ***great attention has been given to ruthenium and gold complexes that seem to be very promising***. The mechanisms through which the metal complexes produce their biological and pharmacological effects are still largely unexplored and it seems that ***gold and ruthenium complexes act on different targets, most likely on protein targets***.

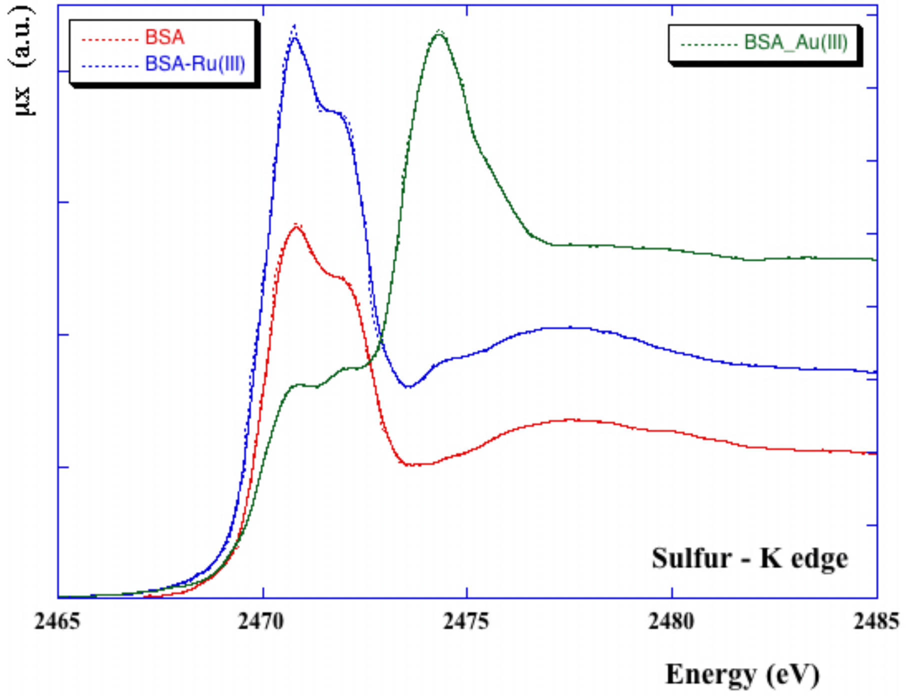

Measurements have been performed at the Sulfur K- edge on **B**ovine **S**erum **A**lbumin (BSA) proteins which have interacted with ruthenium(III) and gold(III) metallo-drugs.

I. Ascone et al., *Exploiting Soft and Hard X-Ray Absorption Spectroscopy to Characterize Metallodrug/Protein Interaction.* ***Inorg. Chem.*** **47**, 8629 (2008)

X-ray detectors

Ionization chambers and SDD

X-ray detectors and basic principles

An X-ray detector is used to convert the energy released by an X-ray photon in the detector material into an electric signal.

The readout and processing of this electric signal by means of a suitable electronics chain can be used to achieve different information including for specific detectors the energy released by the photon and the arrival time of the event.

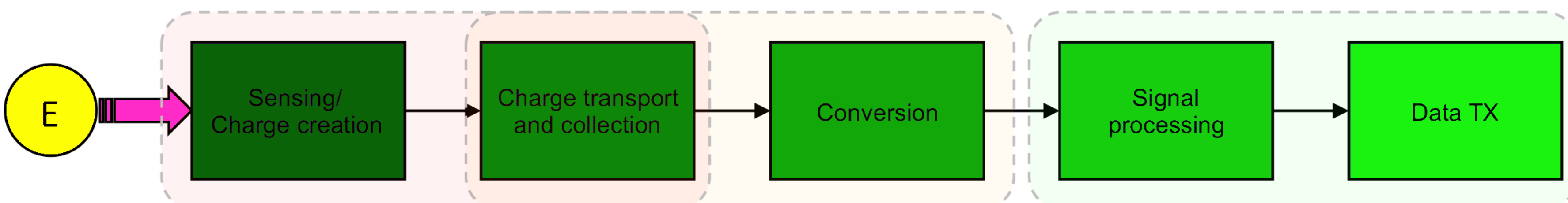

Signal generation and transfer of energy

- *Detection principles mostly used in SR detectors can be direct or not. Direct detection mode using gas or semiconductors*
- *Using gases: electron ion pairs are produced*
- *Using semiconductors: electron hole pairs are produced*
- *Pair creation energy in semiconductors is much lower than ionization energy in gases (Si 3.6 eV; Argon gas 26 eV)*
- *High density of solids implies high interaction probability*
- *The detector to choose depends on the information needed and provided by the detection system*

X ray detectors taken into account

Ionization chambers

Current (= flux) operation mode

Sum the charge generated from stopped X-rays and subsequently digitize it.

SDD

Energy dispersive operation mode

Charge pulses production whose height is directly proportional to the energy of the incident X-ray

Detector chosen as a function of the required information.

General properties:

- *Quantum detection efficiency:* fraction of photons emitted by the source that interact with the detector and are completely absorbed.
- *Count rate*
- *Noise*
- *Energy resolution*

Gas ionization chambers

Visualisation of ion chamber operation

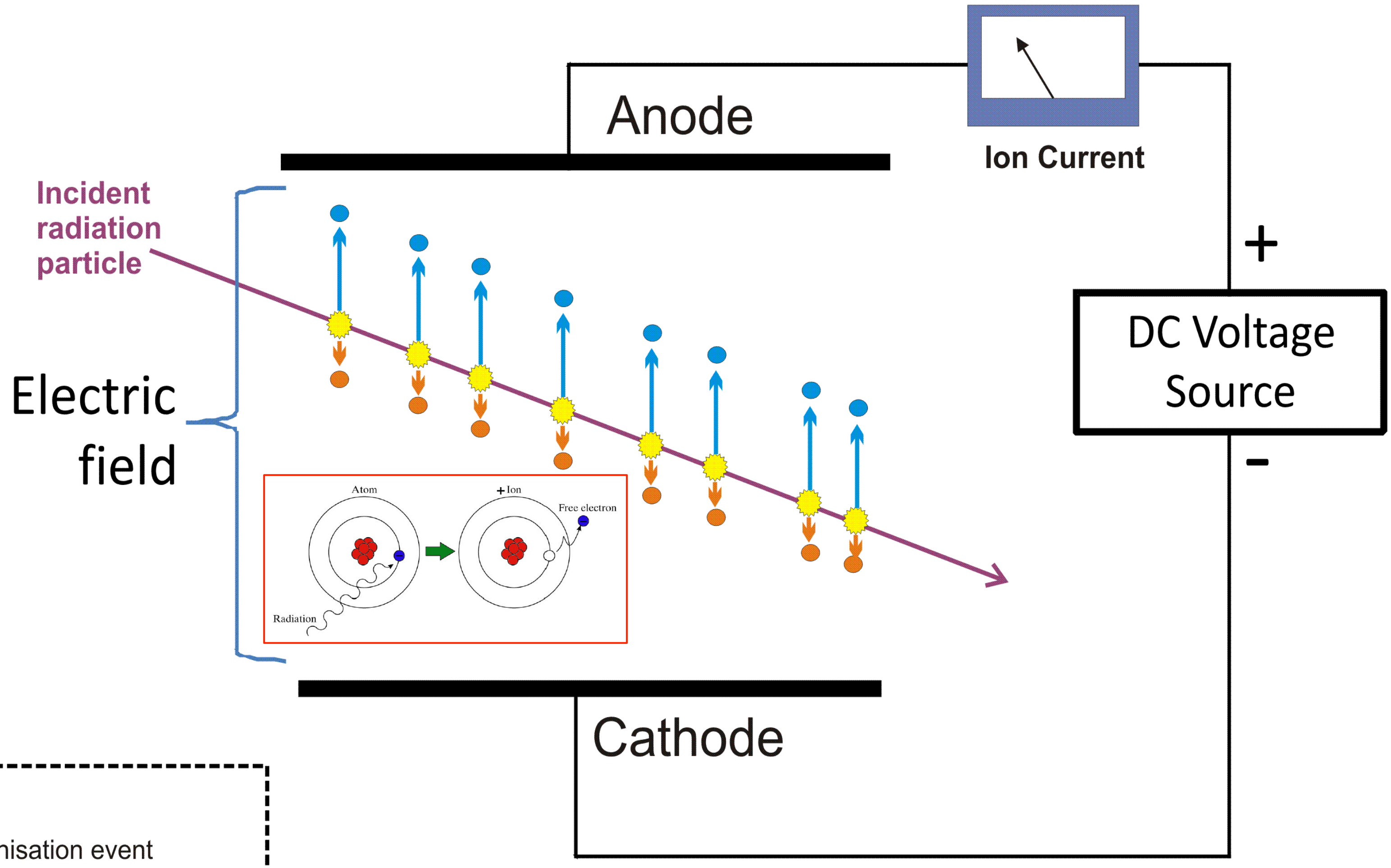

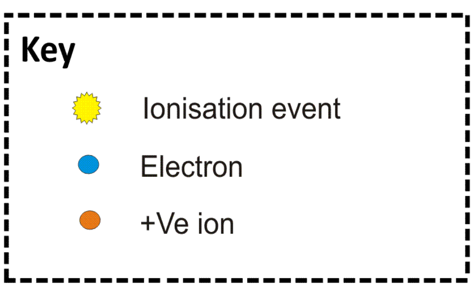

Schematic diagram of parallel plate ion chamber, showing drift of ions. Electrons typically drift 1000 times faster than positive ions due to their much smaller mass.
Credit: Wikipedia – Dougsim

X-ray Ion Chamber

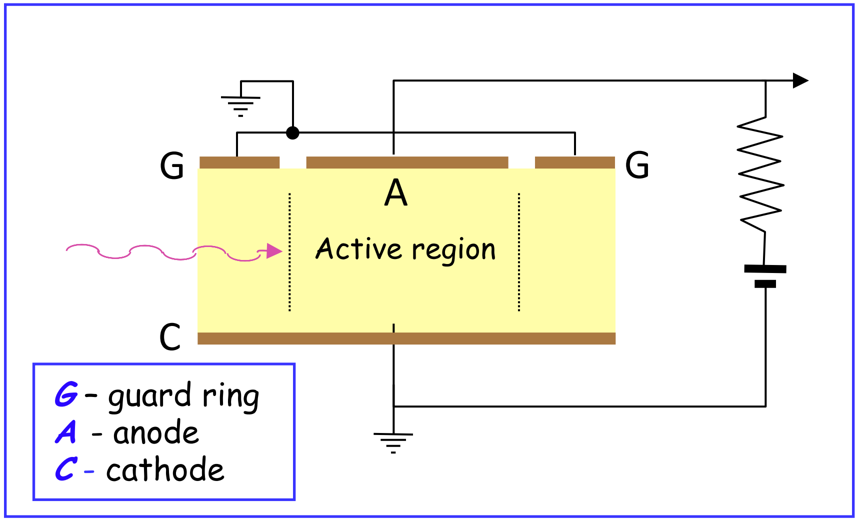

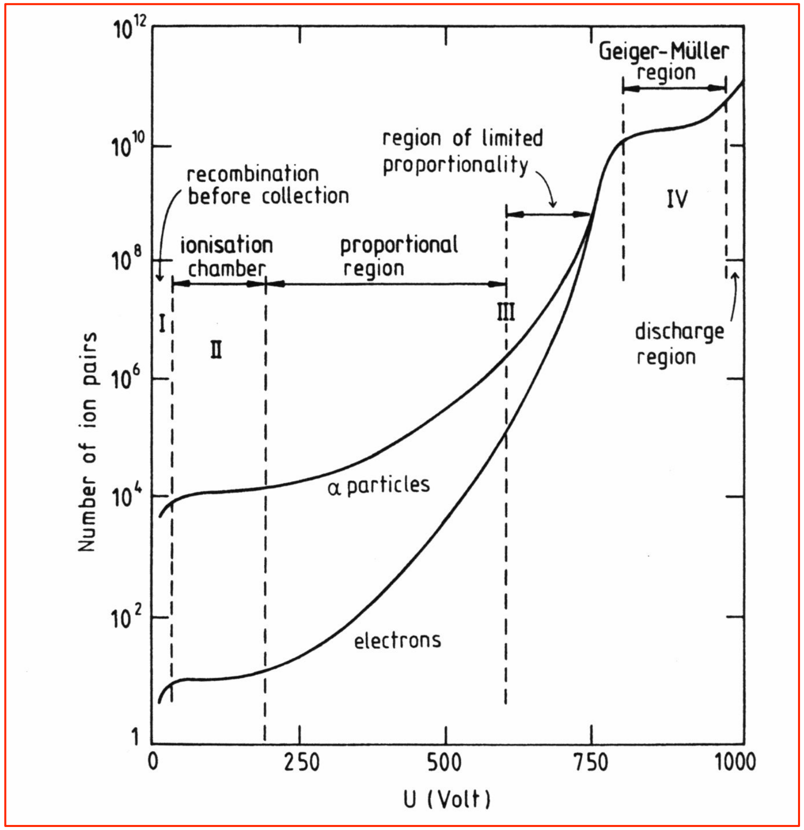

Gas ionization detectors are commonly used as integrating detectors to measure beam flux rather than individual photons. A typical detector consists of a rectangular gas cell with thin entrance and exit windows.

Inside the detector, an electric field is applied across two parallel plates. Some of the x-rays in the beam interact with the chamber gas to produce fast photoelectrons, Auger electrons, and/or fluorescence photons. The energetic electrons produce additional electron-ion pairs by inelastic collisions, and the photons either escape or are photo-electrically absorbed. The electrons and ions are collected at the plates, and the current is measured with a low-noise current amplifier. The efficiency of the detector can be calculated from the active length of the chamber, the properties of the gas, and the x-ray absorption cross section at the appropriate photon energy.

X-ray Ion chamber

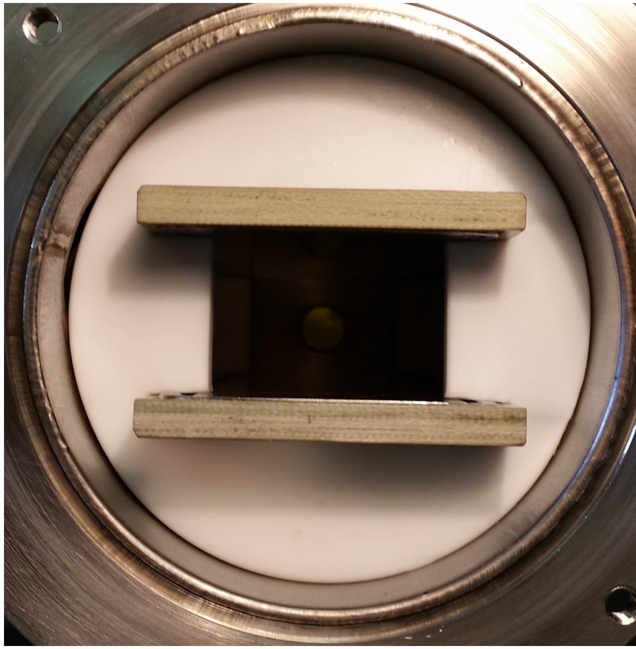

Ion chamber with parallel plates.

Guard ring

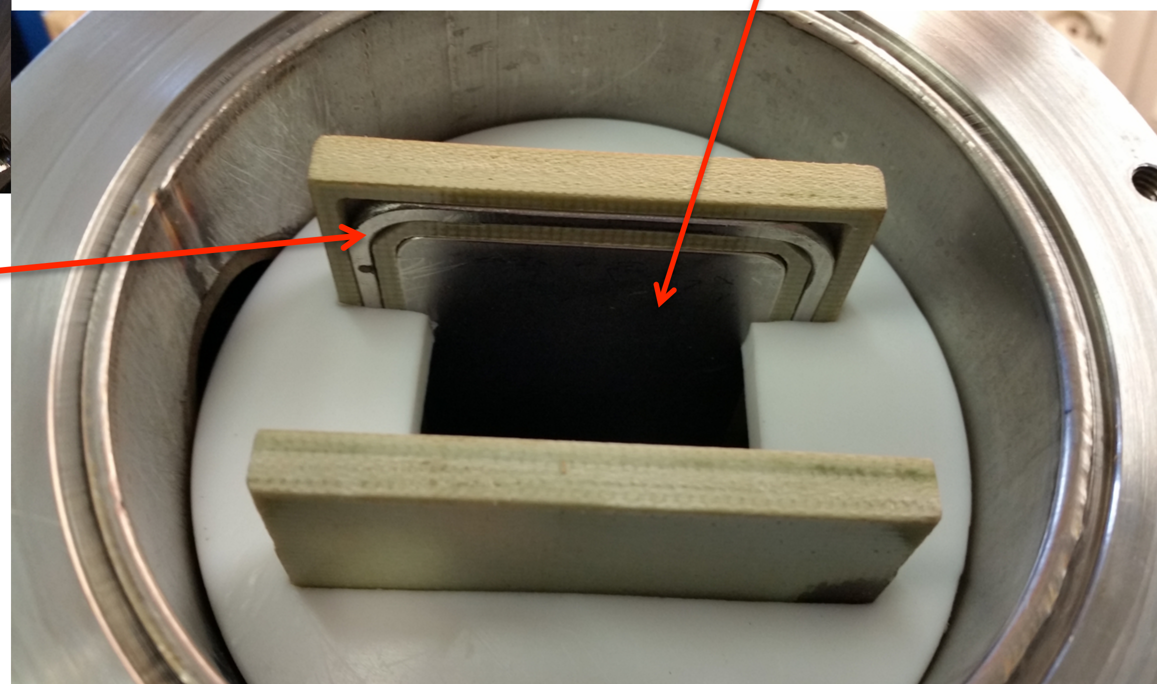

In the parallel plate chamber the charge-collecting electrode is surrounded by an annular ring. The annular ring represents the guard ring (or guard electrode) and is separated from the collecting electrode by a narrow insulating gap, and the applied voltage to the guard ring is the same as that to the collecting electrode.

Direct detection: charge conversion scheme and intensity measurement

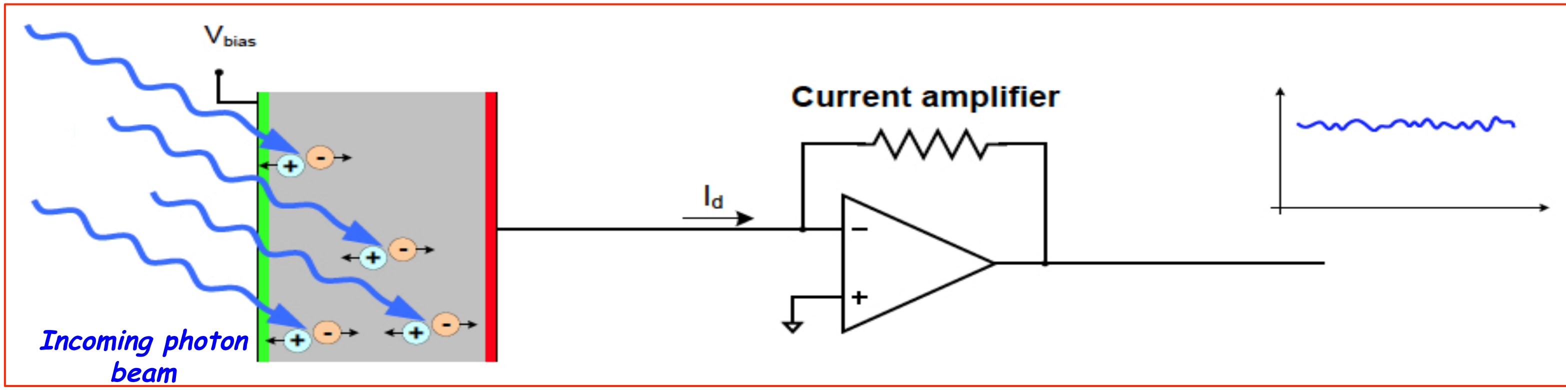

The measured intensity is usually integrated during a well defined time interval and is proportional to the number of incident X-ray photons (N_{ph}).

Intrinsic statistical noise (Poisson statistics): $\sigma_{N_{ph}} = \sqrt{N_{ph}}$ *Effective:* $\sigma_{N_{ph}} = \sqrt{FN_{ph}}$

Fano factor F accounts empirically for deviation from Poisson statistics F ≈ 0.2 for gasses, ≈ 0.1 for semiconductors

The measured intensity is integrated during the exposure time Δt.

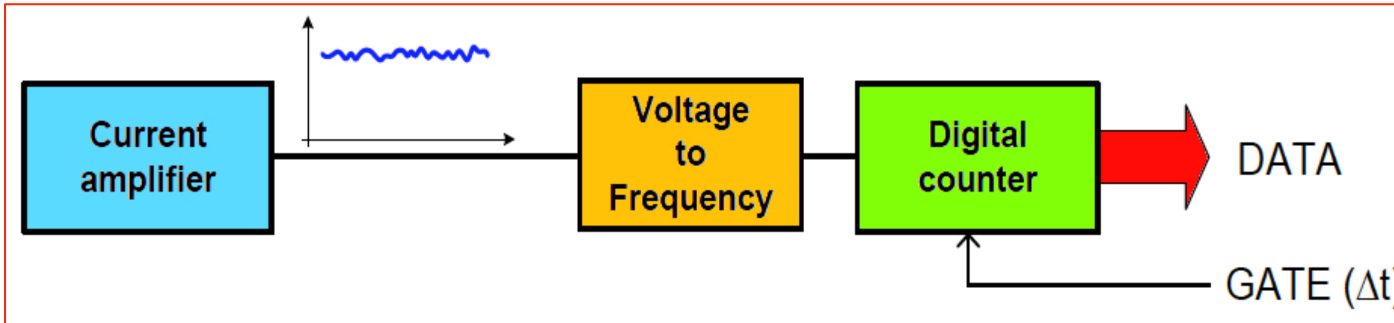

Setup: XAFS in transmission mode

$$\mu(E)x = \ln\left(\frac{I_0}{I_1}\right)$$

Current proportional to the x-ray intensity

Current amplifier and converter of I to V

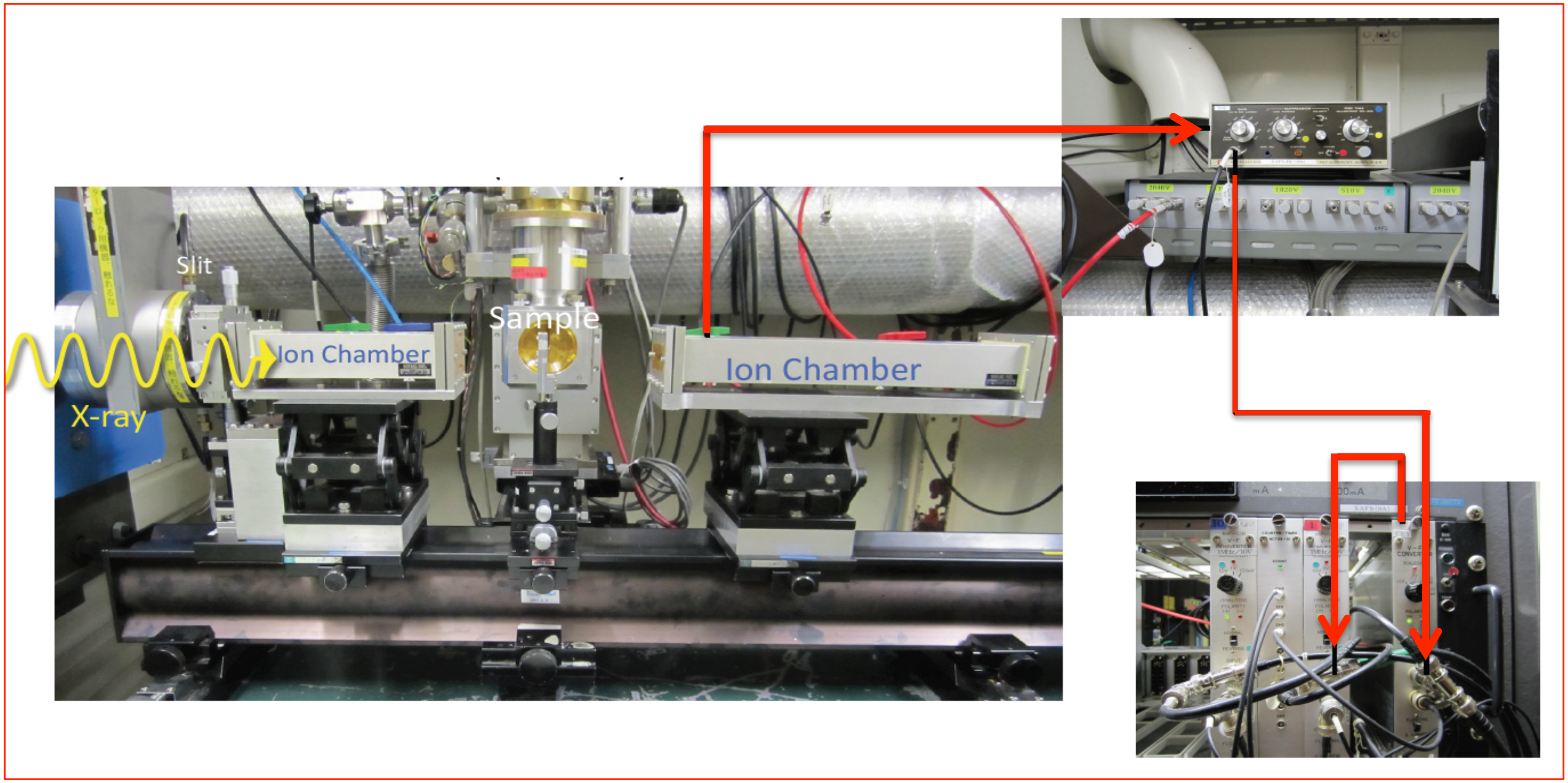

Voltage to frequency converter and counter

Ion chamber characteristics

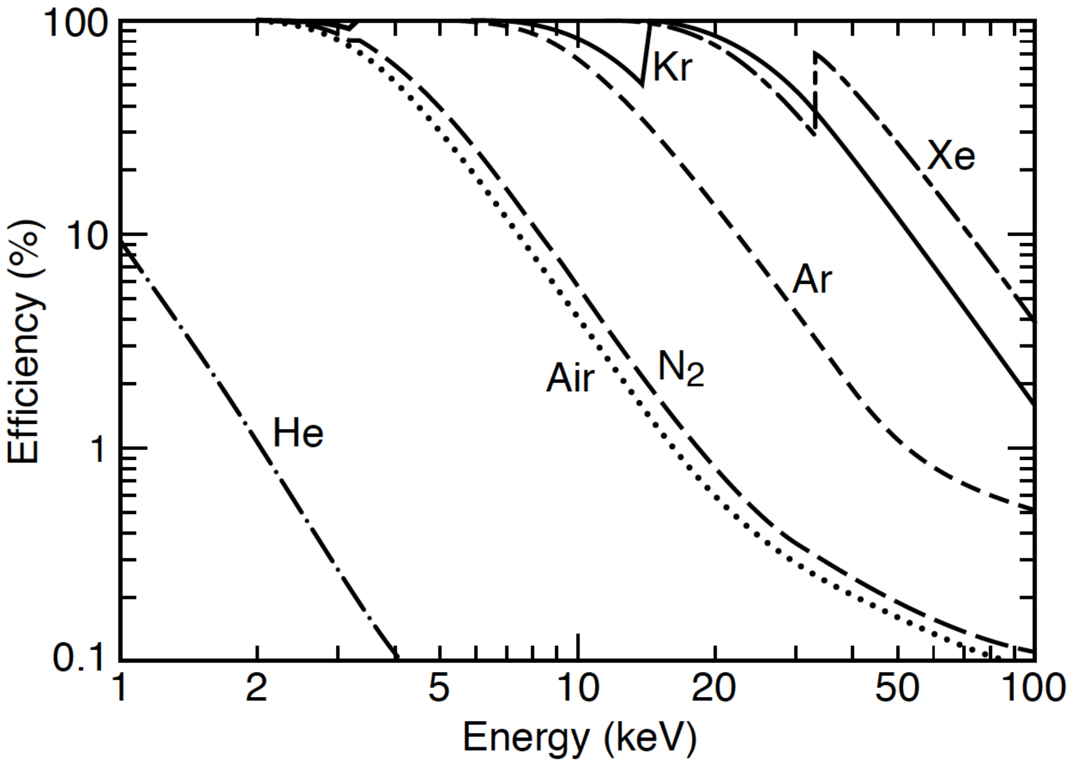

Efficiency of a 10-cm-long gas ionization chamber as a function of energy, for different gases at normal pressure.
The efficiency of the detector can be calculated from the active length of the chamber, the properties of the chamber gas, and the x-ray absorption cross section at the appropriate photon energy

Once the efficiency is known, the photon flux can be estimated from chamber current and the average energy required to produce an electron-ion pair

Element	Energy (eV)
Helium	41
Nitrogen	36
Air	34.4
Neon	36.3
Argon	26
Krypton	24
Xenon	22

Photon flux evaluation

$$I = Ne = I_0 T \gamma e$$

$$N \cong \frac{E}{\langle V_i \rangle}$$

N = Number of electron-ion pairs produced

E = X ray energy

$\langle V_i \rangle$ = Average energy required to produce an electron-ion pair

I_0 = Incoming photon flux (ph/s)

T = Ion chamber window transmission

γ = gas efficiency (electrons/ph)

L = length of the ion chamber plate

$$I_0(ph/s) = \frac{I(A)}{\gamma e(C)} \frac{\langle V_i \rangle (eV)}{E(eV)} \frac{1}{1 - e^{-\mu L(cm)}}$$

$$\mu(cm^{-1}) = \left[\frac{\mu}{\rho}(E)\right] \rho$$

$\left[\frac{\mu}{\rho}\right]$ *= gas mass attenuation coefficient*

ρ = gas density function of pressure (γ)

γ = I_0 10%; I_1 90%

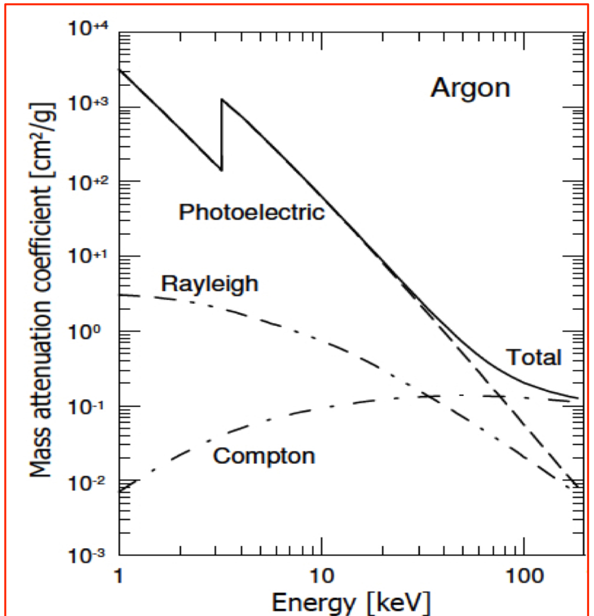

X-ray ion chambers ad windows

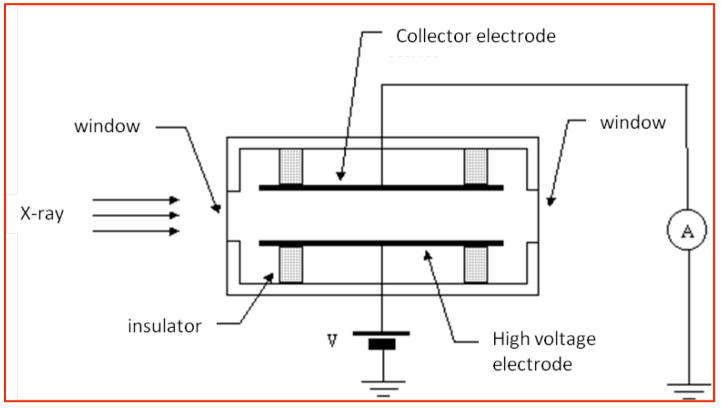

Unmounted and mounted MOXTEK ultrathin windows

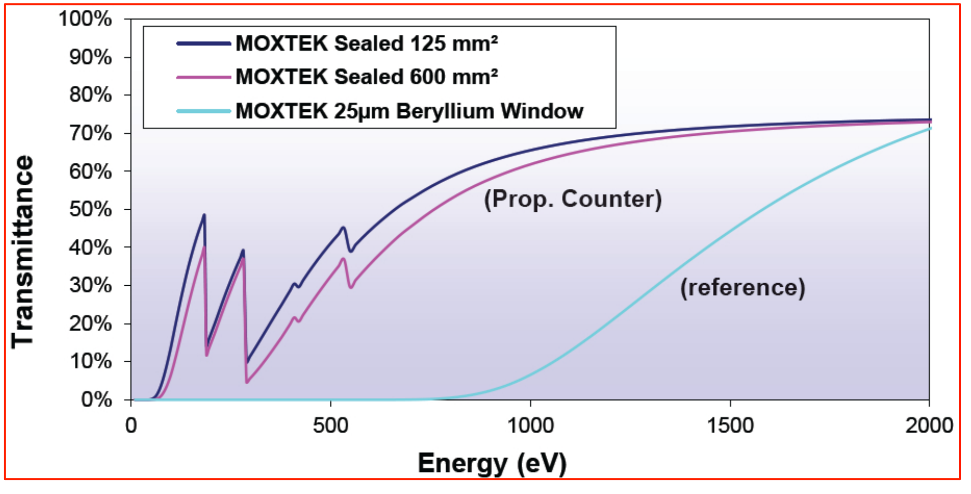

XAFS S_8

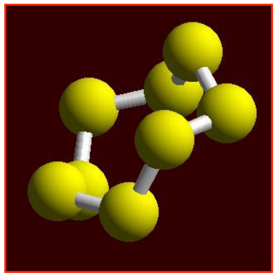

S_8

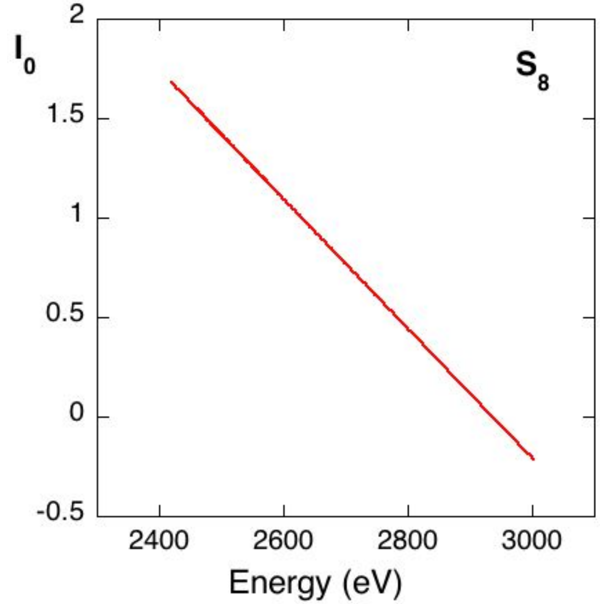

I_0
S_8
2
1.5
1
0.5
0
-0.5
2400
2600
2800
3000
Energy (eV)

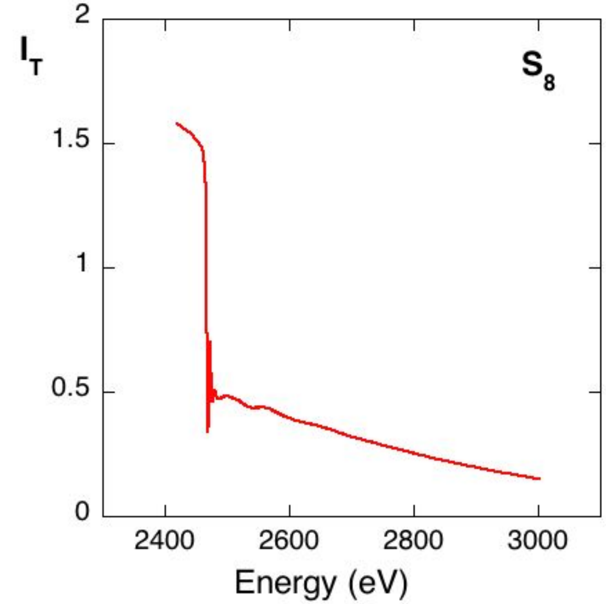

I_T
S_8
2
1.5
1
0.5
0
2400
2600
2800
3000
Energy (eV)

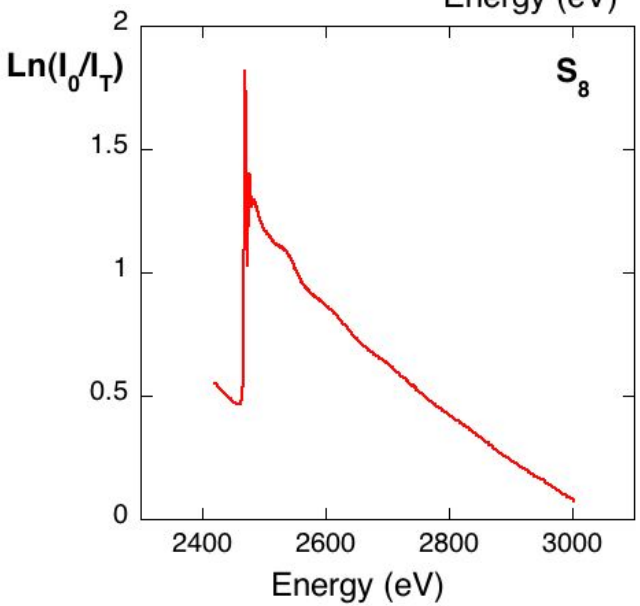

$Ln(I_0/I_T)$
S_8
2
1.5
1
0.5
0
2400
2600
2800
3000
Energy (eV)

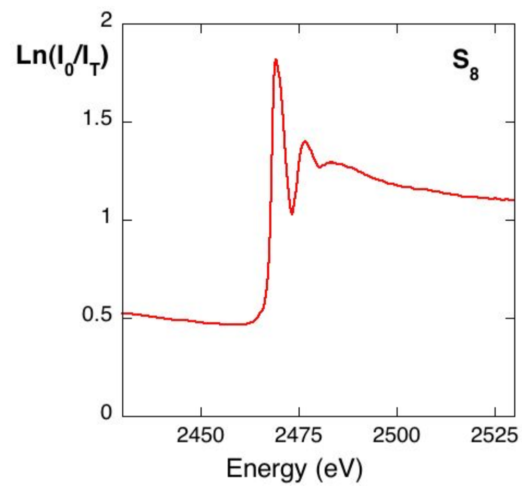

$Ln(I_0/I_T)$
S_8
2
1.5
1
0.5
0
2450
2475
2500
2525
Energy (eV)

SDD
Silicon Drift Detectors
or Energy dispersive detectors

XRF and energy dispersive SDD

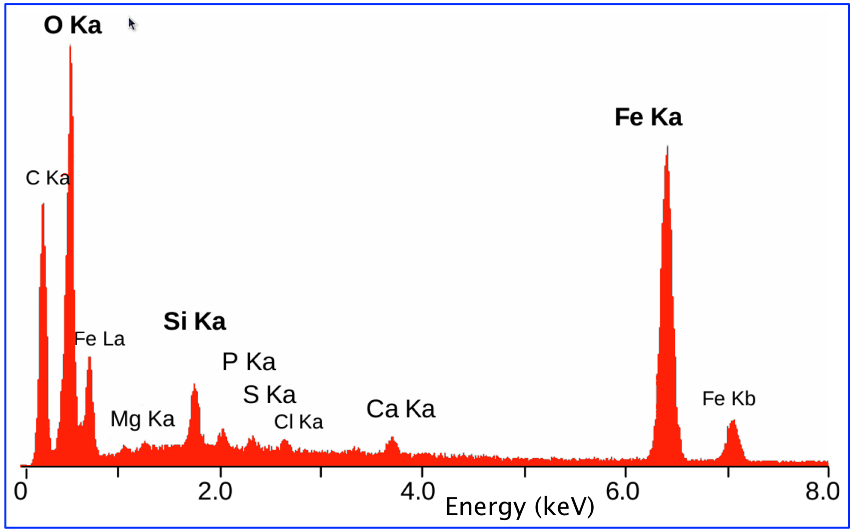

A typical XRF spectrum obtained on mineral particles used to characterize the elemental composition of the sample and to perform this kind of measurements an energy dispersive detector is needed.

$$\mu(E)x = \left(\frac{I_F}{I_0}\right)$$

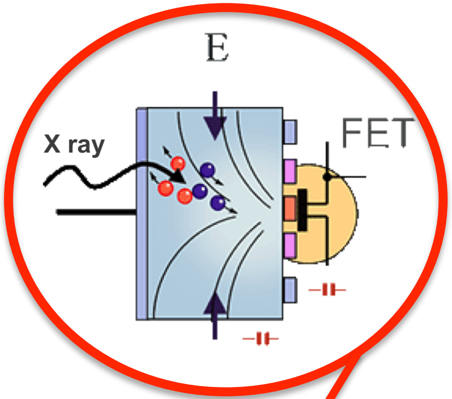

Schematic view of a SDD detector.

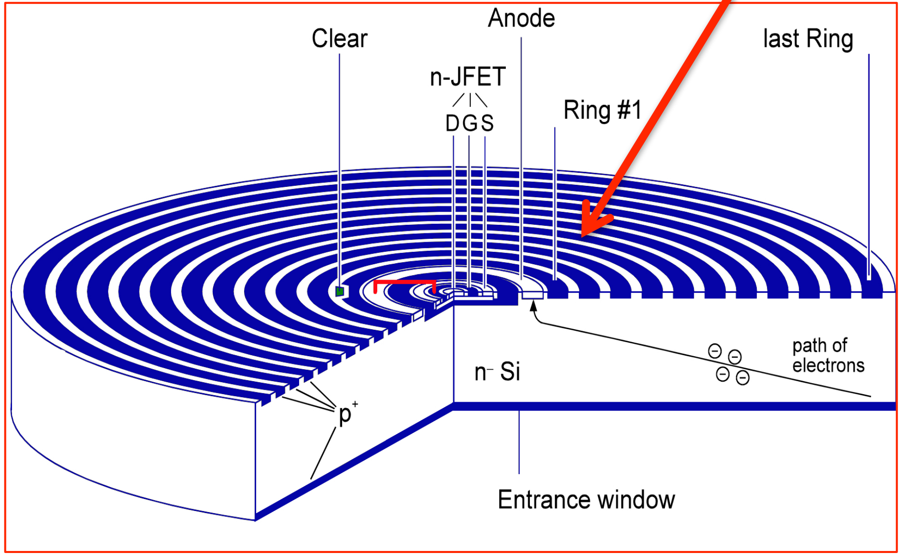

The latest generation of SDD detectors offers: all the advantages of being liquid nitrogen-free, an excellent energy resolution at high count rates and also large active areas.

E. Gatti and P. Rehak, Semiconductor drift chamber-an application of a novel charge transport scheme, Nucl. Instr. and Meth. **A225** (*1984*) 608

Energy Dispersive detectors

Silicon and germanium detectors can make excellent energy-resolving detectors. When a photon interacts in the intrinsic region, tracks of electron-hole pairs are produced (analogous to electron– positive ion pairs in a counting gas). In the presence of the electric field, these pairs separate and rapidly drift to the detector contacts. The average energy required to generate an electron-hole pair is ***3.6 eV for silicon*** and ***2.98 eV for germanium***.

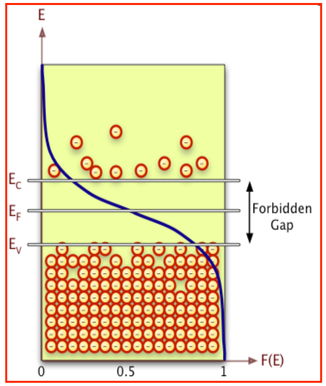

Electrons move to the conduction band of the silicon semiconductor and leave behind holes that behave like free positive charges within the sensor.
Lower band gap materials can offer better resolution due to better ($\Delta E \sim \varepsilon_i$) but must be cooled to limit noise from thermal generation of carriers.
Absorbed radiation energy E is shared between crystal lattice excitations (~2/3) and generation of charge carriers(~1/3) this ratio is ~ same for many semiconductor materials

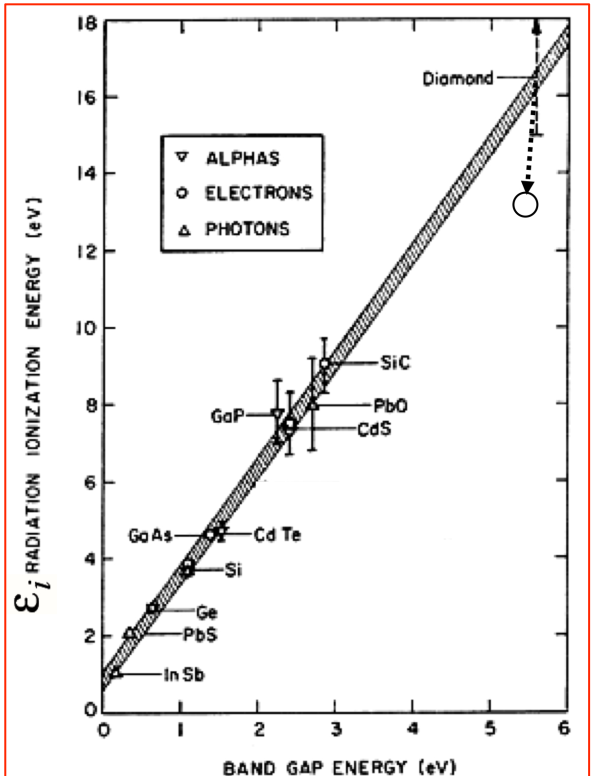

C. A. Klein, J. Appl. Phys. **39** (*1968*) 2029

The ED detector converts the energy of each individual X-ray into a voltage signal of proportional size. This is achieved through a three stage process:

- ***First*** - the X-ray is converted into a charge by the ionization of atoms in the semiconductor crystal.
- ***Second*** - this charge is converted into the voltage signal by the FET preamplifier.
- ***Finally*** - the voltage signal enters the pulse processor for measurement.

The output from the preamplifier is a voltage 'ramp' where each X-ray appears as a voltage step on the ramp. At the same time electronic noise must be minimized to allow detection of the lowest X-ray energies.

SDD working principle

Sideward depletion

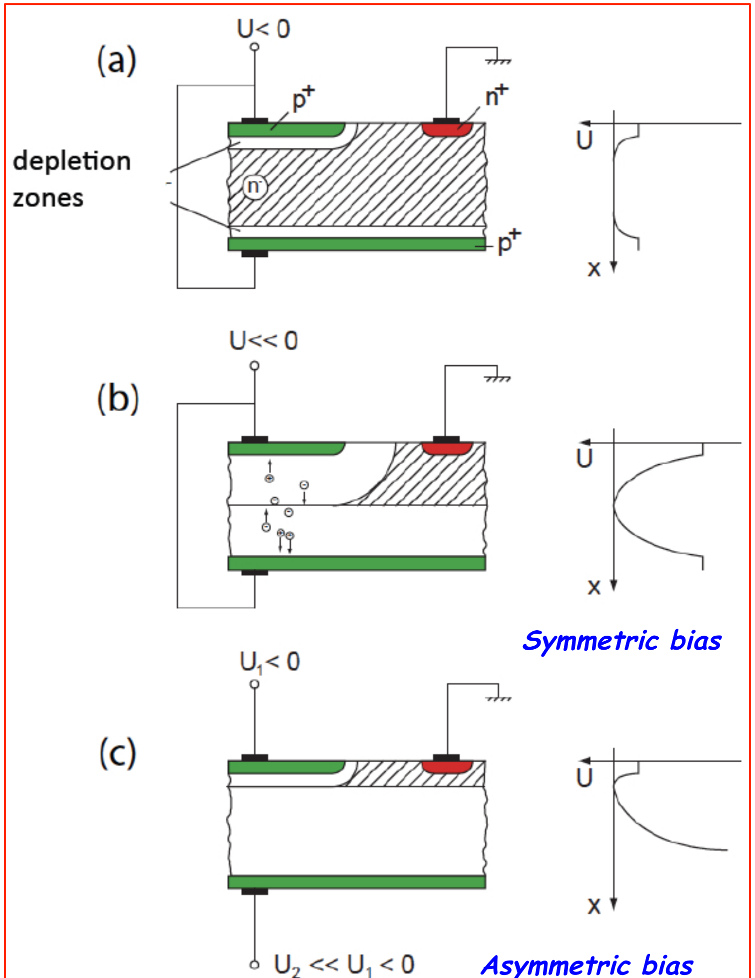

N. Wermes – Semiconductor Detectors- EDIT15

With respect to a conventional p-n diode detector, where the ohmic n+ contact extends over the full area on one wafer side, the ***depletion of the bulk can be also achieved by positively biasing a small n+ electrode with respect to p+ electrodes covering both sides of the wafer***. When the n+ voltage is high enough, the two space charge regions separated by the undepleted bulk touch each other, leading to a small undepleted bulk region only close to the n+ electrode.

In the ***Silicon Drift Detector***, based on ***the principle of the sideward depletion***, an ***additional electric field parallel to the surface of the wafer is added*** in order to ***force the electrons in the energy potential minimum to drift towards to the n+ anode***.

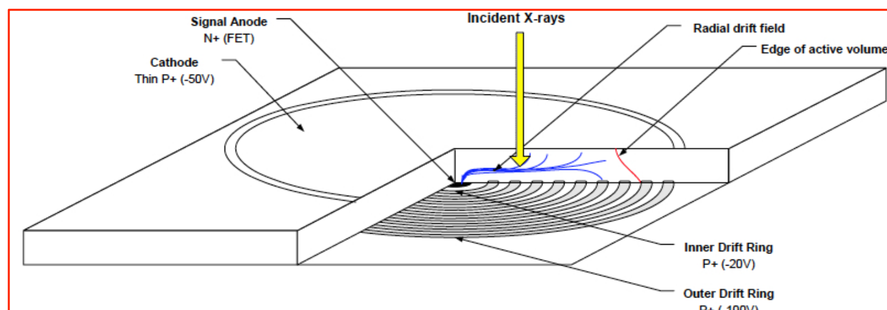

AMPTEK - Application Note AN-SDD-003: Amptek Silicon Drift Detectors

SDD

The silicon drift detector (SDD) sensor is produced using high purity silicon with a large contact area on the side facing the incoming X-rays.
On the opposite side there is a central, small anode contact, which is surrounded by a number of concentric drift electrodes.

*The major distinguishing feature of an SDD is **the transversal field generated by a series of ring electrodes** that **causes charge carriers to 'drift' to a small collection electrode. (Anode)***

The 'drift' concept of the SDD allows for significantly higher count rates.

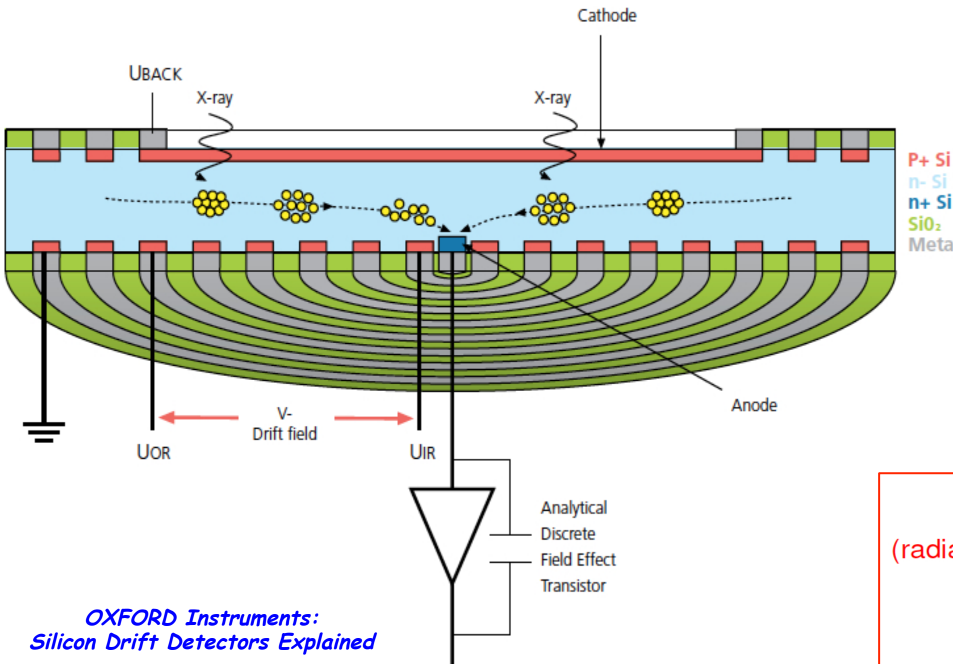

OXFORD Instruments:
Silicon Drift Detectors Explained

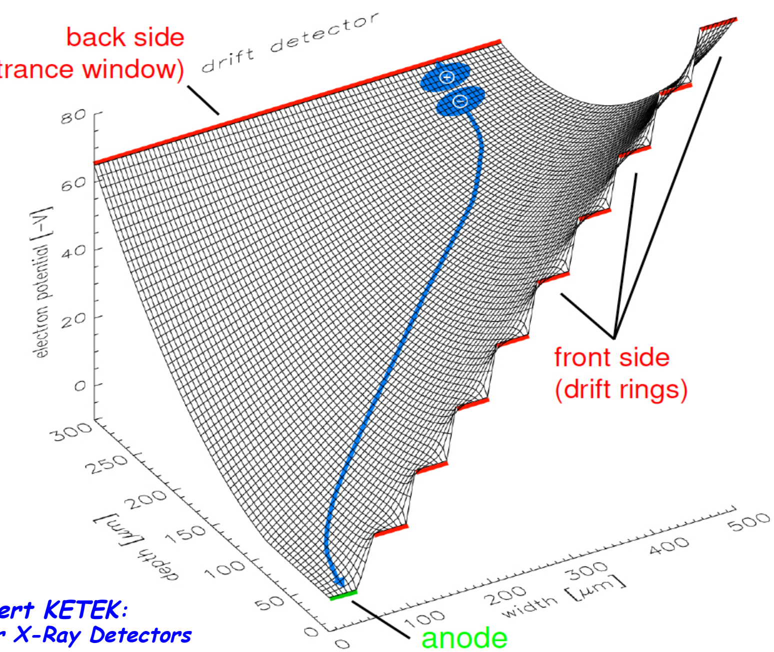

T. Eggert KETEK:
Semiconductor X-Ray Detectors

SDD

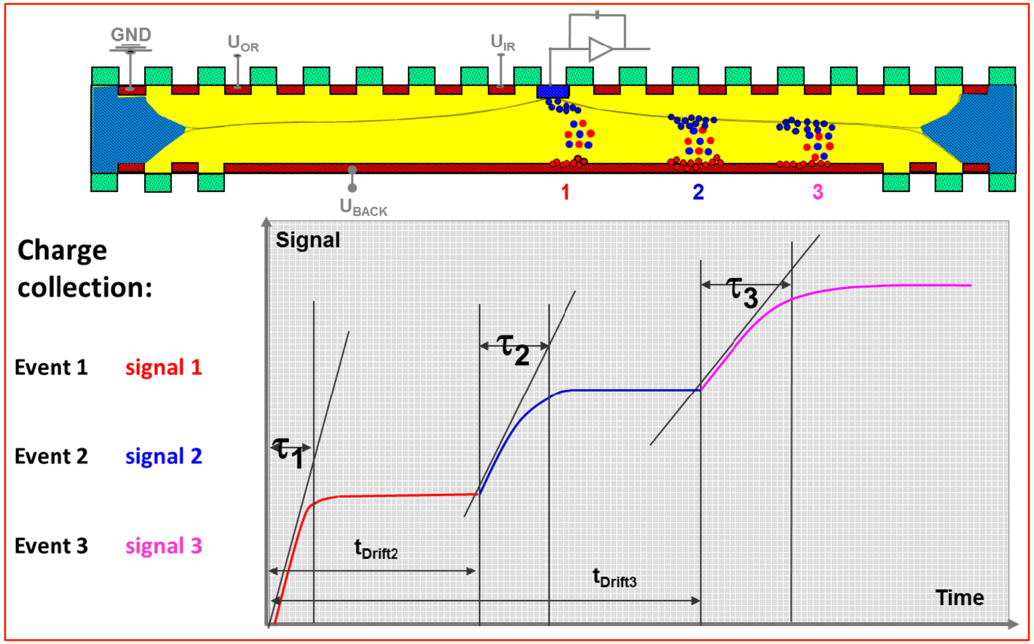

KETEK - High Throughput Large Area Silicon Drift Detectors

The electrons are 'drifted' down a field gradient applied between the drift rings to be collected at the anode.
The charge that accumulates at the anode is converted to a voltage signal by the FET preamplifier.
During operation, charge is built up on the feedback capacitor. There are two sources of this charge, current leakage from the sensor material and the X-ray induced charge from the photons that are absorbed in the detector.

The output from the preamplifier caused by this charge build-up is a steadily increasing voltage 'ramp' due to leakage current, onto which are superimposed sharp steps due to the charge created by each X-ray event. The accumulating charge has to be periodically restored to prevent saturation of the preamplifier. Therefore at a pre-determined charge level the capacitor is discharged, a process called restoration, or 'reset'.

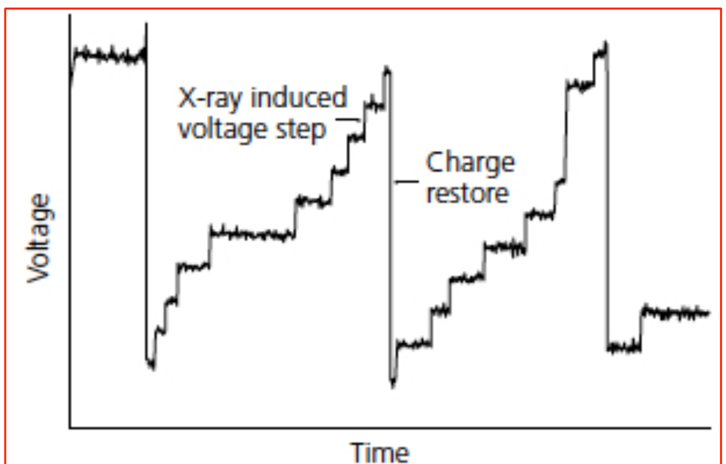

The fundamental job of the pulse processor is to accurately measure the energy of the incoming X-ray, and give it a digital count in the corresponding channel in the computer. It must optimize the removal of noise present on the original X-ray signal and it needs to recognize quickly and accurately a wide range of energies of X-ray events from below 100 eV up to 40 keV. It also needs to differentiate between events arriving in the detector very close together in time to prevent pulse pile-up effects.

Direct detection: charge conversion scheme and measurement

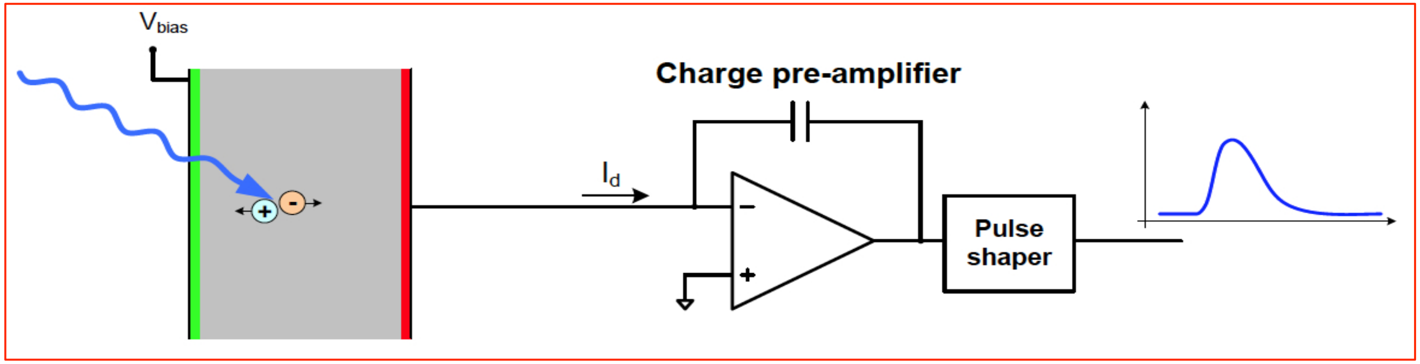

Photon by photon processing and evaluation of the photon energy by measuring the charge generated in the sensor

Pulse discriminator: from simple level discrimination to complex pulse-height analysis (pileup rejection)

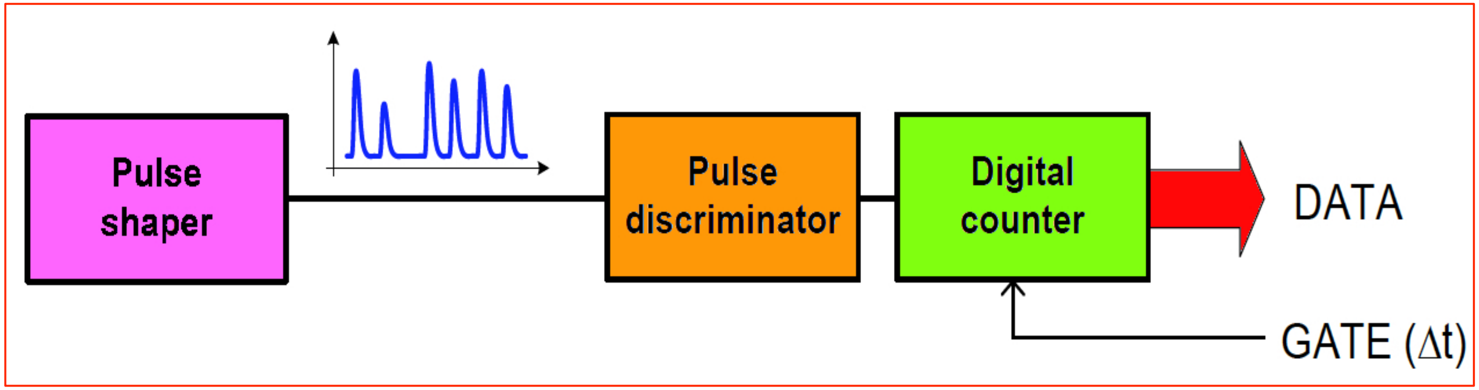

SDD energy resolution

The number of generated charge carriers by a single X ray photon, N_Q, can be estimated as:

$$N_Q = \frac{E}{\varepsilon_i}$$

where the ionization energy, ε_i, is the average energy required to produce an electron/ hole pair. In ***silicon***: ***ε_i = 3.6 eV*** a ***10 keV photon*** produces ***2800 e/h pairs*** .

$$\sigma_{N_Q} = \sqrt{F N_Q}$$

Standard deviation that takes into account ***deviations from Poisson statistics***. F= 0.11 for Si and 0.08 for Ge.

The RMS fluctuation, σ_E, associated to ***X ray → charge conversion*** can be estimated by :

$$\sigma_E = \varepsilon_i \sigma_{N_Q} = \sqrt{F E \varepsilon_i}$$

Usually known as ***Fano noise***

The ***energy resolution*** of the detector at a certain energy is usually defined as the ***full width at half-maximum (FWHM)*** of recorded spectra.

$$FWHM = 2.35\sigma_E$$

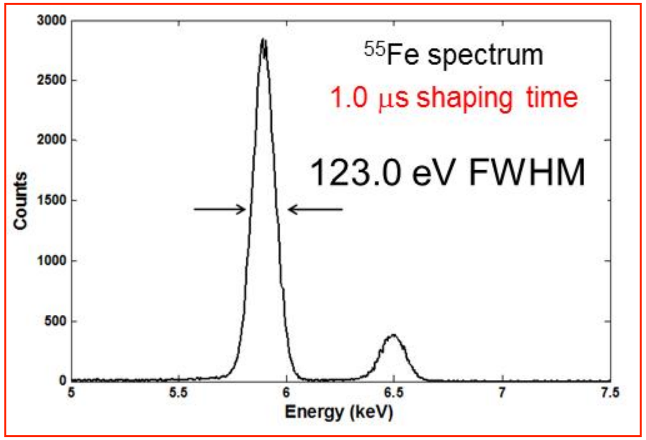

The measured spectral resolution is the quadratic-sum of various noise sources present in the detector:

$$Resolution = \sqrt{(Fano)^2 + (sensor-noise)^2 + (readout-noise)^2}$$

Front-end for SDD

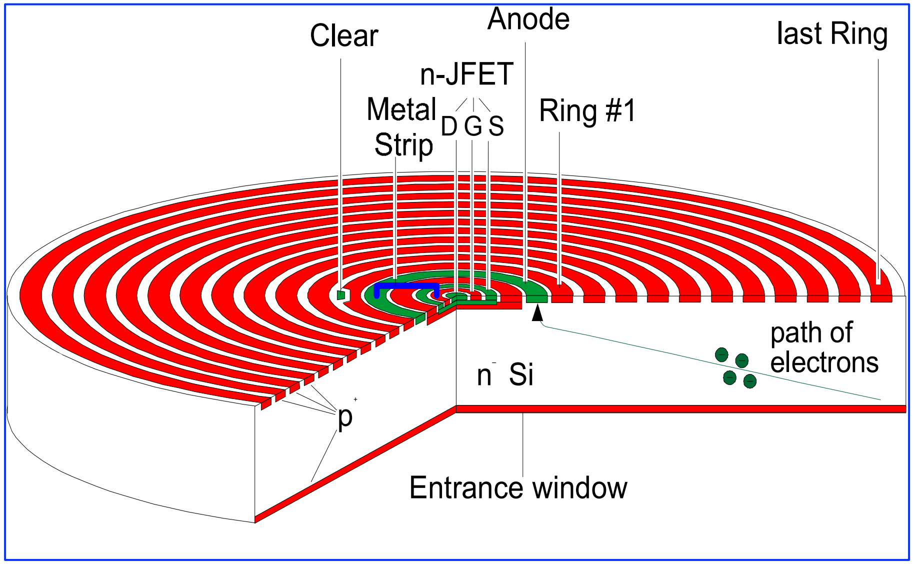

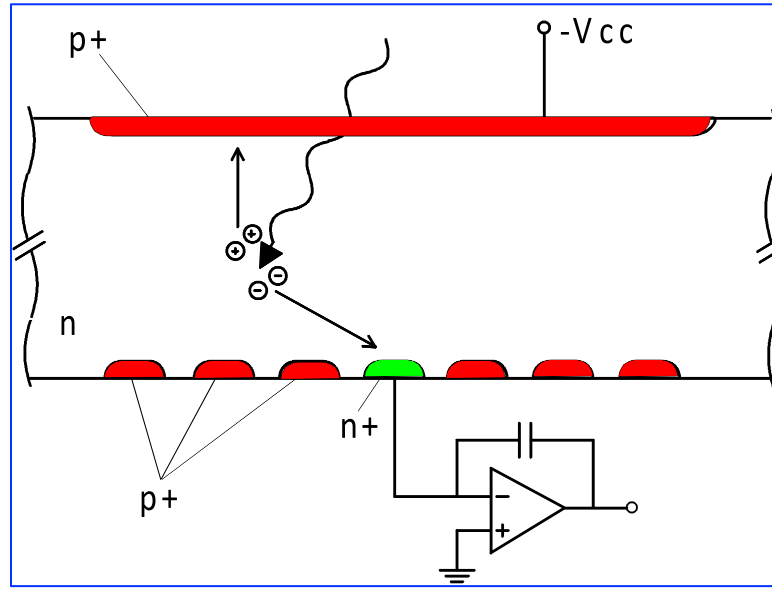

- *JFET integrated on the SDD*
  - lowest total anode capacitance
  - easier interconnection in SDD arrays
  - limited JFET performances (gm, 1/f)
  - sophisticated SDD+JFET technology

- *external FET (JFET, MOSFET)*
  - better FET performances
  - standard SDD technology
  - larger total anode capacitance
  - interconnection issues in SDD arrays

Achievable energy resolution

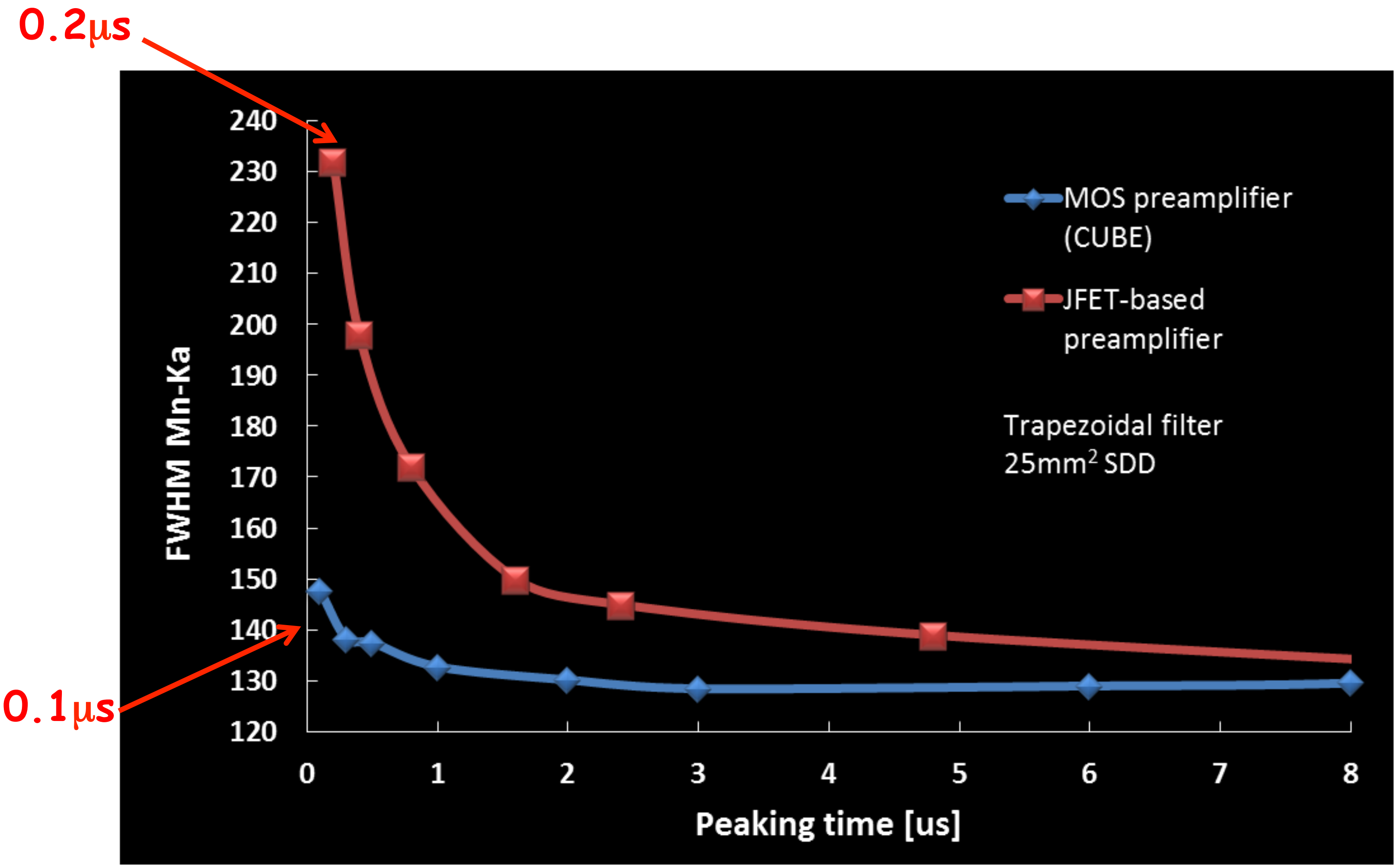

Setup: XAFS in fluorescence mode

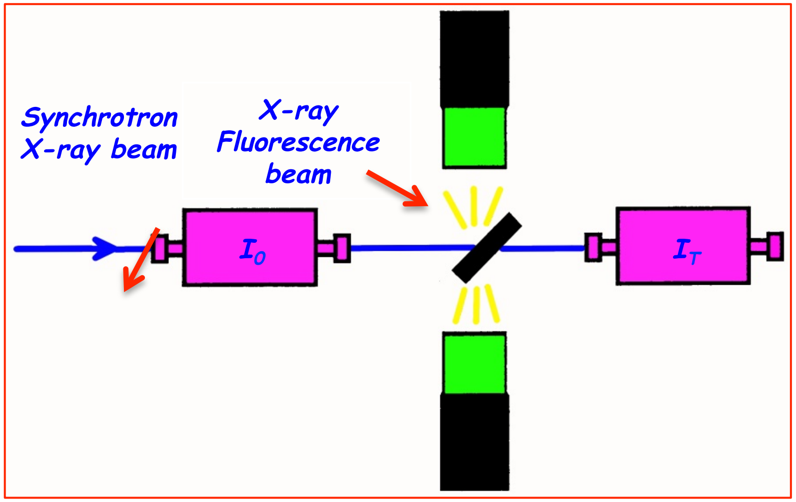

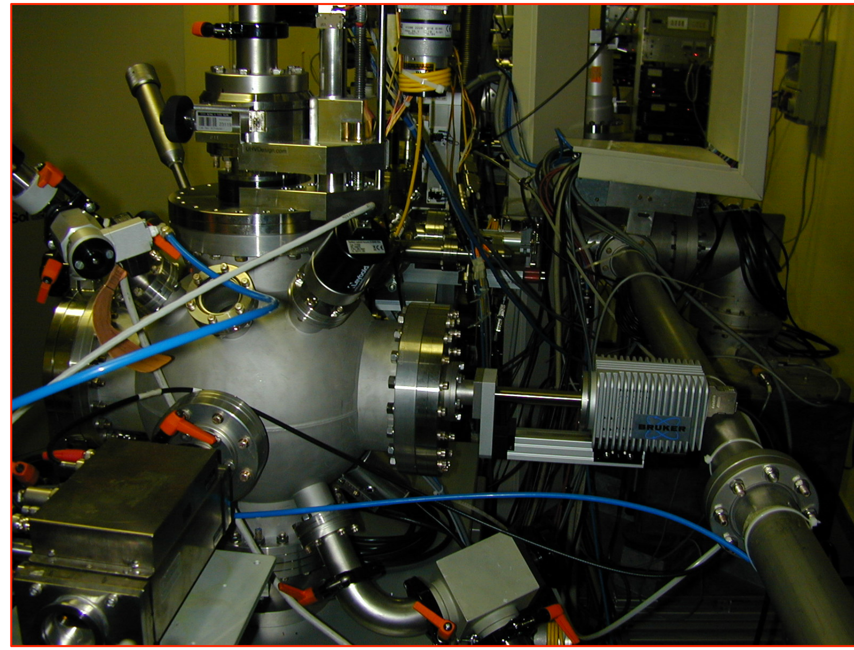

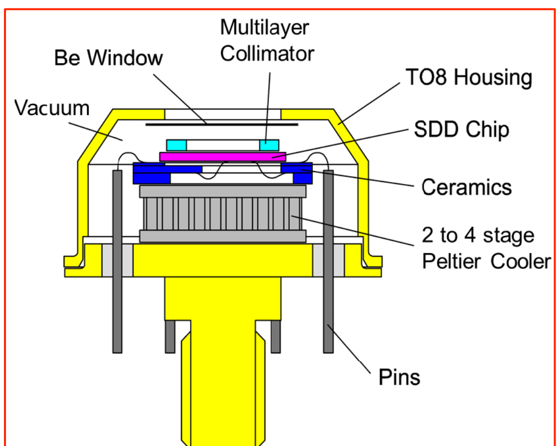

J. Knobloch et al. - KETEK:
High Throughput Large Area Silicon Drift Detectors

Examples of some available multi-element SDD systems

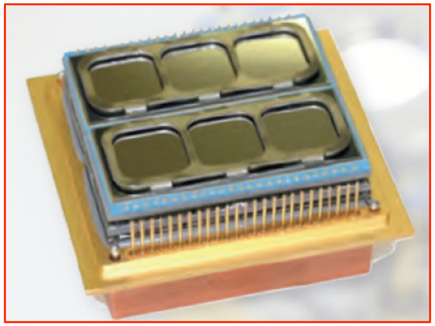

PN-DETECTORS SDD-600 Field
Active area 6 x 100 mm^2
typ. 138 eV @ Mn K, -20 °C
P/B up to 15,000
Input count rate up to 6 Mcps

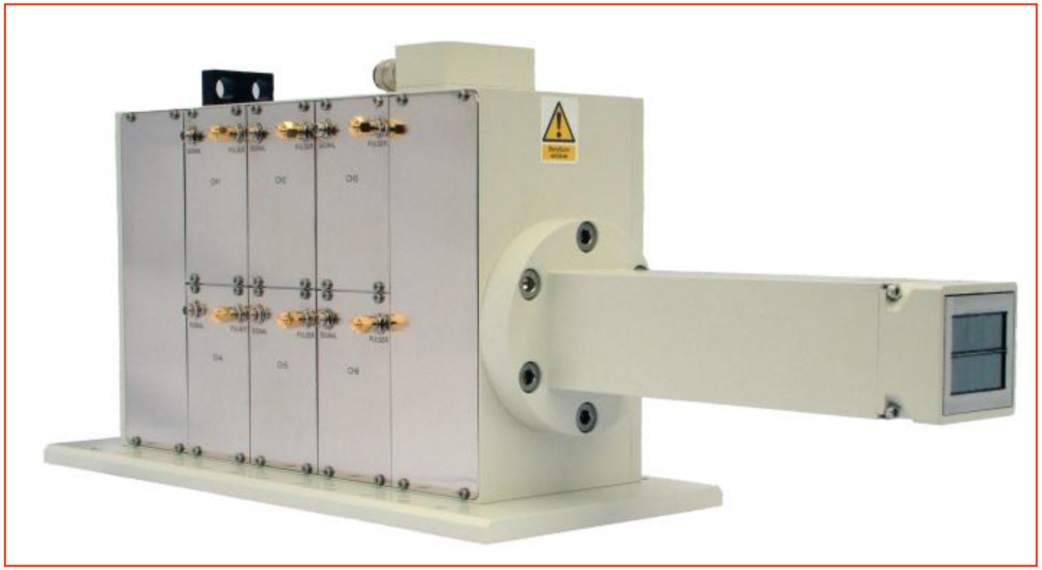

SGX – SENSORTECH - Active area 6 x 100 mm^2

Hitachi Vortex- ME 4
SDD/ASIC e Xpress 3 processor

Thank you for your attention